DOCTORAL DISSERTATION

THE TREATMENT OF STEAM EXPLOSION WASTEWATER GENERATED FROM BIOETHANOL PROCESSING USING SUGAR CANE BAGASSE

NGO VAN ANH

2016

THE TREATMENT OF STEAM EXPLOSION WASTEWATER GENERATED FROM BIOETHANOL PROCESSING USING SUGAR CANE BAGASSE

BY

NGO VAN ANH

Thesis submitted to the Graduate School of Environmental Engineering, The University of Kitakyushu in fulfillment of the requirement for the Degree of DOCTOR OF ENGINEERING

SEPTEMBER 2016

Declaration

I hereby declare that this thesis has not been previously submitted to any other university or institution for obtaining any academic degree. Accept quotations and data which are properly cited, this thesis contains my original works. The thesis is only submitted to The University of Kitakyushu in fulfillment of the requirement for a degree of Doctor of Engineering.

Kitakyushu, Japan

September, 2016

NGO Van Anh

Acknowledgements

First of all, I would like to express my deep gratitude to my supervisor, Prof. Hidenari Yasui for his vital supervision all the time. Without his great insight, support and inspiration, I would not complete this Ph.D. course. Besides, I would like to thank my committee members including Prof. You Ito, Prof. Yoshiaki Miyazato and especially to Assoc. Prof. Mitsuharu Terashima for the helpful comments and suggestions on my research.

Many thanks to officers in The University of Kitakyushu particularly to The International Student Support Center for supporting in daily life. In addition, I received numerous helps from Dr. Liu Bing, Mr. Ian Javis and others labmates in daily experimental life. Their supports and friendship would be unforgettable.

Finally, I would like thank to my husband and family for their love and support during my study.

Kitakyushu, September 2016

Table of Contents

List of figures

List of tables

Abbreviations

AA	Amino acid
ABS	Absorbance
AC	Activated carbon
AD	Anaerobic digestion
ADM1	Anaerobic Digestion Model No.1
AF	Anaerobic filter
AHRs	Anaerobic hybrid reactors
Ammonium-N	Ammonium nitrogen
AOPs	Advanced oxidation processes
APAM	Anionic Polyacrylamide
ASBR	Anaerobic sequencing batch reactor
ASMs	Activated Sludge Models
BC	Brown and Caldwell
CBOD	Carbonaceous biochemical oxygen demand
COD	Chemical oxygen demand
C/N	Carbon/nitrogen
CSTR	Continuous stirred-tank reactor
DHS	Down-flow hanging sponge
DMC	2-methyarcyloyloxyethyl trimethyl ammonium chloride
DOC	Dissolve organic carbon
EGSB	Expanded granular sludge beds
FBR	Fixed-bed reactor

Fur	Furfural
GRABBR	Granular bed anaerobic baffled reactor
GSS	Gas–solids separator
HBu	Butyrate
HMF	5-Hydroxy-methylfurfural
HRTs	Hydraulic retention times
HVa	Valerate
IWA	International Water Association
LCFA	Long chain fatty acid
MPR	Methane gas production rate
MS	Monosaccharide
MS-UASB	Multistage UASB reactor
NaClO	Sodium hypochlorite
NF	Nanofiltration
Nitrate-N	Nitrate nitrogen
NREL	National Renewable Energy Laboratory
OLRs	Organic loading rates
Ortho-P	Orthor phosphorus
PAC	Poly Aluminium Chloride
PAM	Polyacrylamide
PDMC	Poly (2-methacryloyloxyethyl) trimethyl ammonium chloride
PVA	Polyvinyl-alcohol
PZSS	Poly-Zinc-Silicate-Sulfate
RO	Reverse osmosis
SEWW	Steam explosion wastewater

SR	Sulfate reducing
SSF	Simultaneous saccharification and fermentation
TDFS	Total dissolved fixed solids
TDS	Total dissolved solids
TIC	Total inorganic carbon
TKN	Total Kjeldahl nitrogen
TOC	Total organic carbon
Total P	Total phosphorus
TSS	Total suspended solids
TVFA	Total volatile fatty acid
TVS	Total volatile solids
UAFs	Upflow anaerobic filters
UASB	Upflow anaerobic sludge blanket
UPLC	Ultra-performance liquid chromatography
USPHS	United States Public Health Services
UV	Ultraviolet
VLRs	Volumetric loading rates
VSS	Volatile suspended solids

Abstract

In bioethanol processing factories, new technologies using steam explosion pretreatments are developed to improve ethanol production from cellulose (*e.g.* sugar cane bagasse). Along with new methods are the challenges for wastewater treatment from this process. Due to the high organic strength in steam explosion wastewater, high-rate anaerobic biological treatments are also paid attention as the potential processes. However, the operational failure often occurs in the high-rate methane fermentation processes because of the accumulation of volatile fatty acids (VFAs). Mathematical approach based on the basic models (Activated Sludge Models (ASMs) and Anaerobic Digestion Model No. 1 (ADM1)) provides the understanding deeply about biochemical reactions as well as help predict appropriately this phenomena. Although, in many researches the inhibition is assumed on the microbial growth stages whilst acceleration of the decay by inhibitory materials is not considered.

To cope the problem, a lab-scale continuous experiment for the methane fermentation was performed for 110 days by changing the volumetric loading rate from 2.6-9.3 kg-COD/m^3/d to induce an acidic failure, and its dynamic simulation was also conducted using a modified ADM1 equipped with the irreversible inhibition defined as an activity decay. Due to the compositions of steam explosion wastewater are not high fluctuated, it is difficult to express an acidic failure phenomenon. While organics wastes from food processing factories are typical materials having high fluctuated fraction of readily biodegradable organics, therefore, in this study heterogeneous food wastes were chosen as the alternative influent. The modified ADM1 with methanogenic activity decay

reasonably reproduced the responses for soluble material concentrations and methane gas production rate over the experimental period.

On the other hand, due to the lack of technical information for the biological degradability of the liquid waste organics, a batch test was conduct to elaborate a reaction map for the anaerobic degradability of organics in steam explosion wastewater from bioethanol processing. Microorganisms were collected from a lab-scale fixed-bed reactor treating the wastewater. Based on the test, a kinetic model for the anaerobic wastewater treatment was developed with a modification of ADM1 and ASMs.

Along with that, the performance of high-rate reactors (fixed-bed reactor and upward anaerobic sludge blanket reactor) for steam explosion wastewater treatment was evaluated. Two lab-scale reactors with each volume of 10.8 L at 35 °C demonstrated acceptable performance for 160 days of the continuous operation under the volumetric loading rates with 8.51 kg-COD/m^3/d (UASB) and 10.9 kg-COD/m^3/d (FBR), respectively. The average soluble TOC removal efficiencies were 72% (UASB) and 64% (FBR) with a methane conversion efficiency of about 50% for both reactors. Comparing two reactors, FBR operation was more stable and applied higher volumetric loading rate than UASB, the dynamic simulations focused on the fixed-bed reactor's responses. A kinetic model based on a modification of ADM1 and ASMs was used to simulate reasonably the methane production, soluble TOC, suspended solid as well as the soluble effluent constituents in terms of carbohydrate, protein, propionate, acetate, lignin and ammonium nitrogen in FBR.

Although biological treatment resulted in significant soluble TOC removal, the effluent

still retained high lignin concentration and the dark brown color. Therefore, post-treatment experiment (oxidation, coagulation/flocculation and adsorption) were conducted to remove un-degradable materials as well as color from the effluent. Firstly, the effluent from UASB reactor (soluble TOC of 2,675 mg-C/L and color of 12,514 ^{0}) was treated by activated sludge process in 5 days with DO maintained at 1 mg/L. Some biodegradable materials continued to remove in this step and soluble TOC and color decreased to 1,644 mg-C/L and 9,142 ^{0}, respectively. After centrifuging at 8,000 rpm in 5 mins to separate sludge, the supernatant was partial oxidized with different concentrations of sodium hypochlorite (NaClO) (0.01, 0.1, 0.5, 2, 5, 10, 25, 50 and 100 mg/L) and coagulated/flocculated using 50, 100, 150 and 200 mg/L of poly-aluminium chloride (PAC). Then neutralizing pH and waiting for 30 minutes. As the results, soluble TOC and color removal rate obtained 62% and 72%, correspondingly with 5 mg/L NaClO and 200 mg/L PAC. On the other hand, applying adsorption process directly after UASB reactor using 0, 0.5, 1, 2, 3, 4, 5, 6, 7, 8, 9 and 10 g/L of commercial activated charcoal (AC) in 24 hours acquired maximum removal rates (69% for S-TOC and 94% for color) at 10g/L AC. Finally, combining oxidation (50 mg/L NaClO) and coagulation/flocculation (100, 300, 500, 750 and 1,000 mg/L PAC) in 1, 2 and 3 times. At 50 mg/L NaClO, 1,000 mg/L PAC and coagulation/flocculation in 3 times, soluble TOC and color removal rate were 49% and 86%, respectively. Next, using activated carbon (0, 1, 4, 8 and 12 g/L) to treat the remaining un-degradable materials. Soluble TOC and color removal rate achieved 75% and 95% at 12 g/L of AC. Therefore, combining oxidation, coagulation/flocculation and adsorption process could improve the treatment efficiency of S-TOC and color to 87% and 99%, correspondingly.

Chapter 1. Introduction

1.1 Overview of bioethanol processing

Bioethanol is a renewable energy source which is made from the fermentation of sugars obtained from biomass. In recent years, rise in energy demand in worldwide and the decline of oil reserves motivate the search for alternative energy resources, especially for those derived from renewable materials such as biomass (Saxena *et al.* 2009). As shown in Figure 1. 1, global biofuel production increased from 62 to around 120 billion liters in 7 years (2007-2014); and is planned to rise to 140 billion liters in 2020 (IEA 2011).

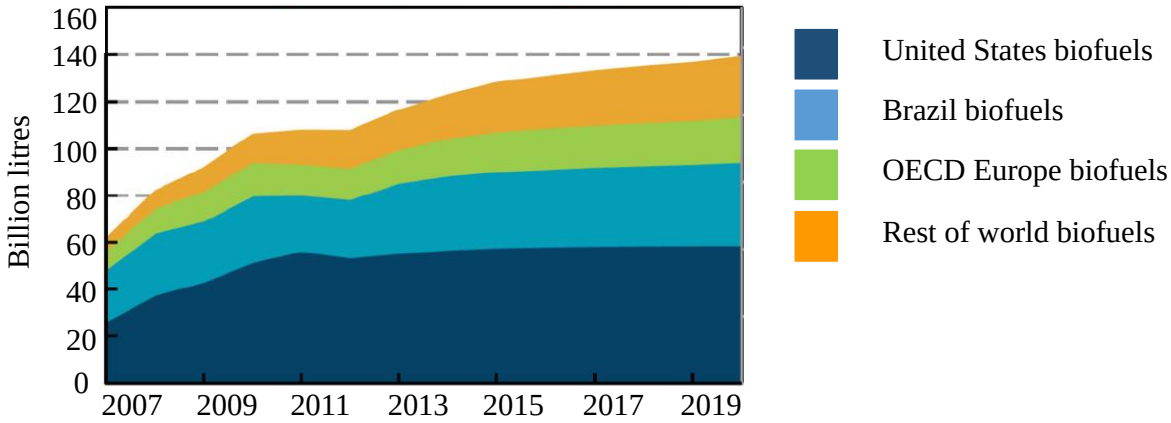

Figure 1. 1. World biofuels production, historical and projected (OECD/IEA 2014)

The feedstock for bioethanol processing can contain either sucrose (sugar cane, sugar beet) or starch (corn, wheat) or be a lignocellulosic material (sugar cane bagasse, wood and straw) (Dias *et al.* 2009). Among the various agricultural crop residues, sugar cane bagasse is the most abundant lignocellulosic material in tropical countries. In Brazil,

sugar cane bagasse is the main agro-industrial residue, being produced at approximately 250 kg per ton of sugar cane (Zanin *et al.* 2000; Wyman *et al.* 2005). The major components of bagasse include cellulose, hemicellulose and lignin which cannot be easily separated into readily utilizable constituents due to its recalcitrant nature. Thus, second generation bioethanol production technology is applied to remove lignin in the bagasse, decrease cellulose crystallinity and increase the surface area for enzymatic activity. In addition, the development of second generation bioethanol made from lignocellulosic biomass can increase the sustainability of feedstock production, reduce production costs by minimizing the utilization of fossil energy sources and reusing the excess material and by-products of the technology employed (Rabelo *et al.* 2011).

The production of ethanol from lignocellulosic material consists of four major unit operations: pretreatment, hydrolysis, fermentation and separation/distillation (Balat et al. 2008). Flow scheme for the conversion of biomass to bioethanol is shown in Figure 1. 2.

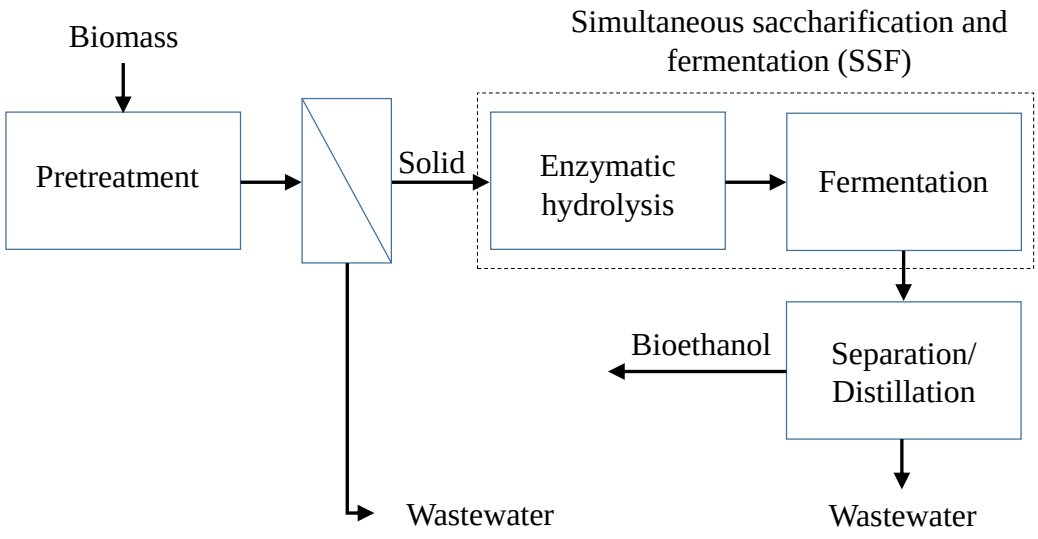

Figure 1. 2. Flow scheme for the conversion of biomass to bioethanol

The first step in bioethanol processing is size reduction and pretreatment (Koehler 2000). In this step, hemicellulose is solubilized and the cellulose is exposed to enhance the rate of hydrolysis and yields of fermentable sugars (Mosier *et al.* 2005). Pretreatment can be conducted in different ways such as physical treatment (uncatalyzed steam explosion, liquid hot water pretreatment, mechanical comminution, and high energy radiation), chemical treatment (catalyzed steam explosion, acid, alkaline, ammonia fiber/freeze explosion, organosolv, pH-controlled liquid hot water, and ionic liquids pretreatments) and biological treatment (Yi Zheng 2009). Table 1. 1 shows various pretreatment options in bioethanol processing (Hamelinck *et al.* 2003, 2005).

In hydrolysis step cellulose may be converted to glucose chemically with acid or enzymatically. Acid hydrolysis processes require high temperature, low pH and have limited conversion efficiency due to glucose degradation. While enzymatic hydrolysis processes conduct at low temperature, low residence time and have fast reaction rate. Sugars from pretreatment and hydrolysis step are fermented by yeast or bacteria to produce ethanol and carbon dioxide.

Table 1. 1. Various pre-treatment options in bioethanol processing

Pretreatment methods	Chemicals	Temperature /Pressure	Reaction time (min)	Xylose yield (%)	Downstream enzymatic effect
Dilute acid hydrolysis	Acid	>433 K	2-10	75-90	<85%
Alkaline hydrolysis	Base			60–75	55%
Uncatalyzed steam explosion		433–533 K	2	45–65	90%
Acid catalyzed steam explosion	Acid	433–493 K			88%
Ammonia fiber explosion	Ammonia	363 K	30		50–90%
CO_2 explosion	CO_2	56.2 bar			75%

1.2 Steam explosion

Among some pretreatment methods, steam explosion is one of the promising biomass fractionation processes. The process comprises steam explosion, liquid separation and hot water systems (180 to 240^0C) at high pressure (1 to 3.5 MPa) from several seconds to minutes, then the materials are suddenly depressurized.

According to Garrote *et al.* (1999) advantages of steam explosion processes compared to other pretreatment technologies include:

- No chemical are used
- Obtain good yield of hemicelluloses
- Reduce equipment corrosion due to a mild pH
- Avoid acid recycling and treatment

Nevertheless, several disadvantages of steam explosion include destruction of a portion of the xylan fraction to volatile compounds (mainly acetic, lactic and formic) (Chiaramonti *et al.* 2012), incomplete disruption of the lignin-carbohydrate matrix produced phenolic compounds (Kaar *et al.* 1998) and some by-products contains the derivatives from sugars (furfural and 5-hydroxy-methyfurfural (HMF)). These materials could have a negative effect on the following hydrolysis and fermentation steps (Davidsson 2013).

1.3 Characterization of wastewater from bioethanol processing

Bioethanol processing generates a lot of waste streams such as condensed pretreatment vapors, boiler and cooling tower blowdown streams, and filtered beer stillage (Steinwinder *et al.* 2011; Divya Ramchandran 2013). In general, the wastewater contains high concentrations of organic compounds (measured as COD, TOC and BOD). In addition, blow-down water has a large salt concentration due to evaporation and scaling.

The National Renewable Energy Laboratory (NREL) conducted a project to develop a process design for treating the wastewater from the cellulosic ethanol production process (Steinwinder *et al.* 2011). In this project, wastewater characterization from ethanol processing was found out. The sample was taken after ethanol distillation and removal of usable solids and analyzed by TestAmerica and Brown and Caldwell (BC) Treatability Laboratory in Nashville, Tennessee. Results are summarized in Table 1. 2.

Table 1. 2. Wastewater characterization from ethanol production using the cellulosic feedstock

Parameters	Units	TestAmerica	Brown and Caldwell
CBOD	mg/L	38,300	-
Soluble CBOD	mg/L	32,600	-
Total COD	mg/L	117,000	124,900
Soluble COD	mg/L	116,000	84,600
TOC	mg/L	32,800	-
TIC	mg/L	732	-
Total solids	mg/L	70,800	88,583
TVS	mg/L	71,300	76,750
TSS	mg/L	14,500	21,650
VSS	mg/L	12,800	19,650
TDS	mg/L	51,900	66,933
TDFS	mg/L	-	9,833
Ammonia-N	mg/L	1,060	-
Nitrate-N	mg/L	12	-
TKN	mg/L	4,950	-
Total P	mg/L	805	-
Ortho-P	mg/L	805	-
Acidity	mg/L	44	-
Hydroxide alkalinity	mg/L as $CaCO_3$	ND	-
Total alkalinity	mg/L as $CaCO_3$	-	2,750
Hardness	mg/L as $CaCO_3$	36	-
Sulfate	mg/L	5,600	4,400

Table 1.2. Wastewater characterization from ethanol production using the cellulosic feedstock (Continued)

Parameters	Units	TestAmerica	Brown and Caldwell
Sulfide	mg/L	ND	-
Sulfide dissolved	mg/L	36.6	-
Silica (SiO_2)	mg/L	1,580	-
Aluminum	mg/L	ND	-
Barium	mg/L	0.0147	-
Cadmium	mg/L	ND	-
Calcium	mg/L	6.79	-
Chromium	mg/L	0.177	-
Copper	mg/L	ND	-
Iron	mg/L	0.814	-
Lead	mg/L	ND	-
Magnesium	mg/L	4.63	-
Manganese	mg/L	0.0957	-
Potassium	mg/L	498	-
Chloride	mg/L	-	-
Sodium	mg/L	15.8	-
Strontium	mg/L	0.0863	-

ND: Non detected

1.4 High rate anaerobic process

The fermentation process in which organic materials are degraded and converted to biogas (methane and carbon dioxide) is termed as an anaerobic digestion. Comparing to aerobic processes some advantage and disadvantages of anaerobic processes are shown in Table 1. 3 (Tchobanoglous *et al.* 2003).

Table 1. 3. Advantages and disadvantages of anaerobic processes

Advantages	Less energy require
	Less biological sludge production
	Fewer nutrients required
	Methane production, a potential source
	Smaller reactor volume required
	With acclimation most organic compounds can be transformed
	Rapid response to substrate addition after long periods without feeding
Disadvantages	Longer start-up time to develop necessary biomass inventory
	May require alkalinity and/or specific ion addition
	May require further treatment with an aerobic treatment process to meet discharge requirements
	Biological nitrogen and phosphorus removal is not possible
	Much more sensitive to the adverse effect of lower temperatures on reaction rates
	May be more susceptible to upset due to toxic substances
	Potential for production of odors and corrosive gases

High-rate anaerobic treatment processes receive increasing interest due to their high organic loading rate (OLRs), low energy consumption, short hydraulic retention times (HRTs) and low sludge production (Rajesh Banu *et al.* 2006; Rajinikanth *et al.* 2009). Figure 1. 3 shows the increase gradually in the number of anaerobic high-rate reactors from 1972 to 2006 (Lier *et al.* 2008).

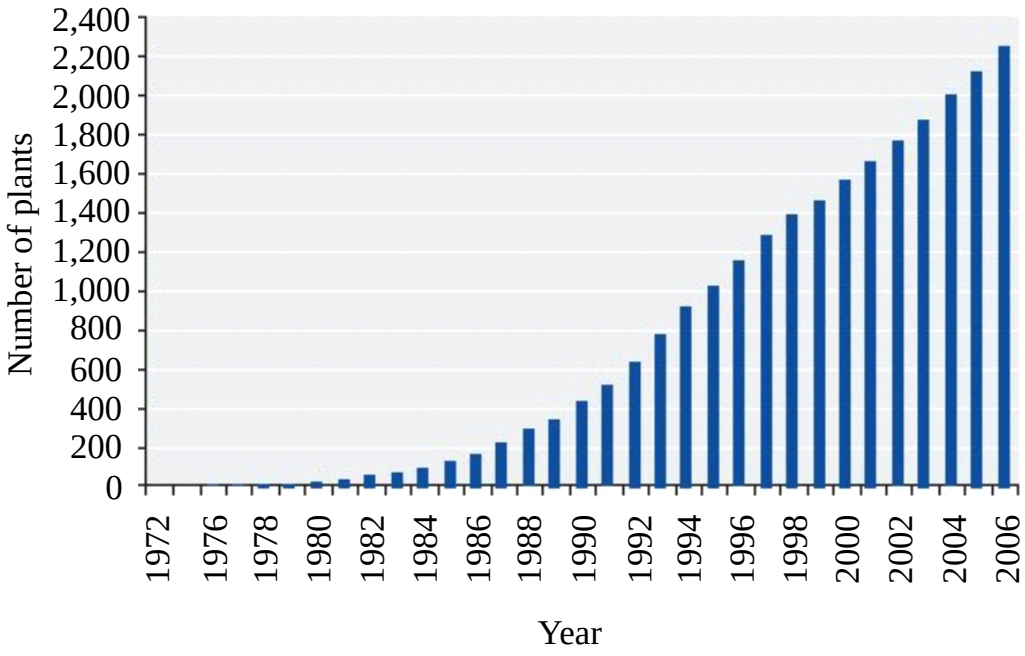

Figure 1. 3. Increase in number of worldwide installed anaerobic high-rate reactors in the period 1972-2006

High-rate anaerobic treatment processes are rapidly becoming popular for industrial wastewater treatment. Table 1. 4 shows anaerobic treatment applications for different industrial wastewaters. The technologies applied high-rate anaerobic digestion include: upflow fixed-bed reactors, upflow anaerobic sludge blanket (UASB), moving-bed biofilm reactor (Mannina & Viviani 2009; Bélafi-Bakó 2010), expanded granular sludge beds (EGSB), sequencing batch reactors and anaerobic hybrid/hybrid upflow anaerobic sludge blanket reactors (Chong *et al.* 2012).

Table 1. 4. Anaerobic treatment applications for different industrial wastewaters

Wastewater type	Reactor type/Operating temperature (^{0}C)	Capacity (m^3)	OLR (kg-COD/m^3/day)	COD removal (%)	Methane yield (m^3/kg-COD)	Reference
Pulp and paper	Baffled/35	0.01	5	60	0.141-0.178	(Grover *et al.* 1999)
Pulp and paper	Anaerobic contact/-	-	-	80	0.34	(Rajeshwari *et al.* 2000)
Slaughterhouse	UASB/-	450	2.1	80	-	(Del Nery *et al.* 2001)
Slaughterhouse	AF/-	21	2.3	85	-	(Johns 1995)
Cheese whey	Baffled/35	0.015	-	94-99	0.31	(Antonopoulou *et al.* 2008)
Cheese whey	Upflow filter/35	0.00536	-	95	0.55 (biogas)	(Orhon *et al.* 1999)
Textile	UASB/35	0.00125	-	>90	-	(Somasiri *et al.* 2008)
Textile	Fluidized bed/35	0.004	3	82	-	(Şen & Demirer 2003)
Coffee	Hybrid (UASB+AF)/ 23	10.5	1.89	77.2	-	(Bello-Mendoza & Castillo-Rivera 1998)
Coffee	UASB/35	0.005	10	78	0.29	(Dinsdale *et al.* 1997)

Table 1.4. Anaerobic treatment applications for different industrial wastewaters (Continued)

Wastewater type	Reactor type/Operating temperature (^{0}C)	Capacity (m^3)	OLR (kg-COD/m^3/day)	COD removal (%)	Methane yield (m^3/kg-COD)	Reference
Brewery	Sequencing batch/33	0.045	1.5-5	>90	0.326	(Shao *et al.* 2008)
Brewery	AF/34-39	5.8	8	96	0.15	(Leal *et al.* 1998)
Sugar mill	UASB/33-36	0.05	16	>90	0.355	(Nacheva *et al.* 2009)
Sugar mill	Fixed bed/32-34	0.06	10	90	-	(Farhadian *et al.* 2007)

1.4.1 Fixed-bed reactor

Fixed-bed reactor is a relatively simple technology compared to fluidized bed reactors. The process offers the advantages of high-load systems, less volume, space and hence less investment. Moreover, in the system biomass can retain and attach to the support materials and help avoid the loss of biomass from the reactor (Rajinikanth *et al.* 2009; Ganesh *et al.* 2010). As the results, the process is very stable and resistant to stress such as overloading of organic or changes in pH and temperature. The performance of fixed-bed reactor much depends on characteristics of the support materials including porosity, surface area, roughness and chemical composition (Show & Tay 1999; Ganesh *et al.* 2010). Many researches focused on the effect of various packing materials (*e.g.*

polyurethane, clay brick, granular activated carbon (GAC), polyvinyl chloride (PVC) plastic media) on COD reduction (Goyal *et al.* 1996; Vijayaraghavan & Ramanujam 2000).

Fix-bed reactor was applied to treat agro-food industrial wastewater for many years. Ganesh *et al.* (2010) investigated the treatment of winery wastewater in upflow anaerobic fixed-bed reactors with different size and specific surface area of support materials. This study showed that the treatment efficiency increased with decrease in size and increase in specific surface area of the support media. In addition, the biomass accumulation in the reactor was defined as a function of specific surface area and size of the support medium. Nikolaeva *et al.* (2009) used waste tire rubber and zeolite as microorganism immobilization supports to treat screened dairy manure. This research proved that the combined support materials were more effective and increased the maximum methane yield.

Recently, biofilm reactors have paid more attention, especially for treatment of wastewaters containing bio-recalcitrant, inhibitory and toxic substances (Bajaj *et al.* 2008; Farhadian *et al.* 2008). However, after bio-treatment the post-treatment need to added to obtain the discharge standards for organic matters, nutrients (ammonia and phosphorus) and pathogens (Rajinikanth *et al.* 2009).

1.4.2 Upflow anaerobic sludge blanket (UASB)

Upflow anaerobic sludge blanket (UASB) is the most popular high rate process and developed by Lettinga and his co-workers in Holland in the early 1970's. The UASB

reactor consists four parts: sludge bed (layer of biomass settled at the bottom of the reactor), sludge blanket (a suspension of sludge particles), gas–solids separator (GSS) and settlement part.

This system has been utilized for anaerobic treatment of various types of industrial wastewaters (Syutsubo *et al.* 1997; Akunna & Clark 2000). Goodwin and Stuart (1994) applied UASB reactor to treat a liquid waste-product from the malt whisky industry with the COD treatment efficiency of 90%. The maximum volumetric loading rate can reach to 15 kg-COD/m^3/d at stable condition. Hampannavar (2010) studied about sugar industry wastewater in an UASB reactor. This research showed that sugar industry wastewater can be treated at maximum loading of 16 kg-COD/m^3/ d at low HRT of 6 and maximum COD removal efficiency of 89.4%.

Garcia *et al.* (2008) listed various factors affecting the treatment efficiency of UASB reactors including temperature, wastewater composition, mixing, pH, organic loading rate and toxicity. Rajagopal *et al.* (2010) mentioned that excessive granulation phenomena in high loaded anaerobic reactors can washed out biomass from the reactor with the effluent, causing digester instability. Other problems such as flotation and disintegration of granular sludge, sludge bulking and deterioration of performance at low temperatures could be happened in the long start-up period (Mahmoud 2008; Lew *et al.* 2011).

Although most of the practical UASB systems are operated under mesophilic conditions, thermophilic operation has higher treatment efficiency. Wiegant et al. (1985) reported the cultivation of thermophilic sludge on sucrose as the seed materials. The system obtained

high COD loading (86.4 kg/m^3/d) and 60% COD removal efficiency. In another study, Harada et al. (1996) showed 39–67% COD removal and over 80% BOD removal in a thermophilic UASB reactor. The results suggested that the wastewater contained high concentration of recalcitrant compounds could affected to biomass concentration in the reactor.

1.5 Post-treatment of wastewater containing lignin

Wastewater from some industries such as pulp and paper mill, palm oil mill, textile and bioethanol processing are characterized by dark color due to the presence of plant component (*e.g.* dyes, inorganic pigments, lignin, tannin) as well as its biodegradation product (*e.g.* melanoidin) (Anjaneyulu *et al.* 2005). Table 1. 5 presents the color concentrations limits of wastewater generated from some industries.

Table 1. 5. Color concentrations limits of wastewater generated from some industries

Industry	Color concentration (Hazen unit)	Color limits from USPHS (Hazen unit)	Reference
Sugar	150-200	5-10	(Cartier *et al.* 1997)
Pulp and paper	100-600	0-10	(Ali & Sreekrishnan 2001)
Textile	1100-1300	0-25	(Correia *et al.* 1994)
Brewery	200-300	5-10	(Pedro Silva *et al.* 2004)

USPHS: United States Public Health Services

Due to the recalcitrant properties, colored compounds especially lignin (biodegradability index <0.02) (Kallas 2006) can also contribute to the failure of biological processes in wastewater treatment plants (Y. Zahrim & Rajin 2014). Lignin is the nature's most abundant aromatic (phenolic) polymer (Suhas *et al.* 2007) as well as a natural polymeric product from an enzyme initiated dehydrogenative polymerization of the three primary

precursors (Boeriu *et al.* 2004; Chakar & Ragauskas 2004). Figure 1. 4 shows the possible structure of lignin (Essington 2003). The available physico-chemical techniques for removing lignin including membrane filtration, adsorption, coagulation/flocculation and advanced oxidation processes (AOPs) (Andersson *et al.* 2011; Shankar *et al.* 2013; Abu Zahrim Yaser 2014).

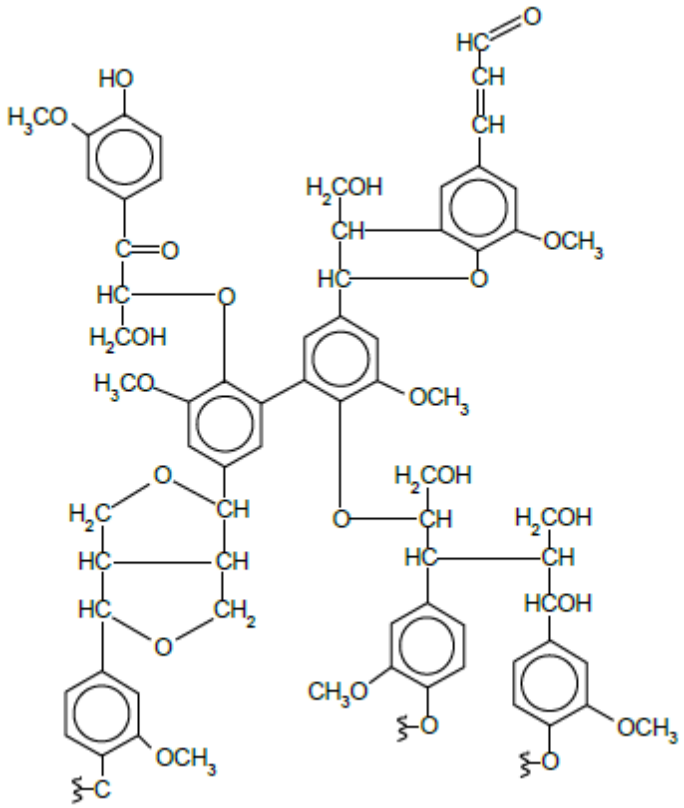

Figure 1. 4. Possible structure of lignin

1.5.1 Oxidation process

Oxidation process changes structure and chemical properties of the organic substances as well as break down the big molecules to smaller fractions. Some oxidants were used to remove lignin from wastewater such as ozone (O_3), hydrogen peroxide (H_2O_2),

permanganate (MnO_4), chloride dioxide (ClO_2), chlorine (Cl_2) or (HOCl), oxygen (O_2) and $OH^{\bullet}$ radical. Some of the important applications of oxidation process in wastewater treatment are summarized in Table 1. 6 (Tchobanoglous *et al.* 2003).

Table 1. 6. Typical application of oxidation process in wastewater treatment

Application	Chemical used	Remarks
Grease removal	Cl_2	Added before pre-aeration
BOD reduction	Cl_2, O_3	Oxidation of organic substances
Ferrous sulfate oxidation	Cl_2	Production of ferric sulfate and ferric chloride
Filter-ponding control	Cl_2	Maintaining residual at filter nozzles
Filter-fly control	Cl_2	Maintaining residual at filter nozzles during fly season
Sludge-bulking control	Cl_2, H_2O_2, O_3	Temporary control measure
Control of filamentous microorganisms	Cl_2	Dilute chlorine solution sprayed on foam caused by filamentous organisms
Digester supernatant oxidation	Cl_2	
Digester foaming control	Cl_2	
Ammonia oxidation	Cl_2	Conversion of ammonia to nitrogen gas
Odor control	Cl_2, H_2O_2, O_3	
Oxidation of refractory organic compounds	O_3	

Oxidation process was used to reduce the concentration of residual organics, control odors, remove ammonia, improve the treatability of nonbiodegradable (refractory) organic compounds and eliminate the inhibitory effects of certain organic and inorganic compounds to microbial growth.

1.5.2 Coagulation and Flocculation process

Coagulation and flocculation involves the addition of chemicals (positively charged ion of metal salt or catalytic polyelectrolyte) to alter the physical state of dissolved and suspended solids to facilitate their removal via a subsequent sedimentation process (Alexander *et al.* 2012). Coagulation is generally defined as the destabilization of suspension, allowing particle collision and growth of flocculants. On the other hand, flocculation describes the process in which the destabilized particles are agglomerated to form larger aggregates (Bratby 2006; Gregory 2006). Finally, the flocs are settled and removed as sludge while supernatant is transferred into subsequent treatment process or discharged into a waterbody (Teh *et al.* 2016). Since lignin particles has negative charge in water, the mechanisms of lignin removal could include charge neutralization, complex chemical reactions/chelation-precipitation, adsorption-precipitation, sweep coagulation, electrostatic patch etc (Abu Zahrim Yaser 2014). Some coagulants used to treat wastewater containing lignin are shown in Table 1. 7.

Table 1. 7. Coagulants used to treat wastewater containing lignin

Industry	Metal	Polymer	Operating condition			Other removal (%)	Lignin removal (%)	Reference
			pH	Dosage (mg/L)	Temp (^{0}C)			
Pulp & paper mill	Aluminium sulfate	-	7	30		-	88	(Bese 2001)
Pulp & paper mill	Ferric chloride + Aluminium sulfate	-	3	$FeCl_3$: 799.97 $AlCl_3$: 800.04		COD: 18 TSS: 49 Color: 48	-	(Irfan *et al.* 2013)
Kraft pulp mill (washing water)	Sodium	-	9	22989.80-114949	25	-	66.7-75	(Sundin & massateknik 2000)
	Calcium	-	9	200.39-2805.46	25	-	66.7-75	
	Magnesium	-	11	680.54-729.15	25	-	77.8-87.5	
	Aluminium	-	9	134.91-1888.71	25	-	73.3-77.5	
Sugar mill	-	PAC	3	300	-	COD: 80	-	(Srivastava *et al.* 2005)
Oily	-	PZSS + APAM	2	Zn/Si ratio: 1-1.5	Ambient	COD: superior TSS: 95 Turbidity: 96.3	-	(Zeng & Park 2009)
Paper and pulp	-	Polydadmac + PAM	-	Polydadmac: 1.2 PAM: 2	Ambient	COD: 98 TSS: 96.8	71.7	(Ariffin *et al.* 2012)
Pulp mill	-	Acrylamide + Starch + DMC	8.35	22.3 and 22.3	Ambient	Turbidity: 95.7	83.4	(Wang *et al.* 2009a)

APAM: Anionic Polyacrylamide

PZSS: Poly-Zinc-Silicate-Sulfate

DMC: 2- methyarcyloyloxyethyl trimethyl ammonium chloride

1.5.3 Adsorption process

Adsorption is a mass transfer process which involves the accumulation of substances at the interface of two phases, such as, liquid–liquid, gas–liquid, gas–solid, or liquid–solid interface. The substance being adsorbed is the adsorbate and the adsorbing material is termed the adsorbent. The properties of adsorbates and adsorbents are quite specific and depend upon their constituents. The constituents of adsorbents are mainly responsible for the removal of any particular pollutants from wastewater (Khattri & Singh 2009). The fundamental concept in adsorption process is that called as the adsorption isotherm. It is the equilibrium relation between the quantity of the adsorbed material and the pressure or concentration in the bulk fluid phase at constant temperature (Da˛browski 2001). Some adsorbents from different wastes used to remove the pollutants in aqueous solutions are shown in Table 1. 8.

Table 1. 8. Some adsorbents from different wastes used to remove the pollutants in aqueous solutions

Adsorbent	Adsorbate	Reference
Rice husk	Cd(II)	(Kumar & Bandyopadhyay 2006)
Rice husk ash	Methylene blue	(Chandrasekhar & Pramada 2006)
Bael fruit shell	Cr (VI)	(Anandkumar & Mandal 2009)
Tea waste	Cu, Pb	(Amarasinghe & Williams 2007)
Hazelnut shell	Ni (II)	(Demirbaş *et al.* 2002)
Sugar cane bagasse	PAHs	(Crisafully *et al.* 2008)
Carbon slurry of fertilizer industry	Ethyl orange, Metanil yellow, Acid blue 113	(Jain *et al.* 2003)
Clarified sludge	Cr(VI)	(Bhattacharya *et al.* 2008)
Raw fly ash	Methylene blue	(Wang *et al.* 2005)
Fly ash	As (V)	(Li *et al.* 2009)

1.6 Anaerobic Digestion Model No.1 (ADM1) and Activated Sludge Models (ASMs)

Anaerobic Digestion Model No.1 (ADM1) (Batstone *et al.* 2002) and Activated Sludge Models (ASMs) (Henze *et al.* 2000) were presented by task groups at International Water Association (IWA) and some of the most implemented mathematical models in many sectors. ASMs describe an activated sludge system with organic oxidation, biological phosphorus removal processes, nitrification and denitrification. In particular, ASM1 was constructed and incorporated into a basic model for COD removal, oxygen demand, bacterial growth and biomass degradation. Figure 1. 5 and Table 1. 9 show an example of process map, process kinetics and stoichiometry for heterotrophic bacterial growth in an aerobic environment.

On the other hand, in ADM1 the degradation of organic compounds is assumed to be divided into the following steps: (1) disintegration of homogenous particles to carbohydrates, proteins and lipids, (2) hydrolysis of the complex organic molecules to monomers as sugars, amino acids and long-chain fatty acids, (3) acidogenesis, (4) acetogenesis and (5) methanogenesis. Acidogenesis and acetogenesis include the dynamics of the volatile fatty acids (VFAs) acetate, propionate, butyrate and valerate. Ultimately, acetate and hydrogen compounds are utilized by the methanogens and converted into methane. In ADM1 there are 24 different components including 7 types of biomass that degrade 8 different components (long chain fatty acids, amino acids, sugars, valerate and butyrate, propionate, acetate and hydrogen). An overview of the structure and biochemical processes in ADM1 is addressed in Figure 1. 6, Table 1. 10 and Table 1.

11 (Batstone *et al.* 2002).

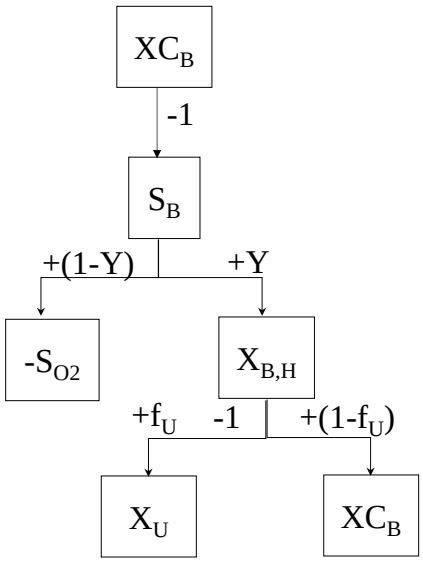

XC_B: Slowly biodegradable substrate

S_B: Biodegradable substrate

S_{O2}: Oxygen

$X_{B,H}$: active heterotroph concentration

X_U: Un-biodegradable particulate concentration

Y: Growth yield

fu: Production of inert materials

Figure 1. 5. Process map of the ASM models

Table 1. 9. Process kinetics and stoichiometry for heterotrophic bacterial growth in an aerobic environment

Component→	i	1	2	3	Process Rate, ρ_j
j process ↓		X_B	S_B	S_{O2}	$[ML^{-3}T^{-1}]$
1 Growth		1	-1/Y	-(1-Y)/Y	$\frac{\mu_{max} S_B}{K_S + S_B} X_B$
2 Decay		-1		-1	bX_B
Stoichiometric parameters: Y: True growth yield		Biomass [M(COD)L^{-3}]	Substrate [M(COD)L^{-3}]	Oxygen (negative COD) [M(-COD)L^{-3}]	Kinetic parameter: μ_{max}: Maximum specific growth rate K_S: Half-saturation coefficient. b:Decay rate (d^{-1})

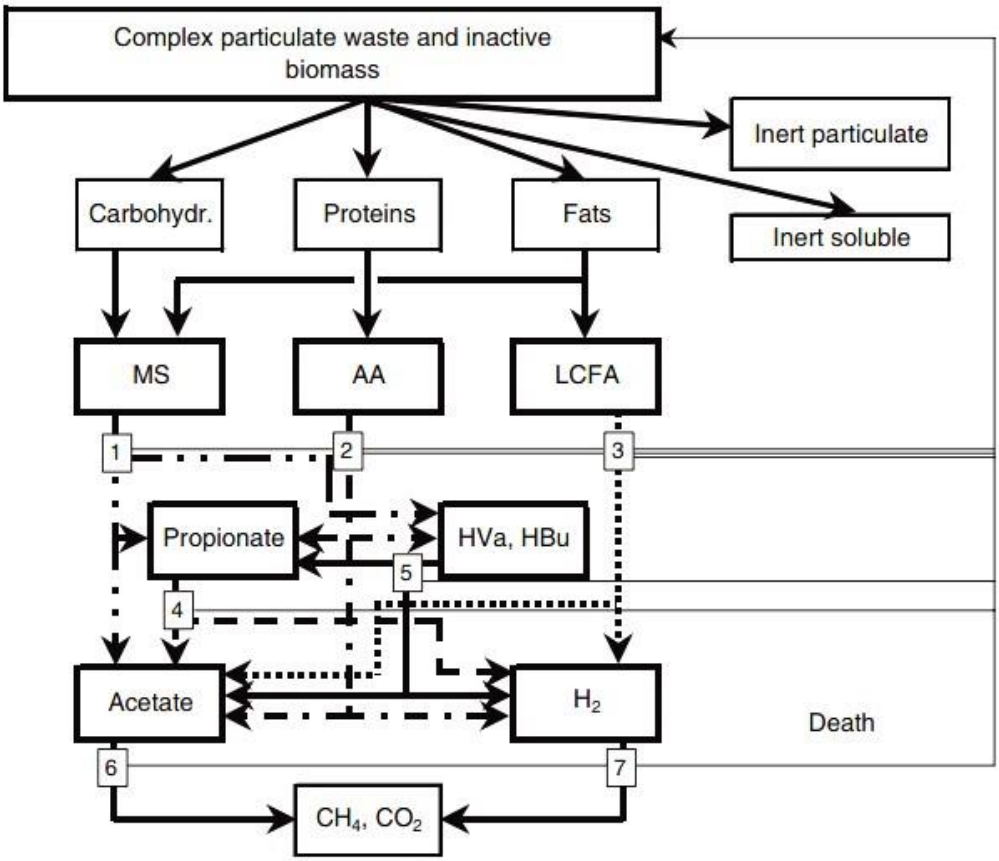

Figure 1. 6. The anaerobic model as implemented including biochemical processes

(1) acidogenesis from sugars; (2) acidogenesis from amino acids, (3) acetogenesis from LCFA, (4) acetogenesis from propionate, (5) acetogenesis from butyrate and valerate, (6) acetoclastic methanogenesis and (7) hydrogenotrophic methanogenesis

Table 1. 10. Biochemical rate coefficients and rate expressions for soluble components

#	Process/state variable	S_{su}	S_{aa}	S_{fa}	S_{va}	S_{bu}	S_{pro}	S_{ac}	S_{h2}	S_{ch4}	S_{IN}	S_I	Rate expressions
r1	Disintegration											$f_{sI,xc}$	First-order type
r2	Hydrolysis of carbohydrate	1											First-order type
r3	Hydrolysis of proteins		1										First-order type
r4	Hydrolysis of lipids	$1-f_{fa,li}$		$f_{fa,li}$									First-order type
r5	Uptake of sugars	-1				(1-Y) $*f_{bu,su}$	(1-Y) $* f_{pro,su}$	(1-Y) $* f_{ac,su}$	(1-Y) $* f_{h2,su}$		-(Y) $*N_{bac}$		Monod type
r6	Uptake of amino acids		-1		(1-Y) $*f_{va,aa}$	(1-Y) $*f_{bu,aa}$	(1-Y) $*f_{pro,aa}$	(1-Y) $*f_{ac,aa}$	(1-Y) $*f_{h2,aa}$		N_{aa}- (Y)$*N_{bac}$		Monod type
r7	Uptake of LCFA			-1				(1-Y) *0.7	(1-Y) *0.3		-(Y) $*N_{bac}$		Monod type
r8	Uptake of valerate				-1		(1-Y) *0.54	(1-Y) *0.31	(1-Y) *0.15		-(Y) $*N_{bac}$		Monod type
r9	Uptake of butyrate					-1		(1-Y) *0.8	(1-Y) *0.2		-(Y) $*N_{bac}$		Monod type
r10	Uptake of propionate						-1	(1-Y) *0.57	(1-Y) *0.43		-(Y) $*N_{bac}$		Monod type
r11	Uptake of acetate							-1		(1-Y)			Monod type
r12	Uptake of hydrogen								-1	(1-Y)			Monod type
r13	Decay of X_{su}												First-order type
r14	Decay of X_{aa}												First-order type
r15	Decay of X_{fa}												First-order type
r16	Decay of X_{c4}												First-order type
r17	Decay of X_{pro}												First-order type
r18	Decay of X_{ac}												First-order type
r19	Decay of X_{h2}												First-order type
$f_{bu,su}$: butyrate from sugars $f_{pro,su}$: propionate from sugars $f_{ace,su}$: acetate from sugars $f_{h2,su}$: hydrogen from sugars $f_{va,aa}$: valerate from amino acids $f_{bu,aa}$: butyrate from amino acids	$f_{pro,aa}$: propionate from amino acids $f_{ac,aa}$: acetate from amino acids $f_{h2,aa}$: hydrogen from amino acids	Monosaccharides (kgCOD/m^3)	Amino acid (kgCOD/m^3)	Long chain fatty acids (kgCOD/m^3)	Total valerate (kgCOD/m^3)	Total butyrate (kgCOD/m^3)	Total propionate (kgCOD/m^3)	Total acetate (kgCOD/m^3)	Hydrogen (kgCOD/m^3)	Methane gas (kgCOD/m^3)	Inorganic nitrogen (kmoleN/m^3)	Soluble inerts (kgCOD/m^3)	N_{aa}: nitrogen in amino acids and proteins (gN/gCOD) N_{bac}: nitrogen in bacteria(gN/gCOD)

Table 1. 11. Biochemical rate coefficients and rate expressions for particulate components

#	Process/state variable	X_c	X_{ch}	X_{pr}	X_{li}	X_{su}	X_{aa}	X_{fa}	X_{c4}	X_{pro}	X_{ac}	X_{h2}	X_I	Rate expressions
r1	Disintegration	-1	$f_{ch,xc}$	$f_{pr,xc}$	$f_{li,xc}$								$f_{xI,xc}$	First-order type
r2	Hydrolysis of carbohydrate		-1											First-order type
r3	Hydrolysis of proteins			-1										First-order type
r4	Hydrolysis of lipids				-1									First-order type
r5	Uptake of sugars					Y								Monod type
r6	Uptake of amino acids						Y							Monod type
r7	Uptake of LCFA							Y						Monod type
r8	Uptake of valerate								Y					Monod type
r9	Uptake of butyrate								Y					Monod type
r10	Uptake of propionate									Y				Monod type
r11	Uptake of acetate										Y			Monod type
r12	Uptake of hydrogen											Y		Monod type
r13	Decay of X_{su}	1				-1								First-order type
r14	Decay of X_{aa}	1					-1							First-order type
r15	Decay of X_{fa}	1						-1						First-order type
r16	Decay of X_{c4}	1							-1					First-order type
r17	Decay of X_{pro}	1								-1				First-order type
r18	Decay of X_{ac}	1									-1			First-order type
r19	Decay of X_{h2}	1										-1		First-order type
Y: yield $f_{sI,xc}$: soluble inerts from composites $f_{xI,xc}$: particulates inerts from composites $f_{fa,li}$: fatty acids form lipids $f_{ch,xc}$: carbohydrates from composites $f_{pr,xc}$: proteins from composites $f_{li,xc}$: lipids from composites			Monosaccharides ($kgCOD/m^3$)	Amino acid ($kgCOD/m^3$)	Long chain fatty acids ($kgCOD/m^3$)	Total valerate ($kgCOD/m^3$)	Total butyrate ($kgCOD/m^3$)	Total propionate ($kgCOD/m^3$)	Total acetate ($kgCOD/m^3$)	Hydrogen ($kgCOD/m^3$)	Methane gas ($kgCOD/m^3$)	Inorganic nitrogen ($kmoleN/m^3$)	Soluble inerts ($kgCOD/m^3$)	

1.7 Research Objectives

For the industrial commercialization, apart from the bioethanol processing system, it is also essential to develop proper treatment systems for the liquid wastes generated from the steam explosion process. In this regard, high-rate anaerobic biological treatments are also paid attention as the processes produce methane gas which can be used for the heat source to convert the steam (Zheng et al. 2014).

However, anaerobic digestion systems are complex processes that unfortunately often suffer from instability because of the inhibition of VFAs on methanogenesis (Mechichi & Sayadi 2005). In order to be able to design, optimize and operate efficiently anaerobic digestion systems, appropriate control strategies as mathematical model approach need to be developed. Although, many researches applied mathematical models to simulate this phenomena but the limitation of these models is that the inhibition is assumed on the microbial growth stages while acceleration of the decay by inhibitory materials is not considered.

On the other hand, technical information for the biological degradability of the liquid waste organics is still limited at present, and consequently conservative low-loaded anaerobic plants are often suggested (Steinwinder et al. 2011).

In addition, one of the challenges of steam explosion wastewater treatment generated from bioethanol processing is the existence of the recalcitrant compounds (lignin) can contribute to the failure of biological processes. Therefore, additional treatments with physico-chemical methods before/after anaerobic digestion to remove lignin need to be integrated into the treatment systems.

The objectives of this study are as follows:

1. To examine the irreversible inhibition in decay stage.
2. To build a new model for anaerobic biological degradation of the organics in steam explosion wastewater from bioethanol processing.
3. To evaluate the performance of high-rate reactors (fixed-bed reactor and upward

anaerobic sludge blanket reactor).

4. To remove lignin and color from wastewater by using the oxidation, coagulation/flocculation and adsorption methods.

The thesis content was composed by 6 chapters.

In chapter 1, the research background is introduced to identify the research objectives. Existing researches about anaerobic treatment, post-treatment of wastewater from bioethanol processing as well as inhibition mathematical models are reviewed in chapter 2. Chapter 3 discusses about the irreversible inhibition in decay stage. Next, an experiment was conducted to model the anaerobic degradation of steam explosion wastewater obtained from sugar cane bagasse in chapter 4. This model was developed with a modification of ADM1 and ASMs. In chapter 5, the performance of high-rate reactors (fixed-bed reactor and upward anaerobic sludge blanket reactor) for steam explosion wastewater treatment was evaluated. Chapter 6 states about physico-chemical methods (oxidation, coagulation/flocculation and adsorption) to remove un-degradable materials from the effluent after anaerobic biological treatment. Finally, the research is summarized in chapter 7.

Chapter 2. Existing researches

2.1 Brief introduction

One of the great challenges of ethanol production is the use of all wastes (both liquid and solid) left over from the process to reduce the environmental impact of the bioethanol process and in order to utilize the energy content in an effective way. Most the liquid residuals has a high organic strength and high nutrients. Therefore, one of the solutions for the use of these wastes is biogas production, which can be a sustainable method for the removal of organic matters from effluents (Zheng *et al.* 2014).

However, in high-rate methane fermentation system the operational failure often occurs due to the inhibition of VFAs on methanogenesis. Many studies used ADM1 to simulate the responses of organic wastes in anaerobic digestion (Kalfas *et al.* 2006; Boubaker & Ridha 2008; Derbal *et al.* 2009; Gali *et al.* 2009). The problem of the model is that the inhibition is only consider on the microbial growth stages (Fukuzaki *et al.* 1990; Siegrist *et al.* 2002; Fezzani & Cheikh 2008) while acceleration of the decay by inhibitory materials is an independent phenomena.

On the other hand, even though biological treatment results in significant COD removal, the effluent still retains high concentration of undegradable materials and the dark brown color (B. Inanc 1999). The color is hardly degraded by the conventional treatments and can even be increased during anaerobic treatments, due to the repolymerization of compounds (Peña *et al.* 2003). Therefore, various physico-chemical treatment methods were explored to remove lignin as well as color from wastewater.

2.2 Anaerobic wastewater treatment from bioethanol processing

Wastewater treatment by anaerobic digestion could be beneficial both economically and environmentally. Anaerobic digestion is a well-known process for sludge reduction and industrial wastewater treatment in many years. In the process, microorganisms convert organic matters to biogas. Recently, utilizing waste from bioethanol process for biogas production through anaerobic digestion are more concern. The proper combination of bioethanol and biogas production processes has been considered as a suitable strategy to enhance the competitiveness of fermentation plants, by producing both ethanol and biogas in a biorefinery concept. Such strategy promotes the utilization of waste from different bio-industries for the input of next treatment (Martin *et al.* 2014; Parajuli *et al.* 2015). The performance of various anaerobic reactors for wastewater treatment from bioethanol processing is summarizes in Table 2. 1.

Table 2. 1. Performance of various anaerobic reactors for wastewater treatment from bioethanol processing

Reactor type	COD loading (kg-COD/m^3/day)	HRT (days)	% COD removal	% BOD removal	References
UASB	15	2.1	90		(Goodwin & Stuart 1994)
UASB	18		>90		(B. Wolmarans 2002)
Thermophilic UASB	Up to 28		39-67	>80	(Harada *et al.* 1996)
Thermophilic UASB	Up to 30	0.3	87		(Syutsubo *et al.* 1997)
Two-stage anaerobic treatment Anaerobic filter UASB	 2.5-5.1 0.6-2.5	 10-19 20-39	 54 93		(Blonskaja *et al.* 2003)
Two-phase thermophilic process Acidogenesis Methanogenesis	4.6-20	 2 15.2	65	85	(Yeoh 1997)
Diphasic (upflow) fixed film reactor (clay brick granules support)	22	3	71.8		(R. Seth 1995)
Diphasic (upflow) fixed film reactor (granular activated carbon support)	21.3	4	67.1		(Goyal *et al.* 1996)
Upflow anaerobic filter (UAF)	20		76		(Tokuda *et al.* 1999)
Downflow fluidized bed reactor with ground perlite	4.5	3.3-1.3	85		(Garcia-Calderon *et al.* 1998)
Anaerobic contact filter (in series)		4	73-98		(Vijayaraghavan & Ramanujam 2000)
Granular bed anaerobic baffled reactor (GRABBR)	4.75		82-90	90	(Akunna & Clark 2000)

Choeisai *et al.* (2014) was conducted a study to evaluate bioethanol wastewater treatment system from a sugar cane molasses. Combining two-phase treatment system including pretreatment unit (a sulfate reducing (SR) tank and multistage UASB reactor (MS-UASB)) and post-treatment unit (UASB and down-flow hanging sponge (DHS)).Temperature was kept in the range of 24.6-29.6^{0}C with HRT of 25 hours and 23 hours for each unit. After 300 days of operation, COD removal efficiency for whole system reached to 74%. The SR reduced SO_4^{2-} completely while the MS-UASB converted 96% COD to methane and 18.7% organic compounds was removed from the UASB and DSH. In addition, 27% TN and 45% TKN removal were obtained in the DHS.

Narra and Balasubramanian (2015) utilized waste generated from ethanol fermentation processes for biogas production through anaerobic digestion. Liquid fraction and solid residues were collected after alkali pretreatment, enzyme production and enzymatic hydrolysis, respectively. Two kinds of conditions including thermophilic and mesophilic temperatures were applied for this study. Solid state bioreactor was used for solid treatment while anaerobic hybrid reactors (AHRs) was set up for liquid treatment. For solid residues treatment, thermophilic digesters had higher biogas yield (131 L) than mesophilic digesters (84 L). Whereas AHRs showed better COD removal efficiency and methane yield for wastewater treatment.

Torry-Smith *et al.* (2003) and Uellendahl and Ahring (2010) studied about biorefinery concept for the production of both second generation ethanol and biogas. The process included: pretreatment of lignocellulosic substrate, enzymatic hydrolysis, fermentation of C6 sugars and lignin separation and fermentation of C5 sugars into ethanol. The output stream from ethanol production became the input flow for an anaerobic process performed in an UASB reactor. The studies were conducted at mesophilic and thermophilic conditions. Results showed that with applying the proposed biorefinery concept about 30% higher carbon utilization compared to a system with only bioethanol production. Higher process efficiency could be attained when removing suspended solids from the input stream before going to the UASB reactor.

2.3 Inhibition model

2.3.1 Reversible inhibition

Anaerobic digestion systems are rather complex processes that operation failure may occur due to some reasons. It could be overloading, entry of an inhibitor or inadequate temperature control. As the results, some phenomena such as a drop in the methane production rate, a drop in the pH, a rise in the volatile fatty acid (VFA) concentration are observed.

To predict the anaerobic system failure, inhibition functions was included in the models. Inhibition forms are shown in Table 2. 2 with reversible form, direct impact of the inhibitor on the microbial yield and decay, two empirical forms, competitive uptake and secondary substrate (Batstone *et al.* 2002). Due to the variation of inhibition forms in anaerobic digestion, Equation 1 is considered as the normal expression for addition of inhibition terms.

$$\rho_j = \frac{k_m S}{K_S + S} X . I_1 . I_2 \ldots I_n \qquad \text{Equation 1}$$

Where the first part of the equation is the uninhibited Monod-type uptake (k_m: Monod maximum specific uptake rate, K_S: Half saturation value) and $I_{1\ldots n}$ = f($S_{I,1\ldots n}$) are the inhibition functions.

Although, many researches applied ADM1 equipped with inhibition function (as listed in Table 2. 2) to simulate the dynamic response in anaerobic digesters, one potential limitation of the model is that the inhibition is only assumed on the microbial growth stages (Fukuzaki *et al.* 1990; Siegrist *et al.* 2002; Fezzani & Cheikh 2008).

Table 2. 2. Inhibition forms

	Description	Equation	Used for
(a)	Noncompetitive inhibition	$I = \frac{1}{1+S_I/K_I}$	Free ammonia and hydrogen inhibition
	Uncompetitive	$\rho_j = \frac{k_m XS}{K_S + S(1+\frac{K_I}{S_I})}$	Not used
	Competitive	$\rho_j = \frac{k_m XS}{K_S\left(1+\frac{K_I}{S_I}\right)+S}$	Not used
(b)	Reduction in yield increased biological decay rate	$Y = f(S_I)$	Not used
		$k_{dec} = f(S_I)$	Not used
(c)	Empirical upper and lower inhibition	$I = \frac{1+2x10^{0.5(pH_{LL}-pH_{UL})}}{1+10^{(pH-pH_{UL})}+10^{(pH_{LL}-pH)}}$	pH inhibition when both high and low pH inhibition occurs
	Empirical lower inhibition only	$I = \exp\left(-3\left(\frac{pH-pH_{UL}}{pH_{UL}-pH_{LL}}\right)^2\right)\Big\vert_{pH<pH_{UL}}$ $I=1\vert_{pH>pH_{UL}}$	pH inhibition when only low pH inhibition occurs
(d)	Competitive uptake	$I = \frac{1}{1+S_I/S}$	Butyrate and valerate competition for C_4
(e)	Secondary substrate	$I = \frac{1}{1+K_I/S_I}$	All uptake to inhibit uptake when $S_{IN} \sim 0$

Nomenclature: K_I = inhibition parameter; ρ_j = rate for process j; S = substrate for process j; S_I = inhibitor concentration; X = biomass for process j

Fezzani and Cheikh (2008) was applied the inhibition function for TVFA (Equation 2) in the uptake of acetate in the modified ADM1

$$I_{TVFA} = \frac{1}{1+S_{TVFA}/K_{I,TVFA}} \qquad \text{Equation 2}$$

Equation 2 was included to consider and predict effectively the inhibition of methanogenic process by high TVFA concentration.

This model could simulate reasonably gas flows, methane and carbon dioxide contents, pH and TVFA with all influent concentrations (43, 67 and 130 g-COD/l) at the HRTs of 24 and 36 days. In addition, the reactor failure at HRTs of 12 days was also predicted and well justified.

A mathematical model with some inhibition terms is developed by (Siegrist *et al.* 2002) to describe the dynamic behavior of mesophilic (35 ± 5^0C) and thermophilic digestion (55 ± 5^0C). In this model, inhibition function by hydrogen and acetate for the anaerobic oxidation of LCFA and propionate, inhibition functions for low pH conditions and inhibition term due to free ammonia for acetotrophic methanogenesis and propionate degradation was taken into account.

The noncompetitive way was expressed for inhibition functions due to acetate and H_2, respectively, were

$$I_{ac,j} = \frac{K_{I,ac,j}}{K_{I,ac,j} + S_{ac}}$$

and

$$I_{h2,j} = \frac{K_{I,h2,j}}{K_{I,h2,j} + S_{h2}}$$

Where $K_{I,ac,j}$ and $K_{I,h2,j}$ are the noncompetitive inhibition constants. While the square functions were added in the inhibition models for free ammonia and pH to increase the strength of these inhibition with increasing free ammonia concentration and decreasing acidic pH. These inhibition functions were listed below:

$$I_{NH3,j} = \frac{K^2_{I,NH3,j}}{K^2_{I,NH3,j} + S^2_{NH3}}$$

and

$$I_{pH,j} = \frac{K_{I,H,j}^2}{K_{I,H,j}^2 + S_H^2}$$

Where $K_{I,NH3,j}$ and $K_{S,H,j}$ are the inhibition constants. A 50% inhibition is reached if $K_{I,i} = S_i$.

2.3.2 Irreversible inhibition

At present, most research works about inhibition focus on reversible inhibition on the growth stage. Hence, if a poisoning due to a severe acidic failure takes place (*e.g.* irreversible loss of active methanogenic biomass), the response of microbial population during/after the event would not be properly predicted from the model.

These two distinct concepts for with/without poisoning may give a technical controversy whether the recovery from the acidic failure should take time because of a need to wait for the relevant biomass growth after their death or would be quick because of the reversible inhibition which should disappear when the concentration of inhibitory materials decreases. To consider the problem, a modified ADM1 equipped with the irreversible inhibition defined as an activity decay would be studied in the later section.

2.4 Post-treatment of wastewater from bioethanol processing

Along with the biological treatment, the physico-chemical methods have been used to remove the color/lignin in the wastewater from bioethanol processing. Several physico-chemical options include coagulation/flocculation (Migo *et al.* 1993; B. Inanc 1999; R. Chandra 1999; A. Mandal 2003; Pandey *et al.* 2003), adsorption (Bernardo *et al.* 1997; Sekar & Murthy 1998; Chandra & Pandey 2000; Lalov *et al.* 2000; A. Mandal 2003; Mane *et al.* 2006), oxidation process (A.D. Dhale 2000; Alfafara *et al.* 2000; Gaikwad & Naik 2000; Pikaev *et al.* 2001; Peña *et al.* 2003; Sangave & Pandit 2004) and membrane (Chang *et al.* 1994; A.G. Vlyssides 1997; Kumaresan *et al.* 2003; Nataraj *et al.* 2006). According to the scope of research, this chapter focuses on 3 first methods.

2.4.1 Oxidation process

Chemical oxidation of wastewater from molasses fermentation with ozone was investigated by Peña *et al.* (2003). Oxidation of more than 4.2 g/h of ozone achieved over 80% decolonization after 20 minutes. COD removal efficiency was not over 25% in any of experimental conditions. However, ozone only transforms the chromophore groups but does not degrade the dark colored polymeric compounds in the effluent. Therefore, TOC values remained constant throughout ozonation.

Sangave and Pandit (2004) employed sonication of distillery wastewater as a pretreatment step to convert complex molecules into a smaller form by cavitation. COD removal efficiency obtained 44% after 72 h of aerobic oxidation and 2 h ultrasound pre-treatment compared to 25% COD reduction without pretreatment.

In another study, Gaikwad and Naik (2000) combined wet air oxidation and adsorption to remove sulfate from distillery wastewater. The post-anaerobic effluent was thermally pretreated at 150 °C under pressure in the absence of air. After that using soda-lime to treat before undergoing a 2 h wet oxidation at 225 °C. The removal rate of COD, BOD, TOC and sulfate were 57, 72, 83, and 94 %, respectively.

2.4.2 Coagulation/Flocculation process

Sari *et al.* (2015) conducted a study to determine decolorization of black liquor wastewater from bioethanol process by using chemical and biological methods. Alum-Poly Aluminium Chloride (PAC) with concentration 1%, ratio 3:1, and total retention time 33 minutes was used in coagulation/flocculation treatment to obtain 96% decolorization. This study showed the possibility for the use of combined physco-chemical and biological in the treatment of black liquor wastewater from bioethanol process.

Pandey *et al.* (2003) addressed physico-chemical treatment of biologically treated distillery effluent using conventional and non-conventional coagulants. 98% of color removal was obtained with conventional coagulants such as ferrous sulfate, ferric sulfate and alum under alkaline conditions. The combination of Percol 47, a commercial organic anionic polyelectrolyte with ferrous sulfate and lime resulted in 99% reduction in color, 87 and 92% reduction in COD and BOD, respectively. Non-conventional coagulants namely wastewater from an iron pickling industry and titanium ore processing industry were also examined. The iron pickling wastewater also removed 92.5% COD and 98% color from the biologically treated distillery effluent.

In another study, Chaudhari *et al.* (2007) used inorganic coagulants ($FeCl_3$, $AlCl_3$ and PAC) to remove color and COD from biodigester effluent of a molasses-based alcohol distillery treatment plant. COD removal efficiency was 55, 60 and 72% while 83, 86 and 92% of color reductions were obtained by using 60mM/l $AlCl_3$, 60mM/l $FeCl_3$ and 30ml/l of PAC, respectively, at their optimum initial pH.

2.4.3 Adsorption process

Mane *et al.* (2006) carried out the study on derivatization of bagasse into an ion exchange material and application of this chemically modified bagasse in the treatment of distillery wastewater. It was found that chemically modified bagasse using 2-diethylaminoethyl chloride hydrochloride and 3-chloro-2-hydroxypropyltrimethylammonium chloride was capable of decolorizing diluted spentwash. Experiment conditions were 0.6 g of chemically modified bagasse in contact with 100 ml spentwash:water solution (1:4 (v/v)

ratio). As the result, 50% decolorization was obtained after 4 h contact with intermittent swirling.

Chandra and Pandey (2000) reported that significant decolorization was observed in packed bed studies on anaerobically treated spentwash using commercial activated charcoal with a surface area of 1,400 m^2/g. 99% decolorization and over 90% BOD and COD removal was obtained with 70% of the eluted sample. Although Sekar and Murthy (1998) showed that commercially available powdered activated carbons can only remove 18% color, however, almost complete decolorization could be achieved when combining coagulation–flocculation with polyelectrolyte followed by adsorption.

The color removal using commercial activated carbon and bagasse fly ash was compared by Mall and Kumar (1997). The results showed that 30 g/l of bagasse fly ash could remove 58% color while 80.7% color removal would be obtained with 20 g/l of commercial activated carbon. In addition, characteristic of the bagasse fly ash was high carbon content and its heating value can be increased by the adsorbed organic material. Therefore, the spent adsorbent can be used to make fire briquettes.

Chapter 3. Expression of Acidic Failure for the Methane Fermentation

3.1 Introduction

In high-rate methane fermentation an acidic failure happens due to the unbalanced reaction rates between the production of volatile fatty acids (VFAs) by acidogens and the consumption of VFAs by methanogens (Mechichi & Sayadi 2005) especially when the composition and concentration of the fed organics are highly fluctuated. Studying about this phenomena will help predict properly and prevent the operational failure in wastewater treatment plant.

Accordingly a primary step to provide robust methane fermentation processes for organic wastes would be to understand the sequential biological degradation in a mathematical manner. In this regard, ADM1 is widely recognised as a platform for the modelling, since ADM1 covers most of the biochemical and physical reactions with respect to disintegration, hydrolysis, acidogenesis, syntrophic reactions, and methanogenesis (Batstone *et al.* 2002; Siegrist *et al.* 2002). Nevertheless, one potential limitation of the model is that the inhibition is only assumed on the microbial growth stages whilst the decay stages are independent of the phenomena. Hence, if an acceleration of decay for methanogens takes place, the response of microbial population during/after the event would not properly obtained from the model.

To cope this problem, a lab-scale continuous experiment for the methane fermentation was performed for 110 days. However, continuous stirred-tank reactor (CSTR) usually applies long HRT in order to allow enough time for the effective degradation of complex compounds (*e.g.* lignocellulosic materials) and to prevent the wash out of slow growing

microorganisms. When fixing HRT the variation of volumetric loading rate occurred by changing the compositions and concentrations of fed organics. On the other hand, due to the compositions of the steam explosion wastewater are not high fluctuated, it is difficult to express an acidic failure phenomenon. While organics wastes from food processing factories are typical materials having high fluctuated fraction of readily biodegradable organics, therefore, in this study heterogeneous food wastes were chosen as the alternative influent. By changing the volumetric loading rate to induce an acidic failure, dynamic simulation was conducted using a modified ADM1 equipped with the irreversible inhibition defined as an activity decay.

3.2 Materials and Methods

3.2.1 Continuous methane fermentation experiment

The continuous methane fermentation experiment was carried out at 35±2°C in a chemostat mode with working volume of 8-litre and stir speed of 100 rpm (Figure 3. 1). Anaerobic inoculum was collected from a mesophilic digester at Hiagari municipal wastewater treatment plant, Kitakyushu, Japan operated at about 38-day hydraulic retention time receiving a mixture of primary and secondary sludge from a conventional BOD-removal activated sludge process. The food wastes for the experiment were obtained once/twice every week from a solid waste processing factory, Kitakyushu, Japan where heterogeneous food wastes were regularly delivered from various food processing sectors over Japan. During the experiment, total 17 composite food waste samples were sequentially fed to the fermenter without dilution or pH adjustment at dilution rate of 0.015–0.020 day^{-1}. To minimize biological degradation during the storage of the samples, the collected food wastes were kept in a refrigerator at 4^0C before the feeding. The food waste samples were roughly homogenized using a lab-scale homogenizer (NISSEI AM-3, Japan) and manually pumped once a day to the fermenter. The methane gas production rate (MPR) at the fermenter was continuously logged using a gas counter after passing it through caustic pellets to remove CO_2 in the biogas (MGC-1, Liter Meter Limited, UK).

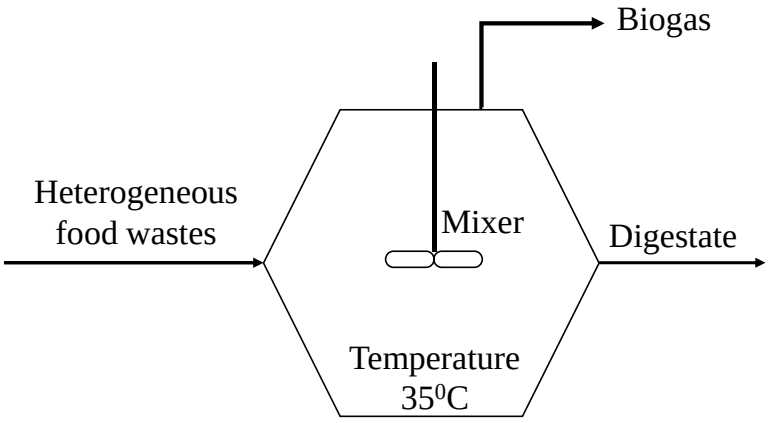

Figure 3. 1. Continuous anaerobic digester

3.2.2 Analytical procedures

Total solid (TS), total volatile solid (TVS), chemical oxygen demand (COD) and lipid concentrations were measured according to #2540, #5220 D and #5520 D in standard methods, respectively (APHA et al. 2012). For measuring the TVS, NaOH was added to the samples to be 4 mol/L to minimize the loss of VFAs from the vaporization during the drying process at 1050C.

Concentrations of carbohydrates (total sugar) and peptide bonds (proteins) were analyzed using Phenol–Sulphuric acid method and Microbiuret method, respectively (DuBois et al. 1956; Itzhaki & Gill 1964). Glucose and egg albumin were used as the standards for the total sugar and the peptide bonds (Kishida Chemicals, Japan). For Phenol-Sulphuric acid method, make standard curve for glucose at 0, 10, 50 and 100 mg/L. Prepare reagents included reagent A, 5% phenol reagent and reagent B, sulfuric acid (H_2SO_4), reagent grade 98%. To analyze carbohydrates, add 1 ml reagent A and 5ml reagent B into 1 ml sample, mix well and wait 10 minutes. Keep samples at room temperature for 20 minutes and measure the absorbance (ABS) at 480 nm wavelength by Clinical Spectrophotometer 7012. In principle, the compounds in the sample will react with phenol to produce a yellow-gold color, which could then be measured using a spectrophotometer. The standard curve for glucose is shown in Figure 3. 2.

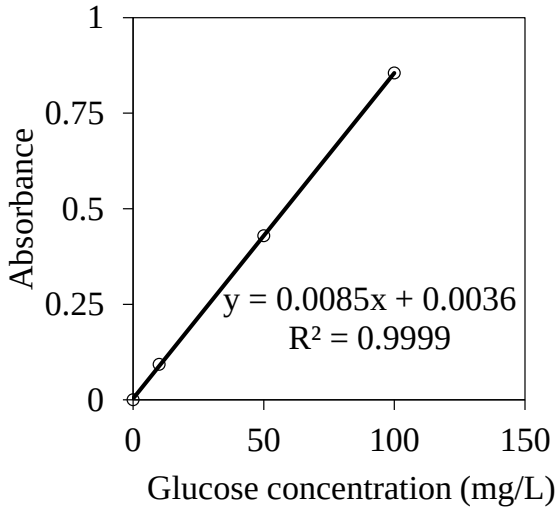

Figure 3. 2. Glucose standard curve

For Microbiuret method, make standard curve for egg albumin at 0, 100, 250 and 500 mg/L. Prepare reagents included reagent A, 0.21% $CuSO_4.5H_2O$ in 30% NaOH and reagent B, 30% NaOH. Before analyzing, samples were pretreated by 2N NaOH in 10 minutes at 100^0C to dissolve insoluble proteins. Then cooling down, settling solid and samples were filtered through filter paper with membrane diameter of 47mm to remove suspended solids. The analysis procedure was conducted as following:

(A_1): 2 ml distilled water + 1 ml reagent A

(A_2): 2 ml sample + 1 ml reagent A

(B_1): 2 ml distilled water + 1 ml reagent B

(B_2): 2 ml sample + 1 ml reagent B.

All mixtures are shaken vigorously. The optical density at 310 nm of mixture (A_2) is read against (A_1) and of (B_2) against (B_1) giving values D_A and D_B, correspondingly. The difference between $D_A - D_B$ was the real absorbance of sample. Readings may be made 5 minutes after mixing using Clinical Spectrophotometer 7012 since the ultraviolet absorption of the copper-protein complex reaches its maximum within this period. In principle, a violet-purplish color was produced when cupric ions (Cu^{2+}) interacted with peptide bonds under alkaline conditions. The difference, $D_A - D_B$ and standard curve for egg albumin are shown in Table 3. 1 and Figure 3. 3.

Table 3. 1. The difference, $D_A - D_B$ for egg albumin standard

Egg albumin concentration (mg/L)	A_1	A_2	$D_A = A_2-A_1$	B_1	B_2	$D_B = B_2-B_1$	$D_A - D_B$
0	0.032	0.032	0	0	0	0	0
100	0.032	0.086	0.054	0	0.014	0.014	0.04
250	0.032	0.159	0.127	0	0.027	0.027	0.1
500	0.032	0.29	0.258	0	0.054	0.054	0.204

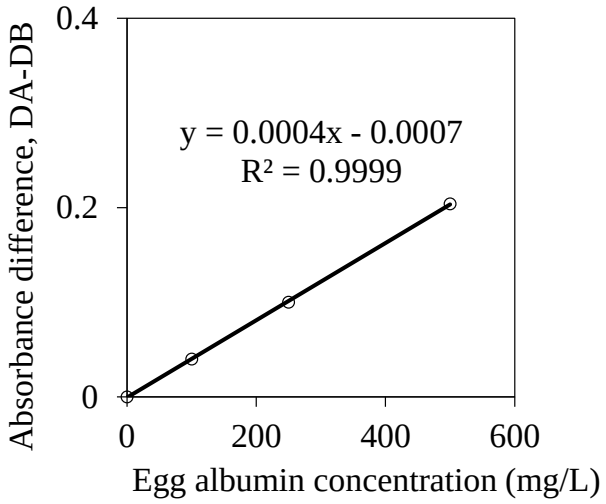

Figure 3. 3. Egg albumin standard curve

The filtrate of the samples with glass fiber filter (Whatman GF/F, USA) was used to measure the soluble VFA concentrations with an ion chromatography system equipped with Ion Pac AS11-HC column whilst the elute flow rate was set at 1 mL/min with 4 mol/L of KOH (ICS-1000, Thermo Fisher Scientific Inc., USA). The retention time was kept at 25 minutes for one sample analysis.

Ethanol concentration was also measured in the food wastes using a gas chromatography, and was found to be trace level. Similarly, concentrations of butyrate, valerate and lactate in the food wastes, and in the digestate were very low throughout the experimental period. Therefore, it was decided that the fate of these compounds were not considered in the study. In addition, considering the protein fractions and food waste concentration to be fed, the nitrogen concentration was supposed to be utmost 2.5-3.2 g-N/L. Hence, this compound did not take into account the inhibition.

3.2.3 Dynamic simulation

To estimate the kinetics, three kinds of mass-balanced parameters were focused; (i) the material concentration in the reactor, (ii) its production rate, and (iii) its decomposition rate. When two parameters out of the three were obtained, the rest can be eventually calculated (*e.g.* from VSS feeding rate as influent stream and VSS concentration in the

reactor, the VSS disintegration kinetics could be estimated). The dynamic simulations of the experiment were performed focusing on a chronological change of MPR, the dominant VFAs (acetate and propionate) and TVS concentration in the fermenter. Using GPS-X ver. 6.3 (Hydromantis Environmental Software Solutions Inc., Canada), these responses were simulated with Equation 3 and Equation 4 on the ADM1 structure, which expressed the reduction of the reaction rates due to presence of inhibitory materials and acceleration of decay due to poisoning respectively.

$$\nu \cdot \left(\frac{K_I^m}{K_I^m + S_{Inhibition}^m} \right) \qquad \text{Equation 3}$$

$$b + b_I \cdot \left(\frac{S_{Inhibition}^m}{K_I^m + S_{Inhibition}^m} \right) \qquad \text{Equation 4}$$

Where ν: specific uptake rate of substrate (d^{-1}), K_I: inhibition half-saturation coefficient (g-COD/L), m: inhibition power factor (-), $S_{Inhibition}$: Inhibitory material concentration (g-COD/L), b: ordinary specific decay rate (d^{-1}), b_I: specific poisoning rate (d^{-1}).

Assuming that high concentration of VFAs and hydrogen would not kill acidogenic nor acetogenic microorganisms, Equation 3 was applied to the specific uptake rates for sugars, amino acids, LCFAs and propionate, which was a comparable formula to that of existing inhibition function (non-competitive type) in ADM1, where $m > 1$ was applied to the propionate uptake process to enhance the hydrogen inhibition effect, and to the acidogenic processes to express the decrease of activity due to high VFAs concentration (Kleerebezem & van Loosdrecht 2006). Although the formula having a power coefficient (Sigmoidal type) (Figure 3. 4) resembled in Hill kinetics, which expressed the change of affinity depending on the concentration of the materials in enzymology (Hill 1910), the expression was totally empirical to jump the output of Equation 3 between ν and zero (If $S_{Inhibition} >> K_I$, then the output $\rightarrow$ zero, otherwise the output $\approx \nu$). In this way the degree of jumping was strengthened when large m was applied. For simplification in this study, the inhibitory VFA material was assumed to be total VFAs whilst the inhibition impacts might vary depending on VFA species and dissociation constants (Wang *et al.* 2009b;

Amani *et al.* 2011).

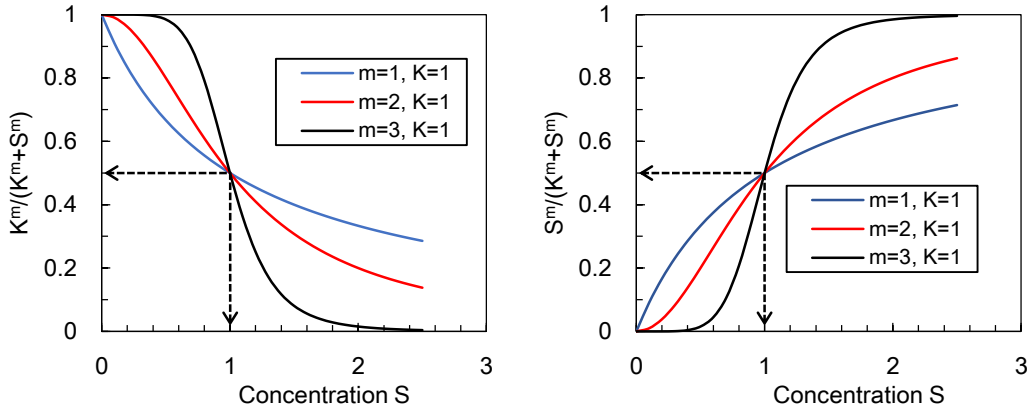

Figure 3. 4. Typical curve shapes for Sigmoidal type

Similar to the above approach, the Sigmoidal type was also incorporated into Equation 4 in order to simulate poisoning phenomena (irreversible inhibitions) on methanogenic microorganisms (i.e., If $S_{Inhibition} >> K_I$, then the output $\rightarrow b+b_I$, otherwise the output = b). This mathematical structure was especially needed to match the datasets and the simulation to express the loss of the methanogenic activity during/ after the acidic failure, as described in the results and discussion section.

3.3 Results and discussions

3.3.1 Composition of the food wastes

The constitution of the food waste samples including ash and organic fractions (carbohydrate, protein, lipid and VFAs) is summarised as shown in Table 3. 2 and Figure 3. 5. Over the 17 samples the ash accounted for 10-20% in TS, and fractions of carbohydrate, protein, lipid contents were averaged to be 24, 40 and 25% respectively. Concentrations of VFAs in the samples were very small with less than 1%. Except sample #15, the sum of the individual materials was closed to 100%, suggesting that the chemicals used as the standards in this study reasonably represented the organic properties of the food wastes.

Table 3. 2. Compositions of the food waste samples

# Unit: g/L	COD	TS	TVS	Carbohydrate	Protein	Lipid	Ash	VFAs
Sample 1	182.7	125.0	95.6	50.3	52.5	0	20.1	0.9
Sample 2	158.0	108.3	77.2	47.6	27.3	1.4	24.3	0.9
Sample 3	218.0	120.8	100.3	59.1	42.7	0	15.0	1.6
Sample 4	110.5	74.9	50.4	21.7	14.6	13.4	19.9	0.7
Sample 5	176.5	162.3	143.7	16.5	19.6	107.0	13.5	0.7
Sample 6	152.5	69.3	53.9	11.0	26.0	16.1	11.7	0.8
Sample 7	196.5	91.2	73.6	6.5	33.4	32.8	13.2	0.8
Sample 8	229.0	85.6	64.3	7.1	31.7	24.8	16.7	0.7
Sample 9	193.0	110.3	91.4	24.5	66.3	0.3	15.2	0.4
Sample 10	159.0	121.7	95.2	11.5	55.9	26.2	21.0	1.6
Sample 11	79.3	58.0	50.2	1.0	51.3	0	5.8	0.5
Sample 12	139.5	96.7	76.0	6.6	17.8	50.5	17.0	1.2
Sample 13	208.0	106.0	87.0	16.3	43.1	26.9	14.8	0.7
Sample 14	158.5	113.3	91.1	20.2	50.5	19.3	17.2	1.0
Sample 15	136.0	74.1	54.0	13.3	58.4	0	15.5	1.2
Sample 16	135.5	71.7	52.1	4.0	52.9	0	12.2	1.6
Sample 17	164.0	72.4	51.6	6.3	22.1	22.8	13.5	0.3

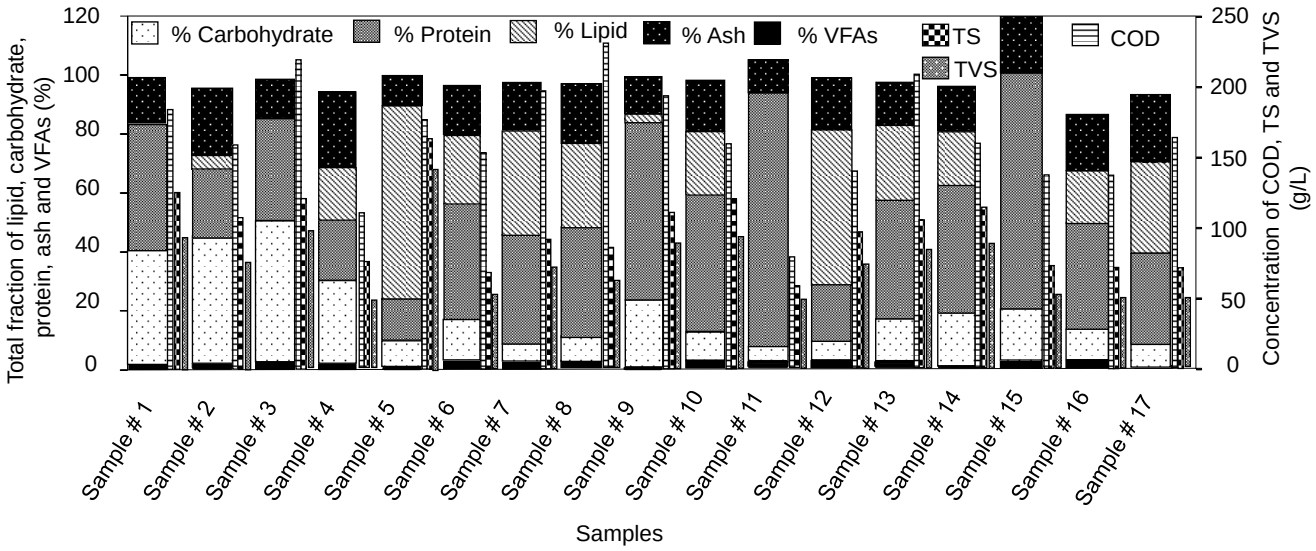

Figure 3. 5. Constituents of the food waste samples

Considering the variation of the organic fraction among the 17 samples (carbohydrate: 7-49%, protein: 12-88%, lipid: 0-52%), kinetics on disintegration and hydrolysis, which were supposed to be mostly inherent properties of the materials rather than the activities of biomass in the fermenter, were individually manipulated in the dynamic simulation according to the sequential feeding of the samples. Due to high complexity of the model structure which includes 17 kinds of disintegration kinetics and 17 kinds of hydrolysis kinetics (Table 3. 3), and 25 kinds of microbial kinetics and 6 kinds of yield stoichiometry (Table 3. 4), computational sensitivity analysis could not be conducted for the calibration. Accordingly the microbial pathways in the model (*e.g.* fractions for acetate production and H_2 production from degradation of sugar) and material-originated fraction (*e.g.* the carbohydrate production and LCFA production from degradation of lipids), the stoichiometries on the intermediates were also not able to be estimated and the set of ADM1 was used as shown in Table 3. 5.

Table 3. 3. List of solubilisation kinetics of the 17 food waste samples

#	Specific disintegration rate (d^{-1})	Specific hydrolysis rate (d^{-1})		
		Carbohydrates	Proteins	Lipids
Sample 1	2.0	2.0	2.0	5.0
Sample 2	2.0	2.0	1.5	5.0
Sample 3	3.0	3.0	2.0	5.0
Sample 4	1.0	1.5	1.0	6.0
Sample 5	0.5	1.0	1.0	10.0
Sample 6	0.5	1.0	2.0	6.0
Sample 7	0.5	1.0	2.0	7.0
Sample 8	0.5	1.0	2.0	6.0
Sample 9	1.0	1.5	2.5	5.0
Sample 10	0.5	1.0	2.0	6.0
Sample 11	0.5	1.0	3.0	5.0
Sample 12	0.5	1.0	1.0	8.0
Sample 13	0.5	1.0	2.0	6.0
Sample 14	0.5	1.0	2.0	6.0
Sample 15	0.5	1.0	3.0	5.0
Sample 16	0.5	1.0	2.0	6.0
Sample 17	0.5	1.0	2.0	7.0
Average	0.88	1.3	1.9	6.1

References: Specific disintegration rate: 0.5 d^{-1} (Batstone *et al.* 2002), 1.0 d^{-1} (Wichern *et al.* 2009); Specific hydrolysis rate of carbohydrate: 0.5-2.0 d^{-1} (Mata-Alvarez 2005), 10 d^{-1} (Batstone *et al.* 2002); Specific hydrolysis rate of proteins: 10 d^{-1} (Batstone *et al.* 2002; Gali *et al.* 2009); Specific hydrolysis rate of lipids: 10 d^{-1} (Batstone *et al.* 2002; Gali *et al.* 2009)

Table 3. 4. List of microbial parameters

Growth and decay kinetics	This study	References
Growth of sugar degraders		
Maximum specific uptake rate (d^{-1})	4	4 [1]
Half-saturation coefficient (g-COD/m^3)	50	50 [2]
Biomass yield (g-COD/g-COD)	0.1	0.1 [2]
Growth of amino acid degraders		
Maximum specific uptake rate (d^{-1})	4	4 [2]
Half-saturation coefficient (g-COD/m^3)	10	24 [2]
Biomass yield (g-COD/g-COD)	0.08	0.08 [2]
Growth of higher fatty acid degraders		
Maximum specific uptake rate (d^{-1})	0.36	0.36 [2]
Half-saturation coefficient (g-COD/m^3)	24	24 [2]
Biomass yield (g-COD/g-COD)	0.06	0.06 [2]
Growth of propionate degraders		
Maximum specific uptake rate (d^{-1})	0.65	0.6 [1]
Half-saturation coefficient (g-COD/m^3)	20	20 [1]
Biomass yield (g-COD/g-COD)	0.04	0.04 [2]
Growth of acetate degraders		
Maximum specific uptake rate (d^{-1})	0.95	0.4 [2]
Half-saturation coefficient (g-COD/m^3)	100	40 [1]
Biomass yield (g-COD/g-COD)	0.05	0.05 [2]
Growth of hydrogen degraders		
Maximum specific uptake rate (d^{-1})	2	2 [1]
Half-saturation coefficient (g-COD/m^3)	1	1 [1]
Biomass yield (g-COD/g-COD)	0.06	0.06 [2]
Decay of microorganisms		
Specific decay rate of sugar degraders (d^{-1})	0.01	0.02 [2]
Specific decay rate of amino acid degraders (d^{-1})	0.1	0.02 [2]
Specific decay rate of higher fatty acid degraders (d^{-1})	0.01	0.02 [2]
Specific decay rate of propionate degraders (d^{-1})	0.001	0.02 [2]
Specific decay rate of acetate degraders (d^{-1})	0.001	0.02 [2]
Specific decay rate of hydrogen degraders (d^{-1})	0.001	0.02 [2]

Table 3.4. List of microbial parameters (Continued)

Growth and decay kinetics	This study	References
Inhibition (reversible) on acidogenic organisms		
Half-saturation inhibition coefficient for VFAs (g-COD/m^3)	3,000	5,200 [3]
Inhibition sensitivity factor for VFAs (*m*, -)	2	Nil
Inhibition (reversible) on propionate degraders		
Half-saturation inhibition coefficient for hydrogen (K_I, g-COD/m^3)	0.004	0.001 [1]
Inhibition sensitivity factor for hydrogen (*m*, -)	2	2 [1]
Inhibition (irreversible) on methanogenic organisms		
Maximum specific poisoning rate for VFAs (b_I, d^{-1})	1.3	Nil
Half-saturation poisoning coefficient for VFAs (K_I, g-COD/m^3)	5,700	Nil
Poisoning sensitivity factor for VFAs (*m*, -)	4	Nil

References: [1)] (Siegrist *et al.* 2002), [2)] (Batstone *et al.* 2002), [3)] (Boubaker & Ridha 2008)

Table 3. 5. List of stoichiometries on the intermediates

Stoichiometric parameters	This study	Reference
Production of long-chain fatty acids from lipids (g-COD/g-COD)	0.95	0.95
Production of propionate from sugar (g-COD/g-COD)	0.27	0.27
Production of acetate from sugar (g-COD/g-COD)	0.514	0.514
Production of hydrogen from sugar (g-COD/g-COD)	0.216	0.216
Production of propionate from amino acid (g-COD/g-COD)	0.1213	0.1213
Production of acetate from amino acid (g-COD/g-COD)	0.7322	0.7322
Production of hydrogen from amino acid (g-COD/g-COD)	0.1465	0.1465
Production of acetate from higher fatty acid (g-COD/g-COD)	0.7	0.7
Production of hydrogen from higher fatty acid (g-COD/g-COD)	0.3	0.3
Production of acetate from propionate (g-COD/g-COD)	0.57	0.57
Production of hydrogen from propionate (g-COD/g-COD)	0.43	0.43

Reference: (Batstone *et al.* 2002)

3.3.2 Fermenter responses

Due to limited accuracy to define the initial biomass concentrations of the inoculum taken from the municipal wastewater treatment plant, the experimental data were not used for the simulation until reasonable reproductions of methane gas production rate and VFAs concentrations were initiated from day 30. Until day 90 the datasets were used to demonstrate the consistent methane fermentation receiving the heterogeneous food waste samples (10 samples, #6-#15), and to estimate the microbial kinetics. During day 90-97 the volumetric loading rate was intentionally increased by feeding the concentrated food waste samples (#16 and #17) (Figure 3. 6). Consequently, from day 97, a remarkable increase of soluble organics in the digestate was observed together with the considerable accumulation of acetate and propionate in the fermenter (Figure 3. 7).

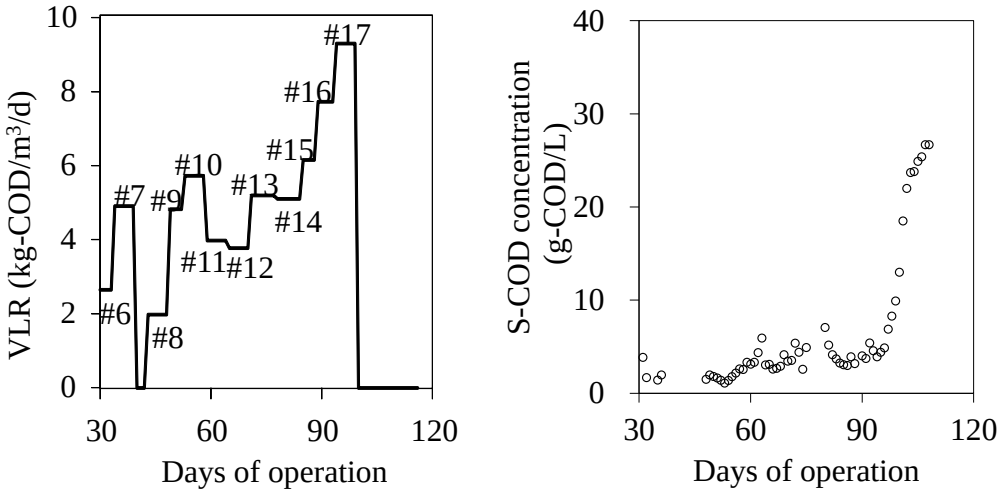

Figure 3. 6. Volumetric COD loading rate of food wastes and measured soluble COD concentration in the fermenter

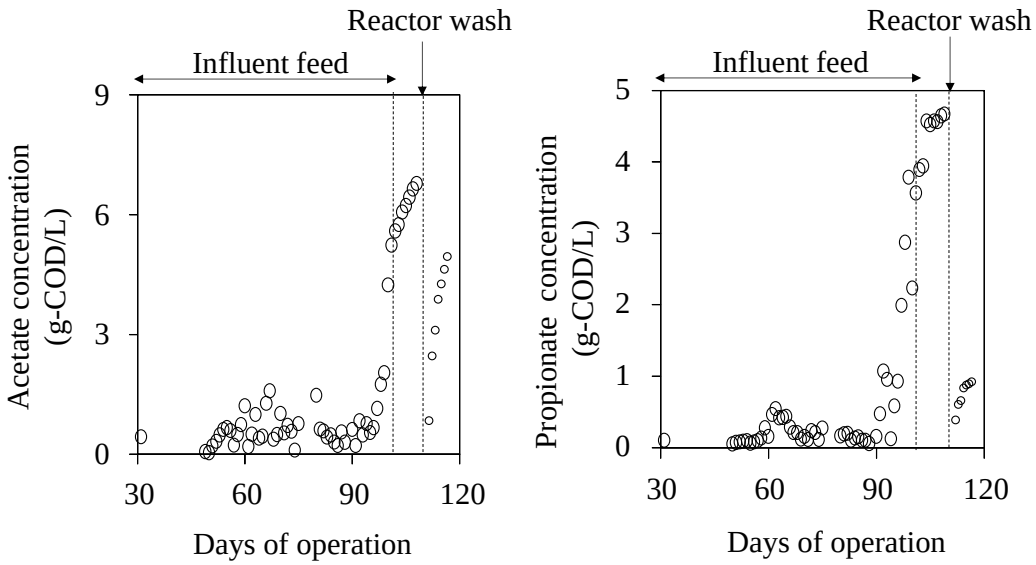

Figure 3. 7. Measured acetate and propionate concentration in the fermenter

When the fermenter pH dropped to about 5 at day 100, the feeding of the food wastes was discontinued. Keeping the condition for 9 days, the acetate concentration and propionate concentration in the fermenter eventually reached to 7.0 g-COD/L and 4.7 g-COD/L, respectively. Then the digestate in the fermenter was centrifuged at 4,000 rpm (12,000 G) for 10 minutes and washed with tap water. This removed 86% of the remaining soluble materials (*e.g.* acetate: 7.0 g-COD/L → 1.0 g-COD/L, propionate: 4.7 g-COD/L → 0.67 g-COD/L), and the fermenter pH was neutralised to 7.5 using 0.5 L NaOH 1mol/L. After washing, the microorganisms was supposed to be almost perfectly recovered as the supernatant SS concentration was below 100 mg/L (SS recovery efficiency > 99%). Even after the fermenter wash, the accumulation of the VFAs was consistently kept due to the unbalance of the reaction rates between the acidogens and methanogens, and no recovery of methane production was observed (Figure 3. 8).

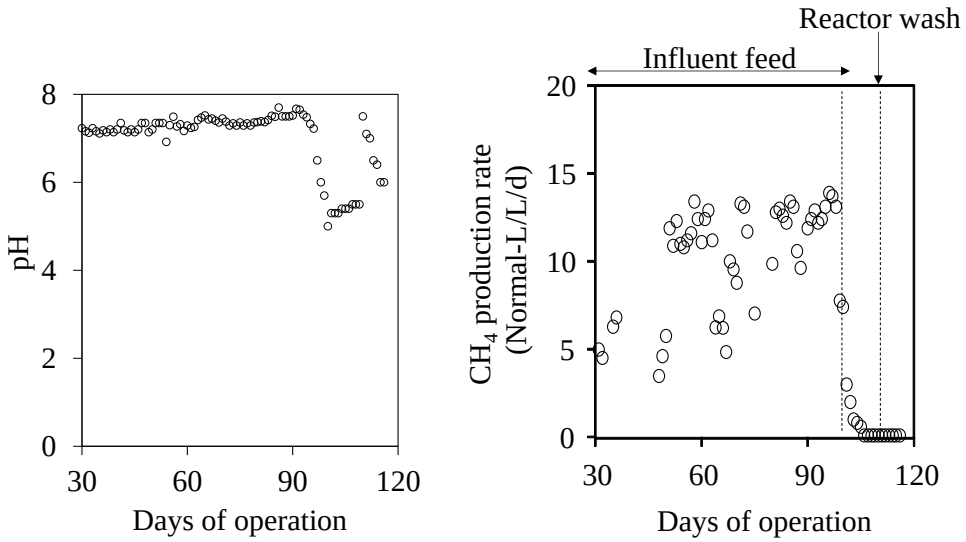

Figure 3. 8. pH and volumetric methane gas production rate in the fermenter

Based on the above datasets, three kinds of dynamic simulation were conducted applying (1) a model using averaged solubilisation kinetics of the 17 food waste samples with the poisoning concept, (2) a model using differentiated solubilisation kinetics (listed in Table 3. 3) with the poisoning concept, and (3) a model using averaged solubilisation kinetics without poisoning (no activity decay on the methanogens) (Figure 3. 9, Figure 3. 10 and Figure 3. 11).

(a) TVS concentration in the fermenter

(b) Soluble COD concentration in the fermenter

(c) Acetate concentration in the fermenter

(d) Propionate concentration in the fermenter

(e) Volumetric methane gas production rate

(f) Soluble sugar concentration

(g) Soluble protein concentration

(h) Lipid concentration

As shown in Figure 3. 9 and Figure 3. 10, the model (1) could roughly reproduce TVS concentration with overestimation of the soluble materials and underestimation of MPR especially between day 90 and day 100, although the loss of methanogenic activity was comparable to that simulated using the model (2). In fact, the calculated concentrations with the model (1) for soluble sugar, soluble protein and lipid in the fermenter also seemed to be slightly inconsistent with the data plots, comparing to those obtained from the model (2).

These responses suggested that a reactor designing procedure using a grab food waste kinetics to build full-scale plants would hold a potential risk when volumetric loading is highly fluctuated. Therefore, to avoid unexpected acidic failure in the practical operation at commercial methane fermentation systems, a development of quick on-site monitoring method to identify the kinetics for the fresh food waste would be desired.

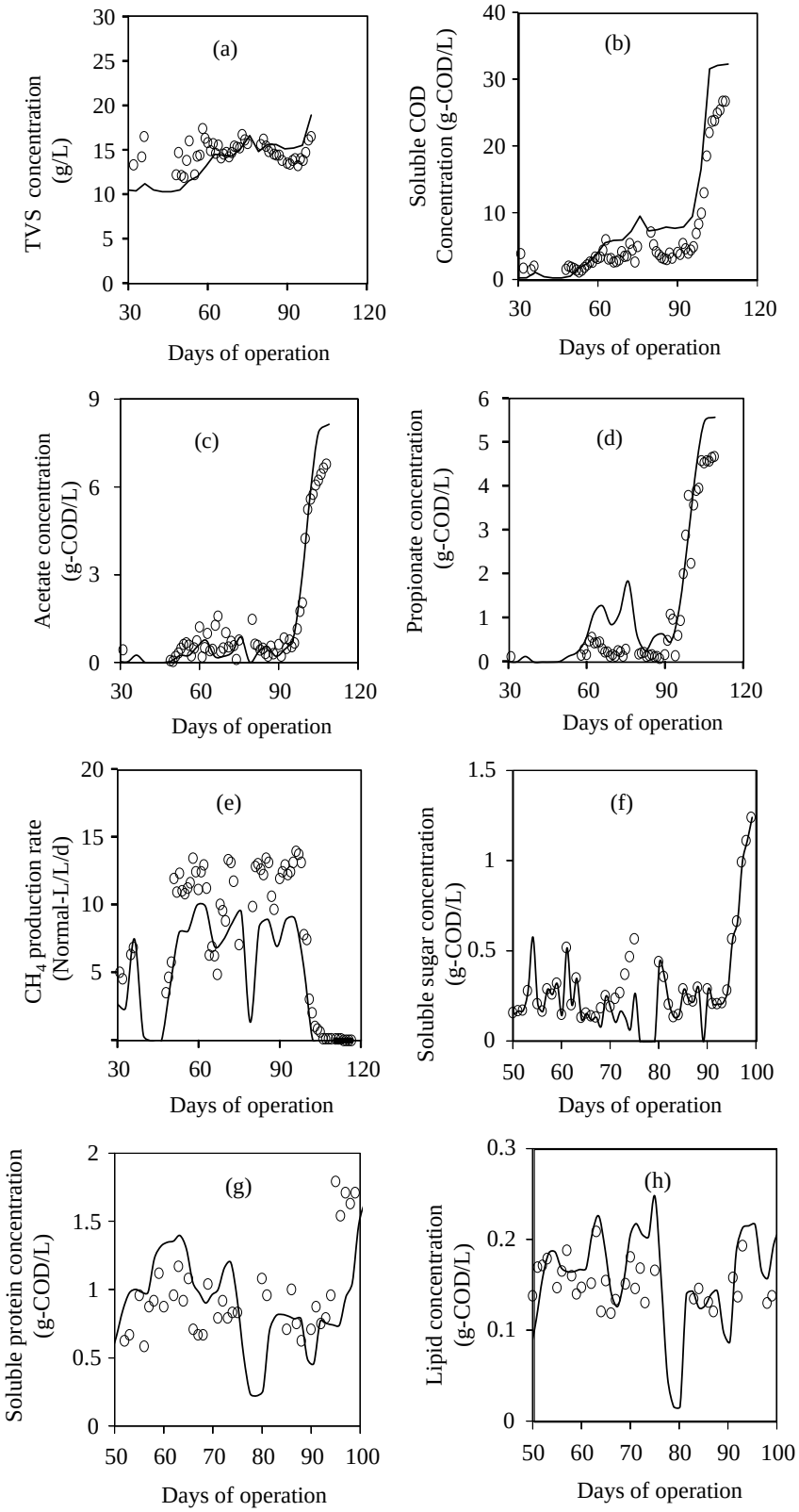

Figure 3. 9. Fermenter responses using model (1)

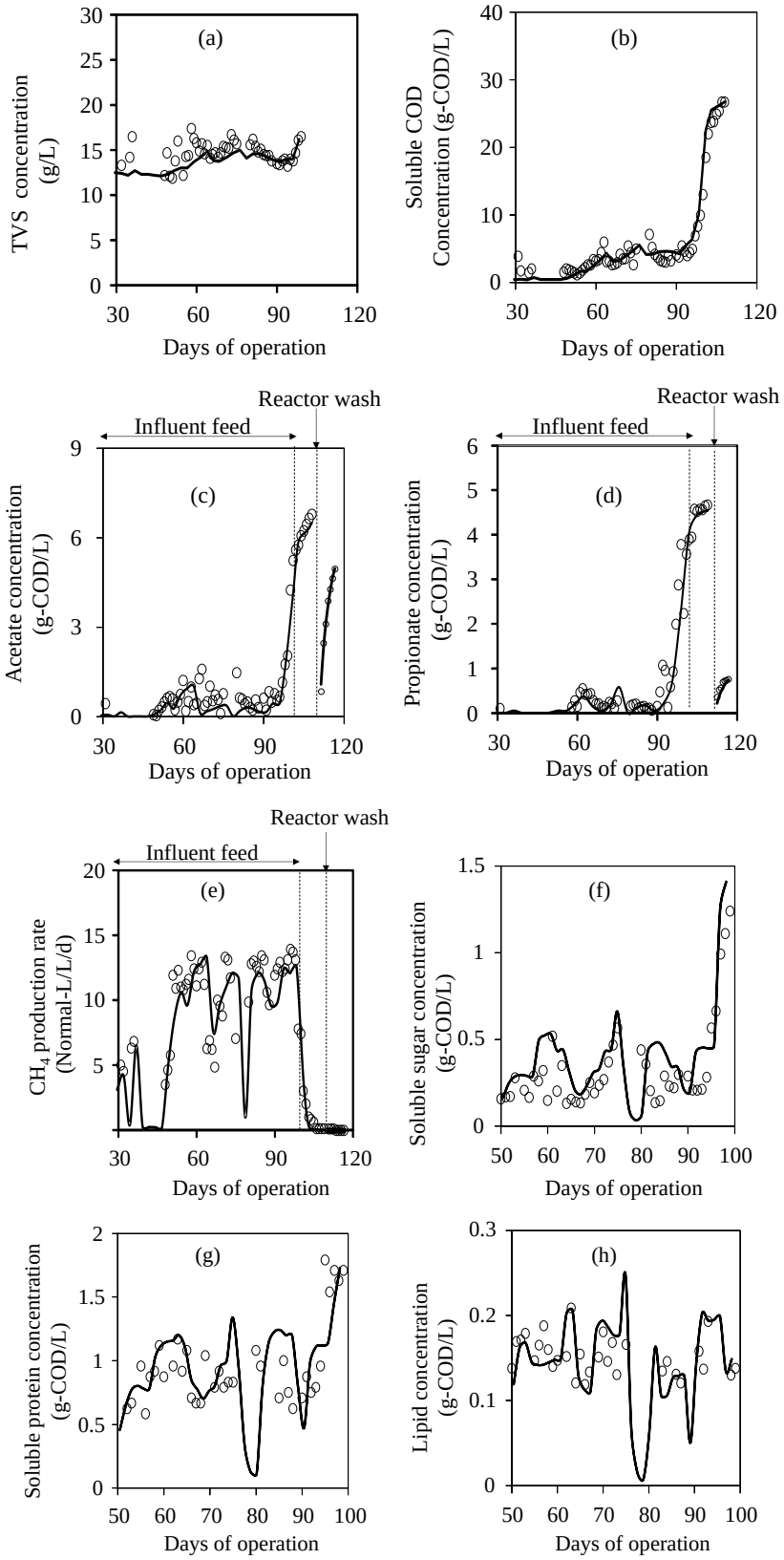

Figure 3. 10. Fermenter responses using model (2)

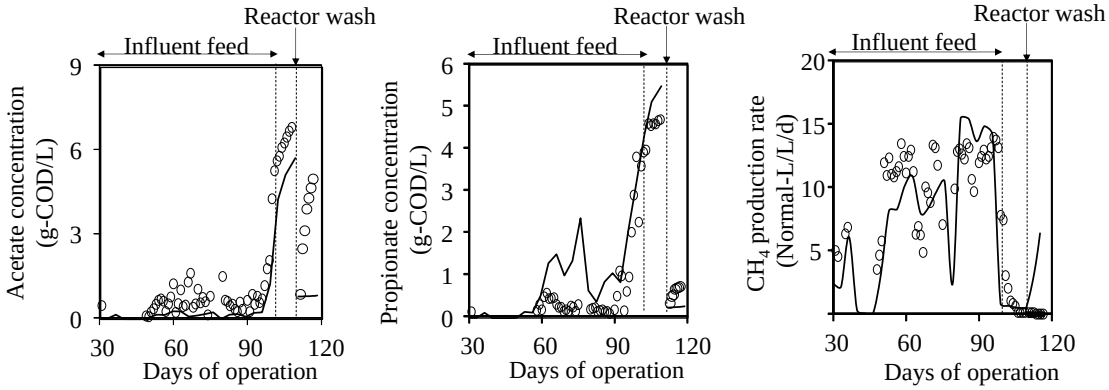

Figure 3. 11. Fermenter responses using model (3)

On the other hand, because the model (3) was emphasized the role of the poisoning concept during the acidic failure, the dynamic simulation was focused on the responses from acetate, propionate and MPR. As shown in Figure 3. 11 the model (3) was not able to reproduce the MPR during/ after the acidic failure event. The MPR in the continuous experiment fluctuated according to the fluctuation of the volumetric loading rate until the acidic failure starting at day 100. Within a couple of days since the event, the MPR sharply decreased and reached to no CH_4 production, which only could be simulated using the model (2) with poisoning concept. When the VFAs concentration and pH in the fermenter were controlled at reasonable levels on day 109 (below 2.0 g-COD/L), the model (3) significantly overestimated the MPR after the reactor wash, which indicated that considerable activity decay for the methanogens took place during the acidic failure. Focusing on the concentration of VFAs in the fermenter between day 100 and day 109, the kinetics of the additional decay for the methanogens were estimated to match the observed MPR data plots for the model (2). Based on the reduction of the active methanogenic biomass, the accumulation of VFAs after day 109 (after the fermenter wash) could be also reasonably simulated as shown in the bold line in the graphs, as well as concentrations of TVS, soluble COD and VFAs.

3.3.3 State variable concentration

The dynamic change of the state variables for two kinds of methanogens (acetoclastic biomass and hydrogenotrophic biomass) and four kinds of acidogens (sugar degrader,

amino acid degrader, LCFA degrader and syntrophic propionate degrader) were calculated as shown in Figure 3. 12.

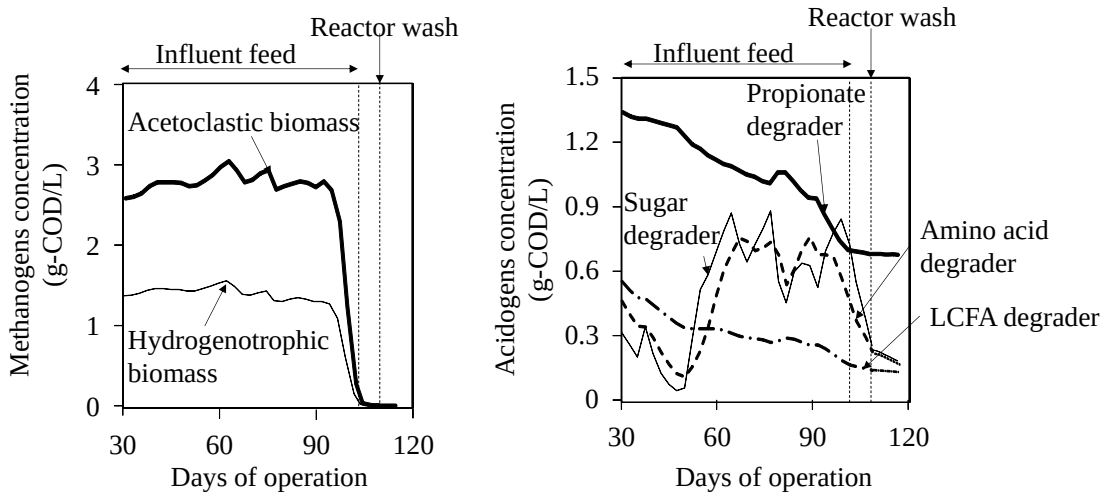

Figure 3. 12. Calculated methanogens and acidogens concentrations in the fermenter

The methanogen concentrations were almost kept constant until day 90 where the accumulation of VFAs started. The calculated two kinds of active methanogens quickly decreased from the day until day 109 along with the elevation of acetate and propionate concentrations (acetoclastic biomass: 2.6 g-COD/L at day 90 → $5 \cdot 10^{-5}$ g-COD/L at the fermenter wash, hydrogenotrophic biomass 1.1 g-COD/L at day 90 → $2 \cdot 10^{-5}$ g-COD/L at the fermenter wash). Since the decrement of MPR was clearly observed when the total VFA concentration reached to about 5-6 g-COD/L, the inhibition half-saturation coefficient, K_I for the methanogens was supposed to be around in the range (K_I = 5.7 g-COD/L). Another inhibition coefficient, m was calibrated to be 4 in order to meet the decrement of MPR during the acidic failure. The specific poisoning rate b_I was roughly determined to be 1.3 d^{-1} in order that the active biomass reached to the above mentioned concentrations. It was found that the pair of m and b_I compensate each other (high m with low b_I could yield a comparable output to that using low m with high b_I). Additional experimental study changing initial VFAs concentration would be needed to estimate the kinetics more accurate manner.

The concentrations of the sugar, amino acid and LCFA degraders were calculated to meet the dynamic change of corresponding substrate concentrations in the fermenter with a set of default kinetics and yield coefficients in the existing ADM1. These concentrations were affected by the availability for corresponding substrate concentrations. The concentration of the propionate degrader was obtained focusing on the reaction rate of the hydrogenotrophic methanogenic biomass and propionate concentration in the fermenter. The maximum specific propionate uptake rate was needed to modify slightly from the default (0.60 d^{-1} in ADM1 to 0.65 d^{-1} in this study). For the VFA inhibitions on the sugar, amino acid and LCFA degraders, K_I = 3 g-COD/L and m = 2 were applied respectively whereas a pair of $K_I = 4 \times 10^{-6}$ g-COD/L and m = 2 was applied to express the hydrogen inhibition for the propionate degrader.

Since the above simulations using the poisoning concept reasonably reproduced the experimental datasets, the inhibition mechanism on the acidic failure was supposed to be more complicated than those described in the available mathematical models applying traditional reversible inhibition concepts. On the other hand, as there are many evidences for the reversible inhibitions in literatures, perhaps both inhibitions should exist in the biological system. Hence proper mapping the two distinct mechanisms to individual reaction stages in a model will be one of the most important studies to install reliable methane fermentation processes for food waste treatments.

3.4 Conclusions

Based on the dynamic responses of the continuous experiments, a modified ADM1 having an irreversible VFA inhibition function on the decay stage of methanogens was built.

The inhibition half-saturation coefficient, K_I = 5.7 g-COD/L, inhibition power factor, m = 2 were applied to simulate the decrement of MPR during the acidic failure, and the specific poisoning rate b_I = 1.3 d^{-1} of the methanogens were used to simulate the decrement of the methane production rate under the acidic failure and discontinuation of the methane production after the fermenter wash.

In order to reproduce the system responses including VFAs and soluble COD concentrations in the fermenter during the continuous experiment for 120 days, a differentiation of the disintegration and hydrolysis kinetics according to the heterogeneous food wastes of 17 samples were needed (disintegration: 0.5-3 d^{-1}, hydrolysis of carbohydrate: 1-3 d^{-1}, hydrolysis of protein: 1-3 d^{-1}, hydrolysis of lipid: 5-10 d^{-1}).

Chapter 4. Anaerobic Degradation Mechanism and Kinetic Model of the Organics in Steam Explosion Wastewater from Bioethanol Processing

4.1 Introduction

Bioethanol is produced from yeast fermentation of sugars extracted from plant biomass. The organic sources are mostly sucrose (*e.g.* sugar cane and sugar beet), starch (*e.g.* maize and wheat) and lignocellulosic materials (*e.g.* sugar cane bagasse, wood and straw) (Dias *et al.* 2009). To maximize food securities and utilization of non-edible biomass, bioethanol production from lignocellulosic material, especially sugar cane bagasse which is the most abundant potential resource has been paid keen attention (Dias *et al.* 2009; Rabelo *et al.* 2011). Since the lignocellulosic material is composed of lignin and lignin-binding cellulose, physical/ chemical pretreatments are essential to recover the cellulose, followed by an enzymatic hydrolysis process to depolymerize the cellulose to monosaccharide (Kuo & Lee 2009). Until now various kinds of pretreatment methods have been utilized (*e.g.* mechanical disintegration, steam explosion, alkali/ acid digestions and biological partial decomposition) (Balat *et al.* 2008). Among them, the steam explosion in a high-pressure vessel equipped with an instantaneous depressurization stage is supposed to be one of the options (Zheng *et al.* 2014).

For the industrial commercialization, apart from the bioethanol processing system, it is also essential to develop proper treatment systems for the liquid wastes generated from

the steam explosion process. In this regard, anaerobic biological treatments are also paid attention as the processes produce methane gas which can be used for the heat source to produce the steam (Zheng *et al.* 2014). Nevertheless, technical information for the biological degradability of the liquid waste organics is still limited at present, and consequently conservative low-loaded anaerobic plants are often suggested (Steinwinder *et al.* 2011).

As the anaerobic degradation of soluble organics is a consequence of a sequential biochemical reactions composed of (1) hydrolysis of the polymers to monomers, (2) acidogenesis and acetogenesis from the monomers to acetate and hydrogen, and (3) methanogenesis to produce methane from acetate and hydrogen, it is interesting to formulate a process map with listing individual kinetics and stoichiometries. This would provide a platform to evaluate the performance of high-rate reactors (*e.g.* fixed-bed reactor and upward anaerobic sludge blanket reactor) and to optimize the wastewater treatment system configuration. Based on this background, an experiment was conducted to model the anaerobic degradation of steam explosion wastewater obtained from sugar cane bagasse. The organics in the liquid and its intermediate products during the biological treatment were analyzed under batch condition with addition of microorganisms collected from a fixed-bed reactor treating the wastewater. The biological responses were dynamically simulated referring ASMs and ADM1 developed by IWA task groups (Henze *et al.* 2000; Batstone *et al.* 2002).

4.2 Materials and methods

4.2.1 Batch experiment

The steam explosion of sugar cane bagasse was conducted under 3.0 MPa (about 230 °C) for 5 minutes followed by a depressurization to ambient pressure. The solid product was washed with tap water as much as 5 times, and steam explosion wastewater was obtained accordingly (Figure 4. 1).

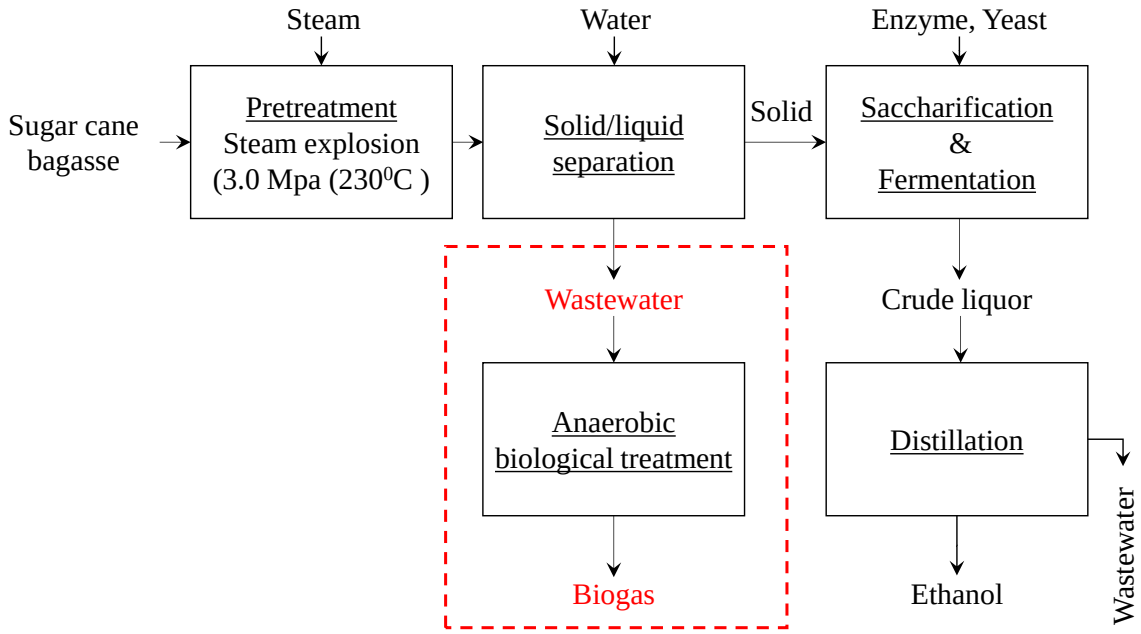

Figure 4. 1. Flow scheme of bioethanol processing for sugar cane bagasse

Since the wastewater was highly acidic (pH = 2.87), pH was neutralized to 7.3 by adding NaOH for the biological experiment. It appeared that the suspended solid concentration in the liquid was very low and below its detectable limit of 5 mg/L. Therefore the biological reaction for the particulate fraction was not considered in this study.

The batch biological experiment (Figure 4. 2) was carried out at 35±2°C in a jar fermenter with working volume of 10-litre and stir speed of 100 rpm. Anaerobic inoculum was collected from a lab-scale continuous fixed-bed reactor operated for over four month by feeding steam explosion wastewater at about 5-day hydraulic retention time under

mesophilic conditions at 35±2°C. 9L of the inoculum having 270 mg-COD/L SS was mixed with 1 L of the wastewater to be 2,625 mg-COD/L (food/microorganism ratio = 9.72), and incubated for 18 days while collecting small amounts of liquid samples from the reactor daily. The methane gas production rate (MPR) of the fermenter was continuously logged using a gas counter after passing it through caustic pellets to remove CO_2 in the biogas (MGC-1, Litre Meter Limited, UK).

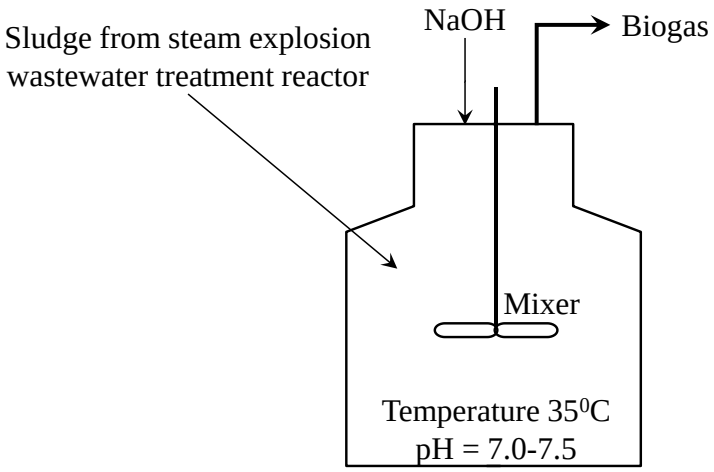

Figure 4. 2. Batch reactor

4.2.2 Analytical procedures

Soluble total organic carbon (S-TOC) and total nitrogen (T-N) concentrations, respectively were measured according to #5310 B and #4500-N B in Standard Methods (APHA *et al.* 2012). Soluble carbohydrate (as total soluble sugar concentration) was calorimetrically analyzed using Phenol-Sulphuric acid method (DuBois *et al.* 1956) with glucose standard (Kishida chemicals, Japan). To estimate protein contents in the samples, a carbon/nitrogen (C/N) ratio of egg albumin (Kishida chemicals, Japan) was determined. Firstly, measuring the egg albumin to identify the percentage of C, H, O and N in the composition. The result is shown in Table 4. 1 and Table 4. 2. From Kjeldahl nitrogen in each sample and the C/N ratio (3.43), soluble protein concentration was estimated.

Table 4. 1. Composition of egg albumin

	Fraction		$C_xH_yO_zN_1$	
	Weight	Mole	x, y, z	Molecular formula
C	50.0%	0.0417	4.0	4
H	9.3%	0.0930	8.9	9
O	26.0%	0.0163	1.5	2
N	14.7%	0.0105	1.0	1

Table 4. 2. COD/MW, C/N and COD/TOC factors of egg albumin

Mass weight (MW)	103.0
COD	144.0
TOC (carbon)	48
Nitrogen (N)	14
COD/MW	1.40
C/N	3.43
COD/TOC	3.00

The Lowry-Follin method (Lowry et al. 1951) was applied to calculate the lignin concentration. The reagents included reagent A, 2% Na_2CO_3 in 0.10 N NaOH. Reagent B, 0.5% $CuS0_4.5H_20$ in 1% $C_4H_4Na_2O_6$. Mix 50 mL of reagent A with 1 mL of reagent B to make reagent C. Reagent D, 1N Folin reagent was diluted from 2N Follin reagent. For the analysis procedure, samples were pretreated by 2N NaOH in 10 minutes at 100^0C to dissolve insoluble proteins. Then cooling down, settling solid and samples were filtered through filter paper with membrane diameter of 47mm to remove suspended solids. Add 5 mL reagent C in 1 mL sample, mix well and allow to stand for 10 minutes or longer at room temperature. 0.5 mL reagent D was added very rapidly and mixed within a second or two. After 30 minutes or longer, the samples were read in Clinical Spectrophotometer 7012 at 750 nm wavelength. As the Lowry-Follin method can detect both protein and polyphenolic compounds (as soluble lignin concentration), the concentration of lignin was calculated by subtracting the protein concentration from the Lowry-Follin method. The factor of the soluble lignin on Lowry-Folin method was determined based on an

alkali-extracted lignin reagent (Tokyo chemical industry, Japan). The egg albumin, alkali-extracted lignin standard and mixture of 2 standards were prepared from 0, 50, 100 and 250 mg/L. Based on the result of absorbance measurements of alkali-extracted lignin, egg albumin and mixture of 2 standards and standard curves the factor of soluble lignin was identified (Table 4. 3 and Figure 4. 3).

Table 4. 3. Absorbance measurements (ABS) at different concentration using Lowry-Folin method

Concentration (mg/L)	Alkali-extracted lignin (ABS)	Egg albumin (ABS)	Mixture (ABS)
0	0.069	0.069	0.069
50	0.18	0.11	0.253
100	0.337	0.226	0.499
250	0.716	0.461	0.975

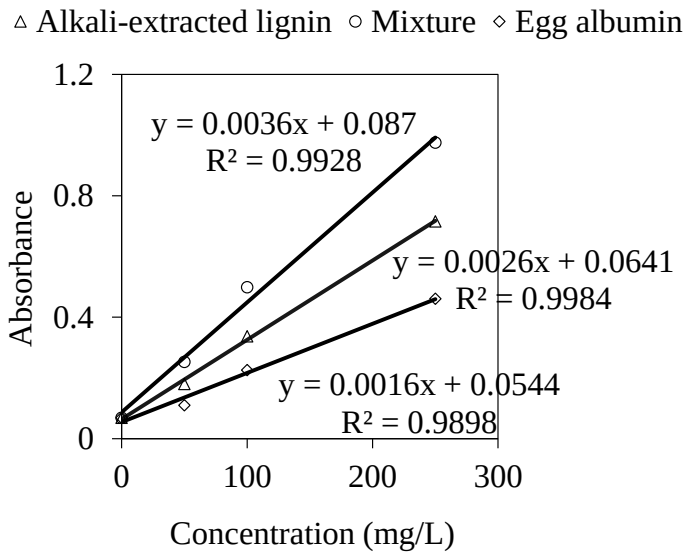

Figure 4. 3. Standard curves for alkali-extracted lignin, egg albumin and mixture of two standards

The filtrate of the samples with 0.2 μm micro filter (25CS020AN, Advantech Japan) was used to analyze two kinds of derivatives from sugars that were generated by the steam explosion process; furfural ($(C_4H_3O)CHO$) and hydroxyl-methyl-furfural (HMF, $(C_4H_3O)CHOHCHO$)). These concentrations were measured using an ultra-performance liquid chromatography system equipped with a refractive index detector (wave length: 275 nm, Acquity Ultra Performance LC, Waters Corporation, USA). Acquity UPLC HSS T3 column (1.8 μm 2.1 × 100 mm) was used while the elute flow rate was set at 0.2 mL/min with mobile phase having 10% acetonitrile and 90% ultra-pure water under 40 °C. Low-molecule fatty acids below C5 were detected using an ion chromatography system equipped with Ion Pac AS11-HC column (ICS-1000, Thermo Fisher Scientific Inc., USA) while the elute flow rate was set at 1 mL/min with 4 mol/L of hepta-fluoro-butyric acid at 35 °C. In addition to formate, acetate, propionate and lactate, a small amount of oxalate was detected in the wastewater but the fate of this compound was not considered in this study because of negligibly low concentrations (*ca.* 19 mg-COD/L). Total nitrogen, total phosphorus, inorganic cations/ anions as well as acid-insoluble materials assumed as silicate were also measured to catch the constituents of the wastewater, but these were not included in the model development. The steam explosion wastewater parameters are listed in Table 4. 4.

Table 4. 4. List of steam explosion wastewater parameters

pH	2.87	Formate	0.40 g-C/L
Total solid	18.4 g/L	Acetate	0.64 g-C/L
Total volatile solid	17.9 g/L	Lactate	0.29 g-C/L
COD	26.3 g-COD/L	Oxalate	0.02 g-C/L
TOC	9.68 g-C/L	Propionate	0.02 g-C/L
Carbohydrate	3.23 g-C/L	Na^+	99 mg/L
Protein	0.33 g-C/L	K^+	40 mg/L
Lignin	3.53 g-C/L	Ca^{2+}	77 mg/L
Furfural	0.43 g-C/L	Mg^{2+}	38 mg/L
Hydroxyl-methyl-furfural	0.64 g-C/L	Cl^-	18 mg/L
Total nitrogen	150 mg-N/L	SO_4^{2-}	111 mg/L
Total phosphorus	31 mg-P/L	Acid-insoluble materials (assumed to be silicate)	305 mg/L

4.2.3 Dynamic simulation

Dynamic simulation of the batch reactor response was performed focusing on a chronological change of methane production rate (MPR) and soluble material concentrations for TOC, the dominant fatty acids (formate, acetate, propionate and lactate), furfural, HMF, total sugar (carbohydrate), protein, ammonia nitrogen and lignin. Based on these degradation and the production of intermediates, a process map and kinetics for individual organics were elaborated. Although ADM1 and ASM1 were initially referred to model the set of reactions, the individual process expressions were considerably modified in order to include the fates of furfural, HMF, lactate and formate. As the material balance of the model was COD basis, COD/TOC factors were prepared to calculate the composite materials (carbohydrate, protein and lignin) as 2.67, 3.00 and 2.92, assuming the elemental compositions $(CH_2O)_n$, $(C_4H_9O_2N)_n$ (U.Satyanarayana & U.Chakrapani 2006) and $(C_{31}H_{34}O_{11})_n$ (King *et al.* 1983), respectively.

A process simulator (GPS-X ver.6.4, Hydromantis Environmental Software Solutions,

Inc., Canada) was used to programme the model and numerically solve the set of differential equations for the dynamic condition. To define the set of active biomass concentrations in the inoculum, a set of first-guess kinetics from the batch experiment was applied to conduct the simulation. When the calculated effluent qualities did not match those monitored, these parameters were manipulated and the simulation was again conducted. The trial & error approach was repeated until calculated responses fairly matched those monitored (Table 4. 5).

Table 4. 5. List of initial biomass concentrations

Microorganisms	Concentration (mg-COD/L)
Sugar degrader	99
Amino acid degrader	13
Propionate degrader	2
Acetate utilizer	3
Hydrogen utilizer	5

4.3 Results and discussions

4.3.1 Decomposition of organics in steam explosion wastewater

As shown in Figure 4. 4 the degradation of soluble total sugar was observed until day 5, and about 66% of the organics was decomposed in that period. The rest of 557 mg-COD/L of the organics remained in the batch reactor almost corresponding to original concentration (642 mg-COD/L) in the inoculum from a continuous fixed-bed reactor, indicating that the carbohydrate could be classified into at least two kinds of fractions having distinct biological degradability. Although the exact chemical composition of the refractory organics was not identified, since soluble lignin was not also degraded throughout the experimental period (Figure 4. 5), it was speculated to be the celluloses bound with lignin (solubilized lignocellulosic material). The significant amount of lignin remaining in the reactor suggested that post-treatments need to be added to remove the un-biodegradable fractions. Similar to the total sugar degradation, the decrement of protein concentration along with time until day 8 (from 543 to 368 mg-COD/L) showed that two kinds of protein fractions coexisted. The un-biodegradable protein fraction was almost equal the concentration of retaining protein (420 mg-COD/L) in the continuous fixed-bed reactor. The ammonia nitrogen produced from the protein decomposition was used to estimate the protein concentration. In the first 5 days the ammonia concentration decreased due to the nutrient supply for the microorganism growth.

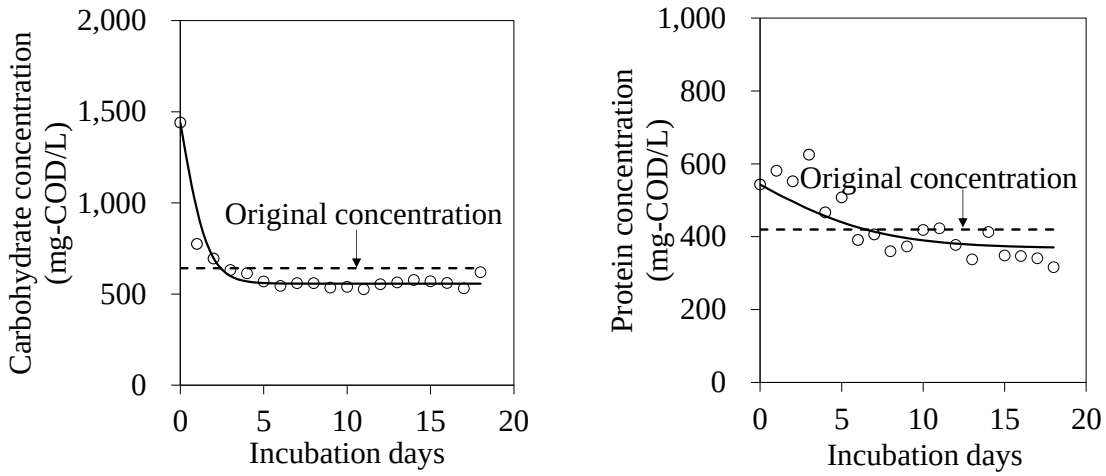

Figure 4. 4. Carbohydrate and protein concentration in the batch reactor

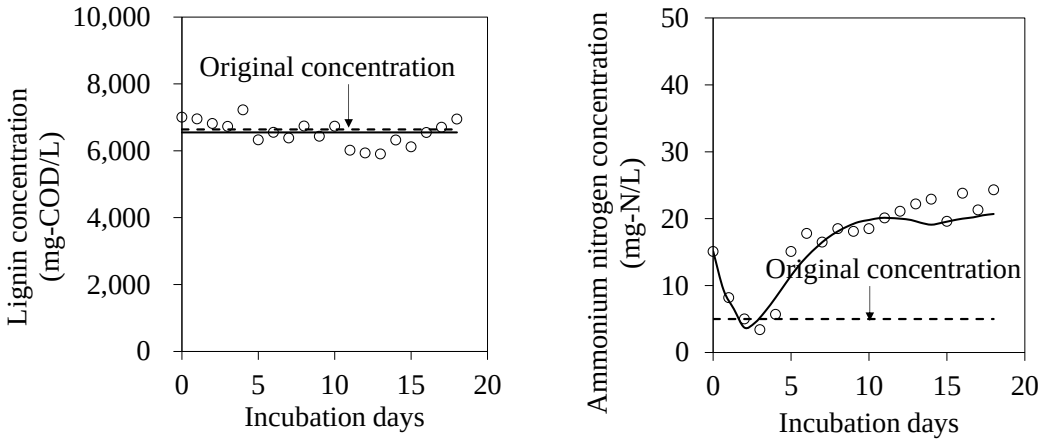

Figure 4. 5. Lignin and ammonium nitrogen concentration in the batch reactor

Furfural and HMF quickly disappeared within 1 day (Figure 4. 6). At day 1 the concentrations of the both organics reached the detectable limits of 1 mg/L. Although some studies (Zaldivar *et al.* 1999, 2000; Klinke *et al.* 2004) pointed out that the compounds inhibited the ethanol fermentation when Saccharomyces and/or ethanologenic E.coli were used, these compounds were identified as readily biodegradable materials for the anaerobic system in this study. The degradation of lactate was also associated with the degradation of soluble total sugar, and 78 mg-COD/L of lactate degradation was completed at about day 2. Like the lactate degradation, formate almost disappeared within 2 experimental days (Figure 4. 7).

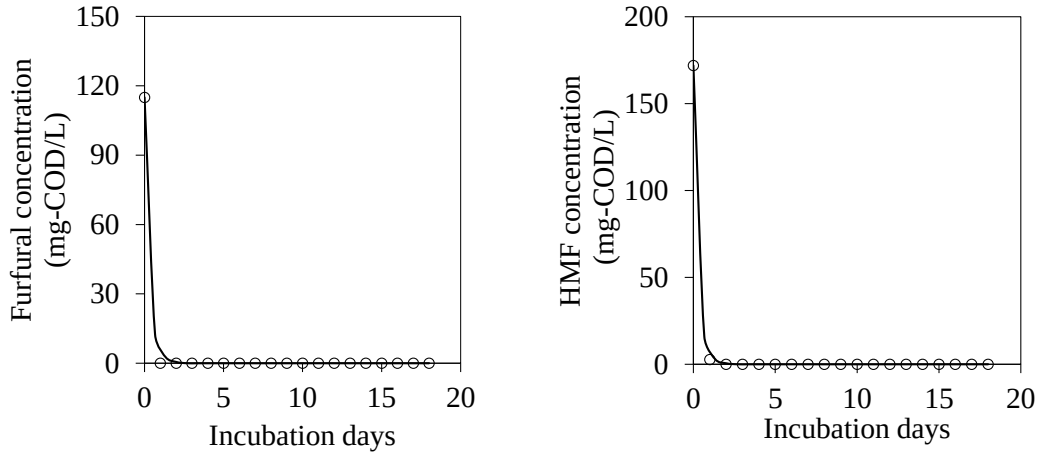

Figure 4. 6. Furfural and HMF concentration in the batch reactor

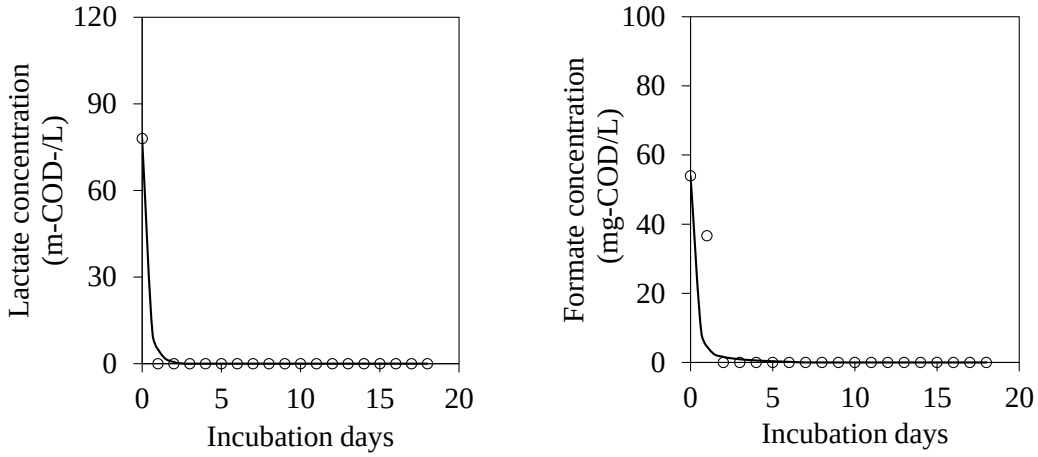

Figure 4. 7. Lactate and formate concentration in the batch reactor

Acetate and hydrogen were thought to be its intermediate products which were eventually generated via pyruvate and Acetyl CoA, considering a thermodynamically feasible reaction (lactate $C_3H_5O_3^-$ + $2H_2O$ → acetate $C_2H_3O_2^-$ + HCO_3^- + $2H_2$ + H^+, $\Delta G° = -12.91$ kJ/mol at pH 7) (Barrow 1981). During the experiment, accumulation of propionate and acetate followed by their rapid reduction yielded the shape of MPR (Figure 4. 8 and Figure 4. 9). This was attributed to an integrated consequence for the reactions by acidogens, acetogens and methanogens, as discussed in a later section.

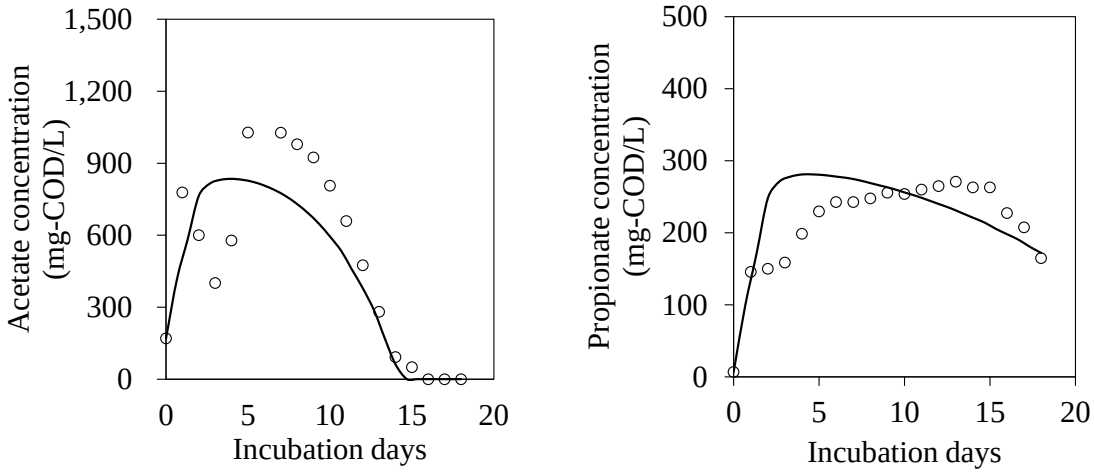

Figure 4. 8. Acetate and propionate concentration in the batch reactor

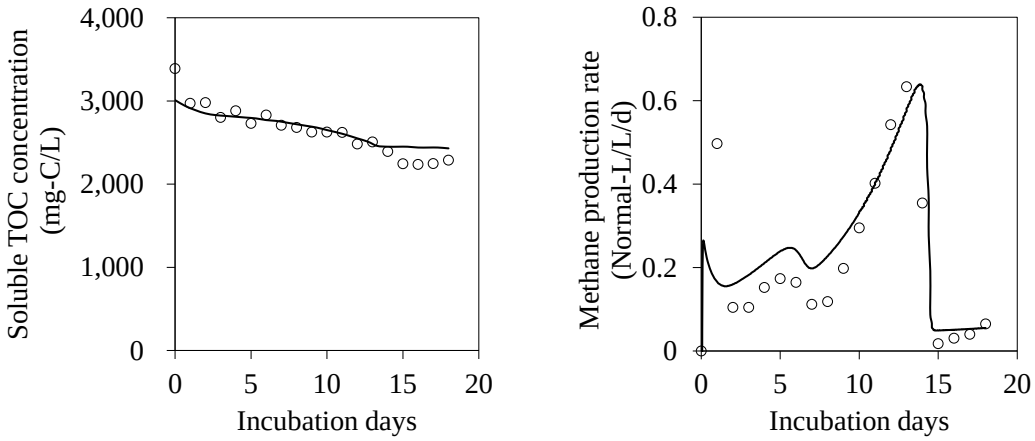

Figure 4. 9. Soluble TOC and methane production rate in the batch reactor

As summarized in Figure 4. 10, 40% of the TOC-based organics including 25% carbohydrate, 4% protein and 11% others (including sugar derivatives and organic acids) in the wastewater was biologically removed in the anaerobic condition. While 60% of un-biodegradable organics was mostly lignin (44%) and small amount of carbohydrate (10%) and protein (6%). Some studies published on the treatment of lignocellulosic wastewater, with most focusing on anaerobic digestion for the biodegradable materials and the production of biogas, which seems the most likely method to obtain the majority of the TOC removal. However, one of the great challenges of steam explosion wastewater is the removal of un-biodegradable materials from wastewater. Therefore, additional treatments with physico-chemical methods after anaerobic digestion to remove lignin need to be further studied and integrated into the treatment systems.

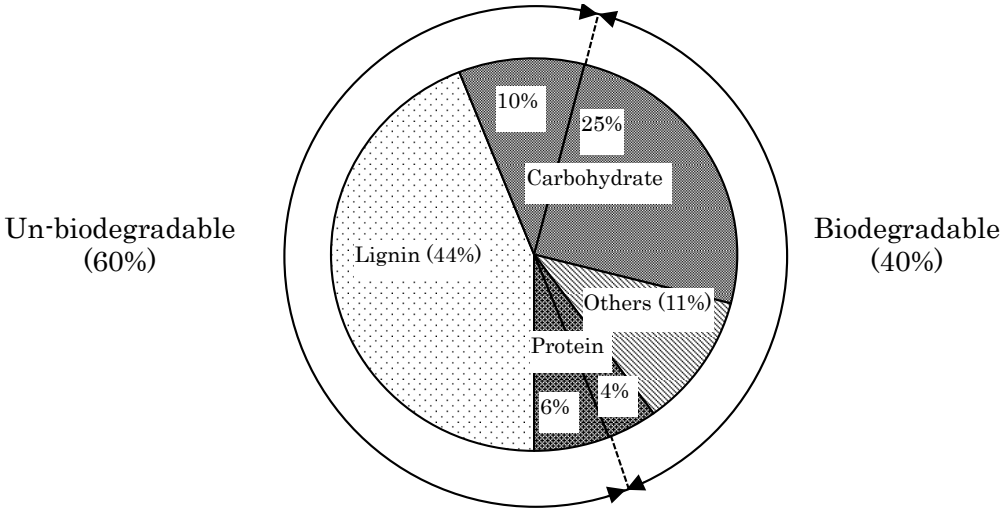

Figure 4. 10. Circle of biodegradable and un-biodegradable TOC

4.3.2 Model structure for the anaerobic biological degradation of steam explosion wastewater

The process map for the anaerobic degradation of organics in steam explosion wastewater is summarized in Table 4. 6, where 22 state variables were defined including un-biodegradable soluble organics (S_{lig}, S_{su_U} and S_{pr_U}), hydrolysable soluble organics (S_{su_B} and S_{pr_B}), active microorganisms (X_{su}, X_{aa}, X_{pro}, X_{ac} and X_{h2}), monomer substrates (S_{su}, S_{fur}, S_{hmf}, S_{lac}, S_{aa}, S_{pro}, S_{for}, S_{h2} and S_{ac}), inorganic nitrogen (S_{IN}), methane (S_{ch4}) and biologically inert particulate generated from biomass decay (X_U).

Table 4. 6. Process map for anaerobic biological degradation of steam explosion wastewater organics from sugarcane bagasse

#	Process/state variable	S_{lig}	S_{su_U}	S_{su_B}	S_{pr_U}	S_{pr_B}	X_{su}	X_{aa}	X_{pro}	X_{ac}	X_{h2}	S_{su}	S_{fur}	S_{hmf}	S_{lac}	S_{aa}	S_{pro}	S_{for}	S_{h2}	S_{ac}	S_{ch4}	S_{IN}	X_U
r1	Hydrolysis of carbohydrate			-1								+1											
r2	Hydrolysis of protein					-1										+1							
r3	Uptake of monosaccharide						Y					-1					(1-Y) *0.27		(1-Y) *0.12	(1-Y) *0.61		-(Y) *N_{bac}[a]	
r4	Uptake of furfural						Y						-1				(1-Y) *0.27		(1-Y) *0.12	(1-Y) *0.61		-(Y) *N_{bac}	
r5	Uptake of HMF						Y							-1			(1-Y) *0.27		(1-Y) *0.12	(1-Y) *0.61		-(Y) *N_{bac}	
r6	Uptake of lactate						Y								-1				(1-Y) *0.33	(1-Y) *0.67		-(Y) *N_{bac}	
r7	Uptake of amino acid							Y								-1	(1-Y) *0.12		1-Y) *0.15	(1-Y) *0.73		N_{aa}[b]-(Y) *N_{bac}	
r8	Uptake of propionate								Y								-1		(1-Y) *0.43	(1-Y) *0.57		-(Y) *N_{bac}	
r9	Uptake of acetate									Y										-1	(1-Y)	-(Y) *N_{bac}	
r10	Uptake of formate										Y							-1			(1-Y)	-(Y) *N_{bac}	
r11	Uptake of hydrogen										Y								-1		(1-Y)	-(Y) *N_{bac}	
r12	Decay of X_{su}						-1					(1-f_U) *0.4				(1-f_U) *0.6							f_U
r13	Decay of X_{aa}							-1				(1-f_U) *0.4				(1-f_U) *0.6							f_U
r14	Decay of X_{pro}								-1			(1-f_U) *0.4				(1-f_U) *0.6							f_U
r15	Decay of X_{ac}									-1		(1-f_U) *0.4				(1-f_U) *0.6							f_U
r16	Decay of X_{h2}										-1	(1-f_U) *0.4				(1-f_U) *0.6							f_U
Y: adopted from ADM1 r3: 0.1 r4: 0.1 r5: 0.1 r6: 0.1 r7: 0.08 r8: 0.04 r9: 0.05	r10: 0.06 r11: 0.06 f_U: 0.08 (adopted from ASM1) N_{bac}: 0.14 N_{aa}: 0.14	Soluble lignin	Unbiodegradable carbohydrate	Biodegradable carbohydrate	Unbiodegradable protein	Biodegradable protein	Sugar degrader (acidogen)	Amino-acid degrader (acidogen)	Propionate degrader (acetogen)	Acetate utiliser (methanogen)	Hydrogen utiliser (methanogen)	Monosaccharide	Furfural	HMF	Lactate	Amino acid	Propionate	Formate	Hydrogen	Acetate	Methane	Inorganic nitrogen	Unbiodegradable particulate

In the model, biodegradable total sugar (cellulose, S_{su_B}) and biodegradable protein (S_{pr_B}) were depolymerized, and accordingly monomer sugar (S_{su}) and amino-acid (S_{aa}) were generated (r1 and r2). For the reactions on the uptake of S_{su}, furfural (S_{fur}) and HMF (S_{hmf}), the conversion stoichiometries of monomer sugar in ADM1 was adopted excluding productions of butyrate and valerate since these fatty acids were not detected. Accordingly the corresponding production of propionate (S_{pro}), acetate (S_{ac}) and hydrogen (S_{h2}) on COD basis was assumed as 27%: 61%: 12% (r3, r4 and r5). As mentioned in the previous section, the conversion stoichiometry S_{ac} and S_{h2} from lactate (S_{lac}) was fixed at 67%: 33% (r6). Similar to r1-r3, productions of S_{pro}, S_{ac} and S_{h2} were assumed from the degradation of S_{aa} under the suggested stoichiometry of ADM1 (12%: 73%: 15%) (r7), as well as the degradation of S_{pro} where S_{ac} and S_{h2} were produced at 57%: 43% (r8).

Apart from acetoclastic methanogen utilizing only S_{ac} for the growth (r9), the reaction of hydrogenotrophic methanogen was modelled to uptake both S_{h2} and formate (S_{for}) depending on the concentrations of the substrates (r10 and r11). To reduce the complexity of the model structure, the decay processes of the above 5 kinds of microorganisms were simplified (r12-r16). The decayed products were defined to be S_{su}, S_{aa} and biologically inert organic particulate (X_U), which was an analogy of ASM3 where no biodegradable particulate was produced. The fraction of produced S_{su} and S_{aa} was assumed to be 40%: 60%, adopted from ADM1. For simplification the biomass yield coefficients (Y) for hydrogenotrophic methanogen from S_{for} and S_{h2} were fixed at the same ratio.

The rate expressions for r1-r16 are listed in Table 4. 7. Contois type was applied to the hydrolysis processes for carbohydrate and protein (r1 and r2). Traditionally a first-order kinetic was used to express hydrolysis of particulates in anaerobic treatments. Considering its soluble nature and mathematical flexibility to include the impact of microorganism concentration on the reaction rates, it was decided to use the equation adopted from ASMs. When a very small half-saturation coefficient was used, the rate expression could be approximated to a first-order type on the microorganism concentration. On the other hand, a very big coefficient provided a first-order type on the soluble material concentration.

Table 4. 7. Process rate expressions for anaerobic biological degradation of organics in steam explosion wastewater

	Process	Rate expression	Maximum specific rate (d^{-1})		Half-saturation coefficient (mgCOD/L, -)	
			This study	References	This study	References
r1	Hydrolysis of carbohydrate	Contois type (by sugar degrader)	10	1.25-18 [1, 2]	8	0.5-22.5 [1, 3]
r2	Hydrolysis of protein	Contois type (by amino-acid degrader)	4	1.04-18 [2, 3]	15	0.26-22.5 [1, 3]
r3	Uptake of monosaccharide	Monod type * $S_{su}/(S_{su}+S_{fur}+S_{hmf}+S_{lac})$	3	0.41-21 [4]	10	3-90 [4]
r4	Uptake of furfural	Monod type * $S_{fur}/(S_{su}+S_{fur}+S_{hmf}+S_{lac})$	10	Nil	10	Nil
r5	Uptake of HMF	Monod type * $S_{hmf}/(S_{su}+S_{fur}+S_{hmf}+S_{lac})$	10	Nil	10	Nil
r6	Uptake of lactate	Monod type * $S_{lac}/(S_{su}+S_{fur}+S_{hmf}+S_{lac})$	10	Nil	10	Nil
r7	Uptake of amino acid	Monod type	2	2.36-4 [4]	10	7.5-70 [4]
r8	Uptake of propionate	Monod type * $K_I^m/(K_I^m+(S_{for}+S_{h2})^m)$	5	0.02-1.07 [4]	10 (uptake) 0.008 (inhibition K_I)[a] 0.05 (inhibition m)[b]	1-57 [4] (uptake) 0.001-0.008 [4] (inhibition K_I) 2 [5] (inhibition m)
r9	Uptake of acetate	Monod type	3.8	0.02-1.41 [4]	5	0.2-71 [4]
r10	Uptake of formate	Monod type * $S_{for}/(S_{for}+S_{h2})$	18	Nil	5	Nil
r11	Uptake of hydrogen	Monod type * $S_{h2}/(S_{for}+S_{h2})$	3	0.02-12 [4]	10	1 [5]
r12	Decay of X_{su}	First-order type	0.01	0.02-0.8 [4]	Nil	
r13	Decay of X_{aa}	First-order type	0.01	0.02-0.8 [4]	Nil	
r14	Decay of X_{pro}	First-order type	0.01	0.01-0.2 [4]	Nil	
r15	Decay of X_{ac}	First-order type	0.01	0.01-0.05 [4]	Nil	
r16	Decay of X_{h2}	First-order type	0.01	0.009-0.3 [4]	Nil	

References: [1)] (Vavilin *et al.* 2008), [2)] (Vavilin *et al.* 1996), [3)] (Mairet *et al.* 2011), [4)] (Batstone *et al.* 2002), [5)] (Siegrist *et al.* 2002)

[a] K_I: Half-saturation inhibition coefficient for hydrogen

[b] m: Inhibition power coefficient for hydrogen

With respect to the degradation of monosaccharide, furfural, HMF and lactate (r3-r6), all compounds were classified in carbohydrate species and supposed to proceed in specific metabolic pathways. The amino-acid degradation was followed by the protein substrates (r7). For the hydrogen inhibition on propionate degradation (r8), as hydrogen concentration could not be measured directly due to extremely low gaseous partial pressure, the kinetics were calibrated to meet the data plots of propionate concentration. To enhance the effect of hydrogen, a power coefficient was applied (Kleerebezem & van Loosdrecht 2006). Acetate concentration was focused to calibrate the kinetics of acetoclastic methanogen (r9), whilst MPR was used to estimate the kinetics of the microorganisms and hydrogenotrophic methanogen (r10 and r11). Although the acidic failure term due to the VFAs accumulation on methanogenesis was expressed in chapter 3, considering the pH changes (Figure 4. 11) during the experimental period, pH was kept stable in the range of 7-7.5, this concept was not included in the model. On the other hand, as the sensitivities of the specific decay rates on the dynamic simulation were limited (r12-r16), the set of kinetics suggested in ADM1 was roughly selected. In addition, comparing to the default values in the references (Vavilin et al. 1996; Batstone et al. 2002; Siegrist et al. 2002; Vavilin et al. 2008; Mairet et al. 2011) almost kinetics parameters in this study were in the reasonable range.

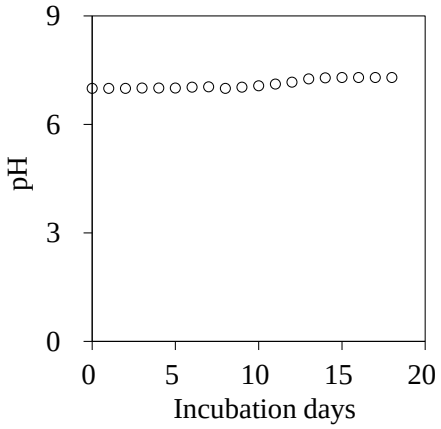

Figure 4. 11. pH changes in the batch reactor

4.4 Conclusions

Using the microorganisms grown in the steam explosion wastewater treatment from sugar cane bagasse, the anaerobic degradability of the soluble organics were evaluated in the batch test and following results were obtained.

The organic detected as total sugar was composed of readily biodegradable fraction and refractory fraction with the ratio of 66%: 34%. Similar to the total sugar, protein was classified into 2 kinds of fractions at 32%:68%. The origin of the un-biodegradable constituent was thought to be lingo-cellulose which was solubilized from the steam explosion pre-treatment.

Furfural and hydroxyl-methyl-furfural were immediately decomposed together with lactate and the biodegradable polysaccharide

Based on the responses from the batch experiment, the process map and the set of rate expressions were made. 22 state variables including 5 microorganisms were defined in the model.

40% of the TOC-based organics in the wastewater was biologically removed in the anaerobic condition, although temporal accumulation of acetate and propionate was observed during the test.

Chapter 5. High-rate Anaerobic Treatment of Steam Explosion Wastewater from Bioethanol Processing

5.1 Introduction

In bioethanol processing factories, new technologies using steam explosion pretreatments are developed to improve ethanol production from cellulose (*e.g.* sugar cane bagasse). However, the wastewater from this step with high chemical oxygen demand (COD), high soluble total organic carbon (S-TOC), low pH, strong odor and dark brown color (Steinwinder *et al.* 2011) causes serious environmental problems.

The great challenges of ethanol production is the use of all wastes left over from the process to reduce the environmental impact of this process and in order to utilize the energy content in an effective way. Therefore, biogas production can be a sustainable solution for the organic matter removal from effluents (Zheng et al. 2014).

High-rate anaerobic treatment processes are rapidly becoming popular for industrial wastewater treatment. Advantages of the process are low energy consumption, short hydraulic retention times (HRTs) and high organic loading rates (OLRs) (Rajesh Banu et al. 2006; Rajinikanth et al. 2009). The technologies applied high-rate anaerobic digestion include: fixed-bed reactors (FBR), upflow anaerobic sludge blanket (UASB), moving-bed biofilm reactor, expanded granular sludge beds (EGSB), sequencing batch reactors and anaerobic hybrid/hybrid upflow anaerobic sludge blanket reactors (Rajinikanth et al. 2009). This chapter focused on the anaerobic wastewater treatment from the bioethanol production using high-rate reactors (UASB and FBR). To express the reactor

performances and biological degradability of the wastewater organics in mathematical manner, a kinetic model was developed based on a modification of Anaerobic Digestion Model No. 1 (ADM1) and Activated Sludge Models (ASMs).

5.2 Materials and methods

5.2.1 Continuous anaerobic reactors

A lab-scale continuous upward anaerobic sludge blanket reactor was operated at 35±2°C with a working volume of 6 liters while a lab-scale continuous fixed-bed reactor (filled with short plastic tube with 10 mm height and 8 mm diameter corresponding to 350 m^2-carrier surface/m^3-reactor) with a working volume of 10.8 liters was also simultaneously operated (Figure 5. 1). Granules from an UASB reactor which was operated to treat food waste, was used as seed sludge for a lab-scale continuous UASB. Anaerobic inoculum for fixed-bed reactor was collected from a mesophilic digester at Hiagari municipal wastewater treatment plant, Kitakyushu, Japan operated at about 38-day hydraulic retention time receiving a mixture of primary and secondary sludge from a conventional BOD-removal activated sludge process. Since steam explosion wastewater (SEWW) was highly acidic, NaOH 1 mol/L and a pH controller were set up during the experiment while increasing the volumetric loading rate from 2.23 to 8.51 kg-COD/m^3/day (UASB) and 4.46 to 10.94 kg-COD/m^3/day (FBR) in a step-wise manner. The methane gas production rate at the fermenter was continuously logged using a wet gas meter (Shinagawa Corporation, Japan).

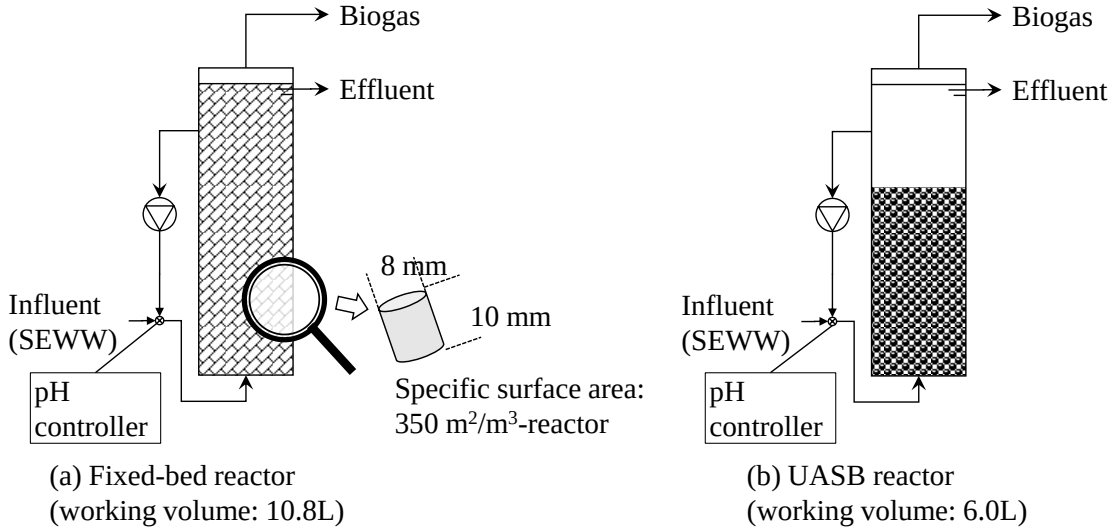

Figure 5. 1. Continuous anaerobic reactors (a): Fixed-bed reactor (FBR); (b): Upward anaerobic sludge blanket reactor (UASB)

5.2.2 Analytical procedures

Total solid (TS), suspended solid (SS), total volatile solid (TVS), chemical oxygen demand (COD), soluble total organic carbon (S-TOC), total nitrogen (T-N), ammonium nitrogen, total phosphorus (T-P) and inorganic cations concentrations, respectively were measured according to #2540 B, D, E, #5220 D, #5310 B, #4500-N B, #4500-NH_3 F, #4500-P E and 3120-B in Standard Methods (APHA *et al.* 2012). Phenol-Sulphuric acid method (DuBois *et al.* 1956) was used to measure soluble carbohydrate (as total soluble sugar concentration). From carbon/nitrogen (C/N) ratio and Kjeldahl nitrogen soluble protein concentration was estimated. Glucose and egg albumin were used for these standards, respectively (Kishida chemicals, Japan). As protein and polyphenolic compounds (as soluble lignin concentration) were analyzed by the Lowry-Follin method (Lowry *et al.* 1951), the concentration of lignin was calculated by subtracting the previous protein concentration. The factor of the soluble lignin on Lowry-Folin method was determined based on an alkali-extracted lignin reagent (Tokyo chemical industry, Japan). An ultra-performance liquid chromatography system equipped with a refractive index detector (wave length: 275 nm, Acquity Ultra Performance LC, Waters Corporation, USA) was used to measure two kinds of derivatives from sugars furfural ($(C_4H_3O)CHO$) and hydroxyl-methyl-furfural (HMF, $(C_4H_3O)CHOHCHO$)). The elute flow rate was set at 0.2 mL/min with mobile phase having 10% acetonitrile and 90% ultra-pure water under 40 °C while Acquity UPLC HSS T3 column (1.8 µm 2.1 × 100 mm) was used in the system. An ion chromatography system equipped with Ion Pac AS11-HC column (ICS-1000, Thermo Fisher Scientific Inc., USA) was applied to detected low-molecule fatty acids below C5 and inorganic anions. The elute flow rate was set at 1 mL/min with 4 mol/L of hepta-fluoro-butyric acid for fatty acids and 4 mol/L of KOH for anions measurement at 35 °C. In addition to formate, acetate, propionate and lactate, a small amount of oxalate was detected in the wastewater but the fate of this compound was not considered in this study because of negligibly low concentrations (ca. 19 mg-COD/L).

5.2.3 Dynamic simulation

Due to the model structure complexity of UASB reactor, the dynamic simulations focused on the fixed-bed reactor's responses including the methane production, soluble TOC,

suspended solid as well as the soluble effluent constituents in terms of carbohydrate, protein, propionate, acetate, lignin and ammonium nitrogen. The system responses were simulated using GPS-X ver. 6.4 (Hydromantis Environmental Software Solutions Inc., Canada). The simulation layout for the fixed-bed reactor is shown in Figure 5. 2. For simulating the reactor performances and biological degradability of the wastewater organics in mathematical manner, a kinetic model was developed based on a modification of ADM1 and ASMs. Although ADM1 and ASMs were initially referred to model the set of reactions, the individual process expression were considerably modified in order to include the fates of furfural, HMF, lactate and formate. An anaerobic biological reaction map for the organics in steam explosion wastewater is shown in Figure 5. 3. Considering the soluble nature of organics in SEWW, the process map included hydrolysis (r1-r2), acidogenesis (r3-r7), acetogenesis (r8), methanogenesis (r9-r11) and decay (r12-r16). Monosaccharide, furfural, HMF and lactate was classified in carbohydrate species while formate and hydrogen were degraded by the hydrogenotrophic methanogen. The decayed products were defined to be carbohydrate, protein and un-degradable particulate, which was an analogy of ASM3. Contois type (from ASMs), Monod type and first-order type (from ADM1) were applied to express the reaction rates. Although the acidic failure term due to the VFAs accumulation on methanogenic organisms was expressed in chapter 3, considering the pH changes during the experimental period this concept was not included in the study. However, a noncompetitive inhibition function was added for the hydrogen inhibition on propionate degradation. Although diffusion resistance of soluble substrates in the biofilm was not incorporated in the model, by applying high half-saturation coefficients (K_s) of process rates the impact of biofilm to organic digestion performance was considered. Kinetics for individual organic in SEWW were defined from simulation results of the batch biological experiment, which was conducted by mixing anaerobic sludge from a lab-scale continuous fixed-bed reactor and SEWW (chapter 4). Based on the MPR response, the degradation of organics in SEWW as well as the production of intermediates, kinetic parameters were determined. As the material balance of the model was COD basis, COD factors were shown as in Table 5. 1.

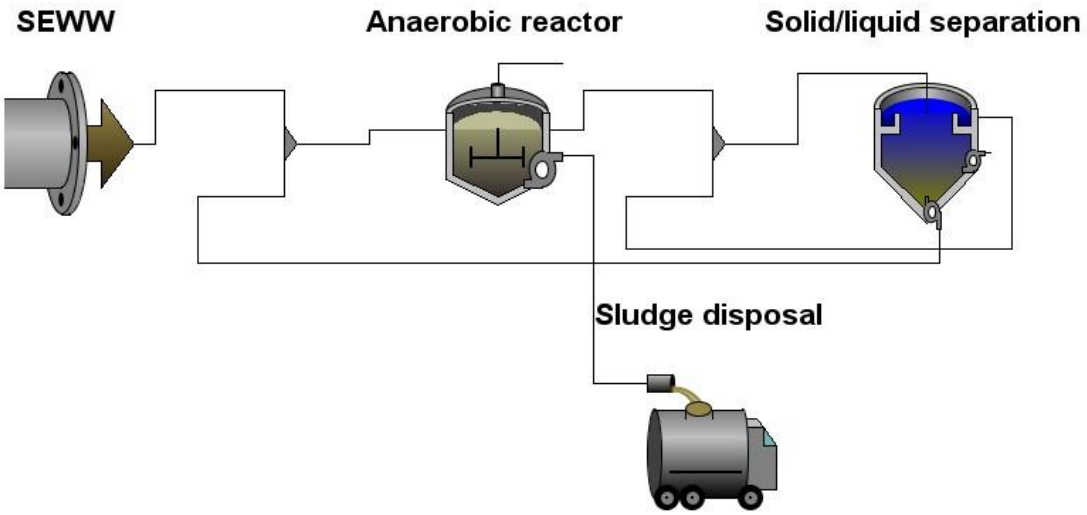

Figure 5. 2. Simulation layout of the fixed-bed reactor

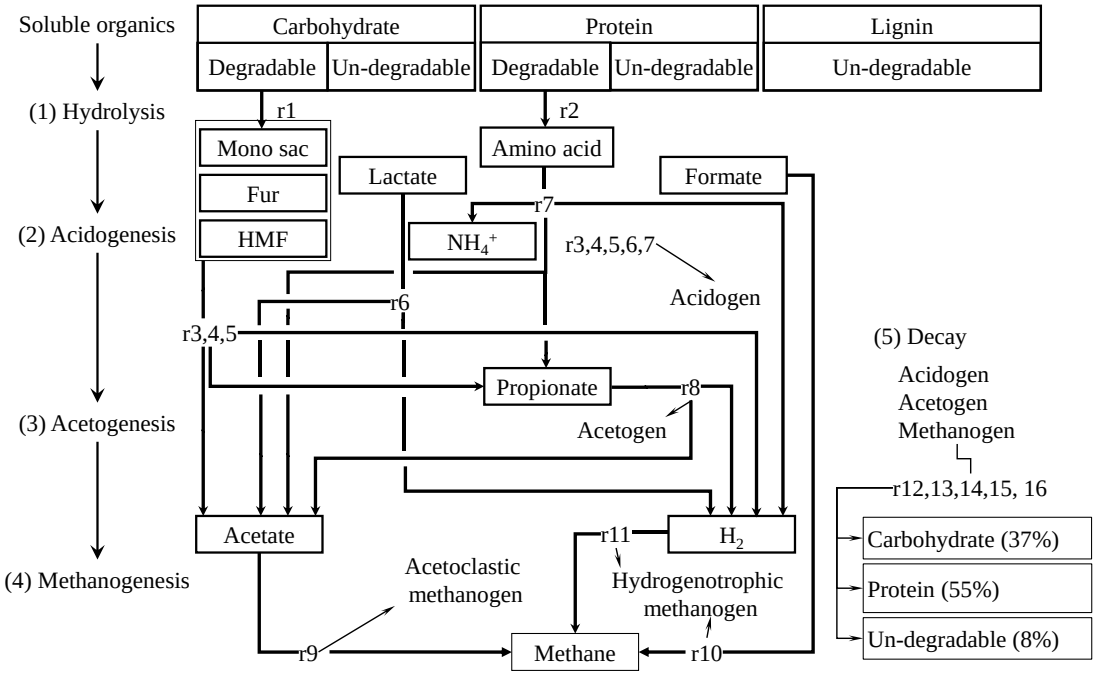

Figure 5. 3. Anaerobic biological reaction map for the organics in steam explosion wastewater

5.3 Results and discussions

5.3.1 Compositions of steam explosion wastewater

The characterizations of 3 steam explosion wastewater samples used for the continuous experiment are shown in Table 5. 1. In general, the wastewater was acidic with pH in the range of 2.61-3.03. This wastewater also contained high COD (more than 21,000 mg-COD/L) and TOC concentrations (8,784-9,684 mg-C/L), strong smell and dark brown color which mainly comes from high lignin concentration (from 5,521 to 6,929 mg/L). Carbohydrate (8,070-13,642 mg/L) contributed significantly to the compositions of the steam explosion wastewater while concentrations of protein, sugar derivatives (furfural and hydroxyl-methyl-furfural) and low-molecule fatty acids accounted for small amount. Total nitrogen, total phosphorus, ammonium nitrogen, inorganic cations/anions were also measured to catch the constituents of the wastewater, but these concentrations were not remarkable.

Table 5. 1. List of steam explosion wastewater parameters for continuous experiment

Parameter Unit: mg/L except pH	COD factor	Steam explosion wastewater		
		Sample 1 (day 0-66)	Sample 2 (day 67-107, 143-160)	Sample 3 (day 108-142)
pH		2.61	2.87	3.03
Total solid		17,419	18,347	17,073
Total volatile solid		17,000	17,900	16,700
COD		24,100	26,250	21,390
TOC		8,784	9,684	9,375
Carbohydrate	1.07	9,825	8,070	13,642
Protein	1.4	581	650	691
Lignin	1.87	6,020	5,521	6,929
Furfural	1.67	510	689	1,743
Hydroxyl-methyl-furfural	1.52	1,009	1,129	544
Formate	0.35	1,294	1,529	700
Acetate	1.07	1,583	1,597	797
Lactate	1.07	1,687	732	412
Oxalate	0.18	107	70	156
Propionate	1.51	ND	45	15
Butyrate	1.82	ND	ND	52
Total nitrogen		175	196	209
Total phosphorus		30	31	21
Ammonium nitrogen		5.5	6.5	7.4
Na^+		113	99	145
K^+		42	40	23
Ca^{2+}		87	77	76
Mg^{2+}		40	38	28
Cl^-		21	18	8
SO_4^{2-}		80	111	87
Acid-insoluble materials (assumed to be silicate)		316	305	259

ND: Non detected

5.3.2 Volumetric loading rate and suspended solid

Figure 5. 4 showed the volumetric loading rate and suspended solid concentration in fixed-bed reactor and UASB reactor. As can be seen that the volumetric loading rate were started to 2.23 kg-COD/m^3/d (UASB) and 4.46 kg-COD/m^3/d (FBR) at initial phase and continue to increase to achieve the VLR of 8.51 and 10.94 kg-COD/m^3/d, respectively after 160 days of operation. The concentration of suspended solid fluctuated in the narrow range of 100-300 mg/L in FBR and 64-280 mg/L in UASB. According to the characteristics of two reactors, UASB need much time to make granules which were applied to treat wastewater. Therefore the amount of biomass in FBR was little higher than that in UASB.

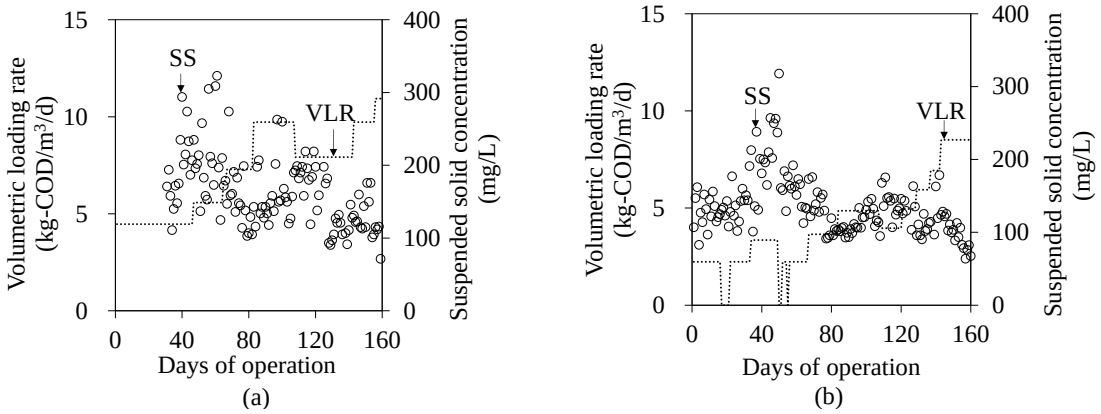

Figure 5. 4. Volumetric loading rate and suspended solid concentration in two reactors ((a): FBR, (b): UASB)

5.3.3 Soluble TOC concentration

Soluble TOC concentration in two reactors is summarized in Figure 5. 5. In FBR with the VLR of 4.46 kg-COD/m^3/d the S-TOC removal efficiency was the highest at 72.4%. It is clear that the increase in VLR from 4.46-10.94 kg-COD/m^3/d caused the reduction in S-TOC removal efficiency and obtained the average value of 64%. Nevertheless, during the operation the fixed-bed reactor kept an acceptable S-TOC concentration (3,300 mg-C/L). In contrast with FBR when the VLR increased from 2.23-3.35 kg-COD/m^3/d, a remarkable increase in soluble organics (from 2,000-4,000 mg-C/L) in UASB reactor was observed. As the result, the feeding of wastewater was discontinued at day 51. After that,

S-TOC decreased and kept stable at the value of 2,700 mg-C/L together with the average S-TOC removal efficiency of 72%. Possibly, due to the difference in VLR, UASB reactor achieved higher S-TOC removal efficiency than FBR. Although, during the experiment no significant increase in S-TOC in FBR proved that the adaptation of biomass in FBR was better than that in UASB reactor.

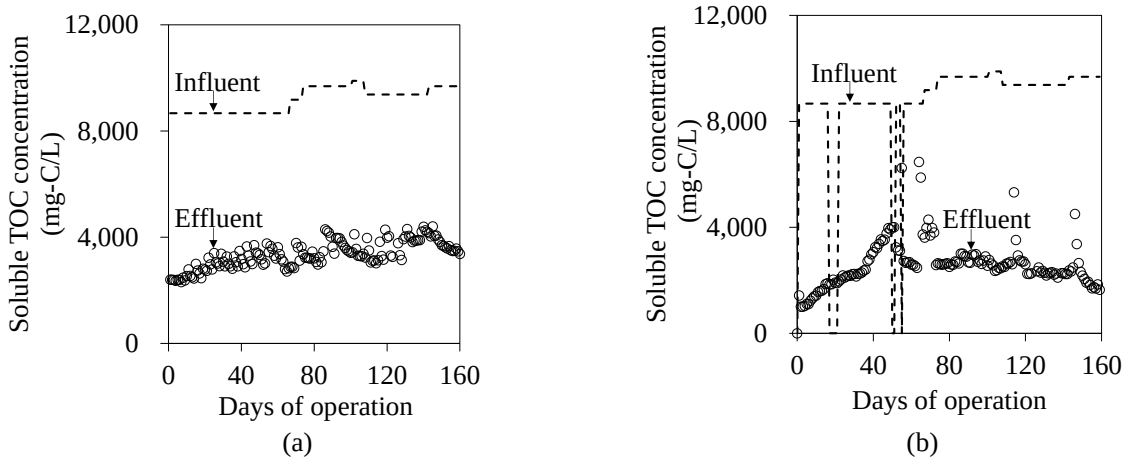

Figure 5. 5. Soluble TOC concentration in two reactors ((a): FBR, (b): UASB)

5.3.4 Methane production rate and methane conversion efficiency

pH changes, CH_4 production rate and CH_4 conversion efficiency in two reactors were plotted as shown in Figure 5. 6. pH in both reactors was always kept stable around 7.00 due to the presence of NaOH 1 mol/L and pH controller. Methane production rate was correspondingly to the increase and decrease of volumetric loading rate. It suggests that the substrates in the reactor were biodegraded and converted into methane gas. Due to the technical problems during the start-up period for UASB, the VLR was stopped from day 18-22, the MPR was also decreased from that day. After that, increasing the VLR to 3.35 kg-COD/m^3/d at day 34 the accumulation of S-TOC in UASB in the period of 10 days (from day 40) was observed together with the decrease in MPR from 7.1 to 1.5 Normal-L/L/d. Then, the VLR was discontinued at day 51-52, soluble organics were degraded gradually and converted to methane until day 142. Since the VLR increased to 8.51 kg-COD/m^3/d, S-TOC started to increase in several days, as the result a decline in MPR was seen. Nevertheless, about 50% of steam explosion wastewater COD was converted to

methane in both reactors as calculated in Figure 5. 6.

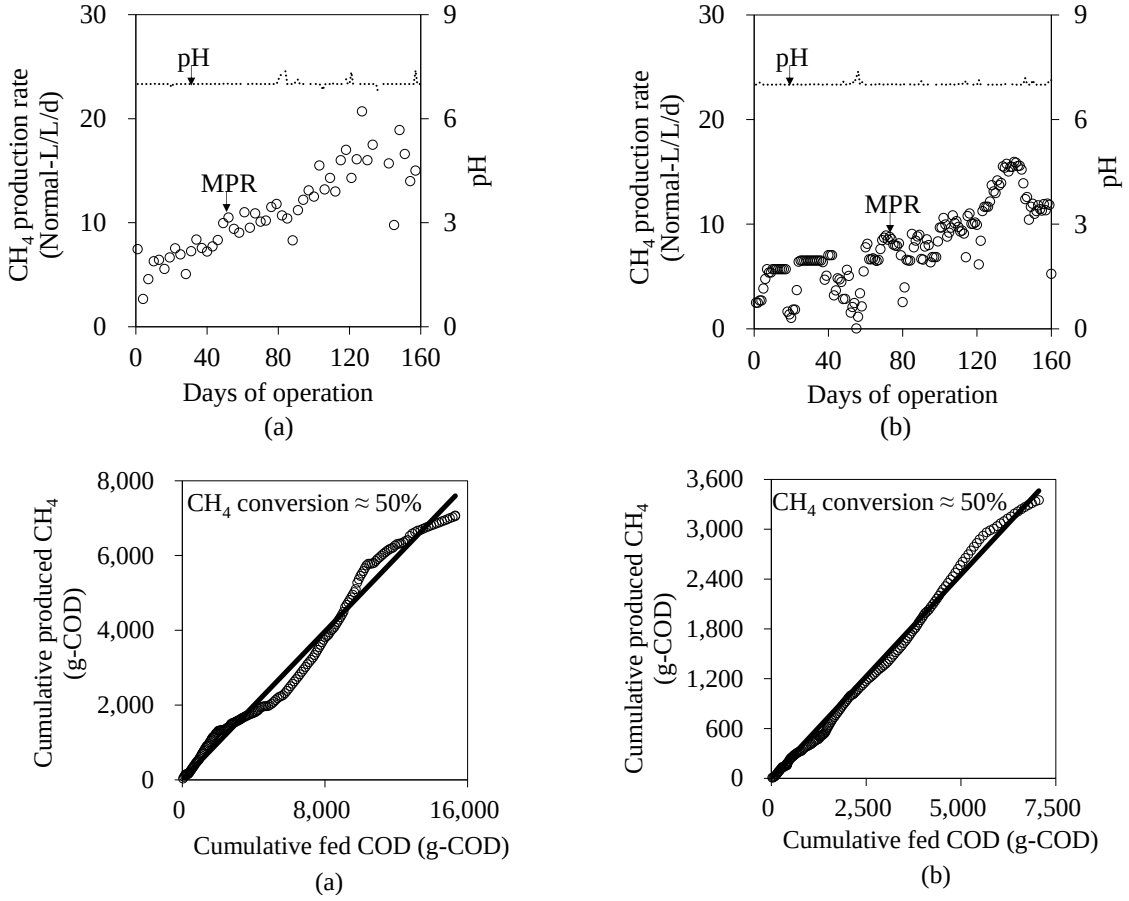

Figure 5. 6. pH changes, CH_4 production rate and CH_4 conversion efficiency in two reactors ((a): FBR, (b): UASB)

5.3.5 Compositions in the effluent

The soluble effluent constituents in terms of carbohydrate, protein and lignin are summarized in Figure 5. 7. Comparing the total carbohydrate concentration in the influent, the rest of around 713 mg-COD/L (FBR) and 670 mg-COD/L (UASB) of the un-biodegradable organic retained in the reactor indicating that almost carbohydrate was degraded, while the remarkable amount of un-biodegradable protein (293 mg-COD/L in FBR and 270 mg-COD/L in UASB) still retained during 160 days of operation. In addition, soluble lignin was not degraded through the experiment period and considered as the soluble inert. The ammonia nitrogen (Figure 5. 8) produced from the protein

decomposition was kept in the low concentration (3.5-7 mg-N/L in FBR and 2.5-30 mg-N/L in UASB). As can be seen in Figure 5. 8 from day 83, when the VLR in FBR increased to 9.72 kg-COD/m^3/d, the accumulation of propionate in the reactor was observed. Although the VLR decreased slightly to 7.92 kg-COD/m^3/d at day 108, the concentration of propionate was still high at 2,300 mg-COD/L. However, after the period of adaptation, propionate was decomposed to acetate, as the result acetate was kept at acceptable level (100-250 mg-COD/L) in FBR. In addition, as explained in previous section, in the start-up period for UASB, a remarkable accumulation of propionate (2,200 mg-COD/L) was occurred and VLR was stopped from day 18-22. After fixing the problems and increasing the VLR to 3.35 kg-COD/m^3/d at day 34 the considerable increase in propionate (more than 2,700 mg-COD/L) in 10 days (from day 40) was observed. Nevertheless, when the operation of UASB was stable, the concentration of acetate and propionate was kept in an acceptable range (less than 1,000 mg-COD/L).

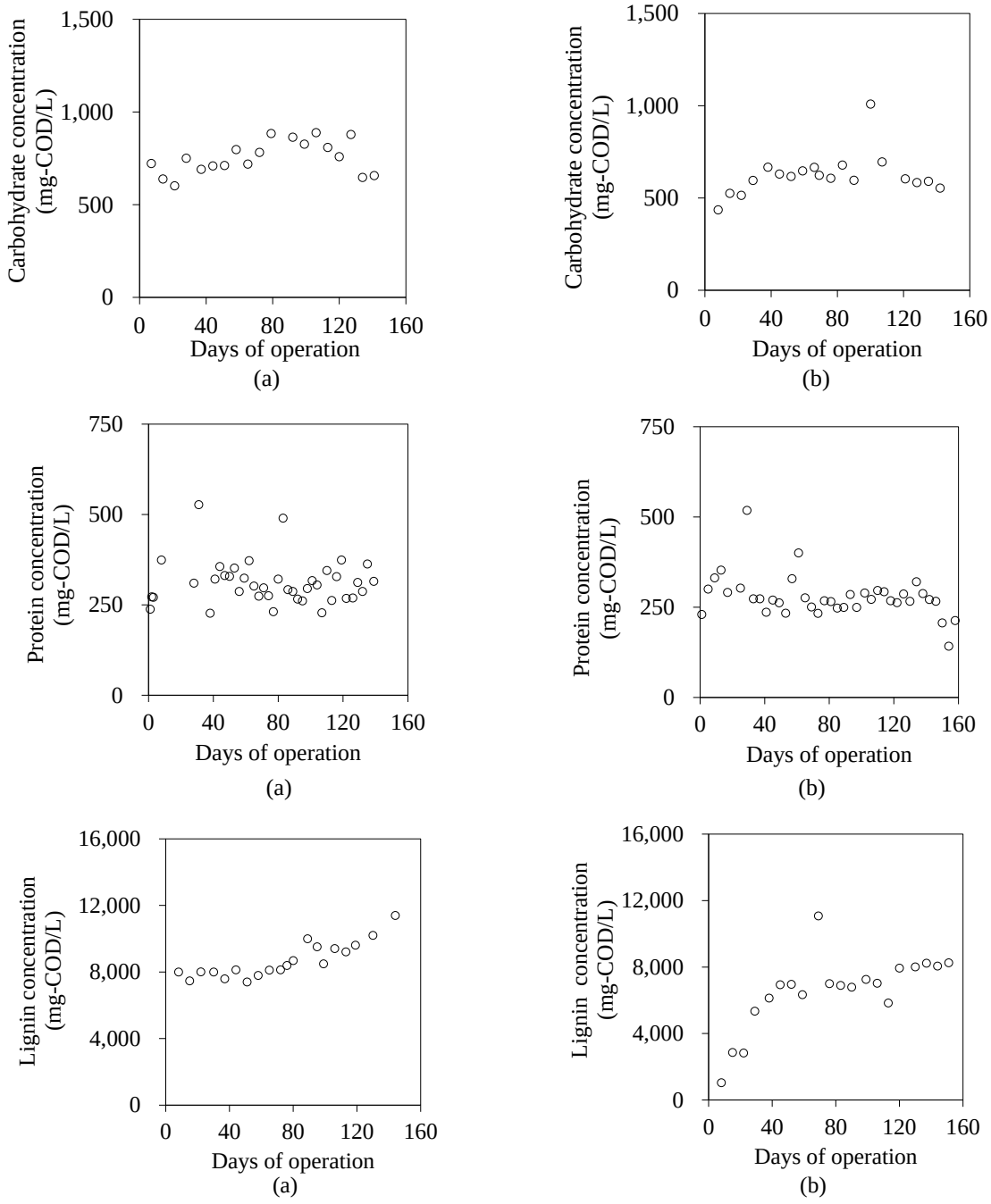

Figure 5. 7. Carbohydrate, protein and lignin concentration in two reactors ((a): FBR, (b): UASB)

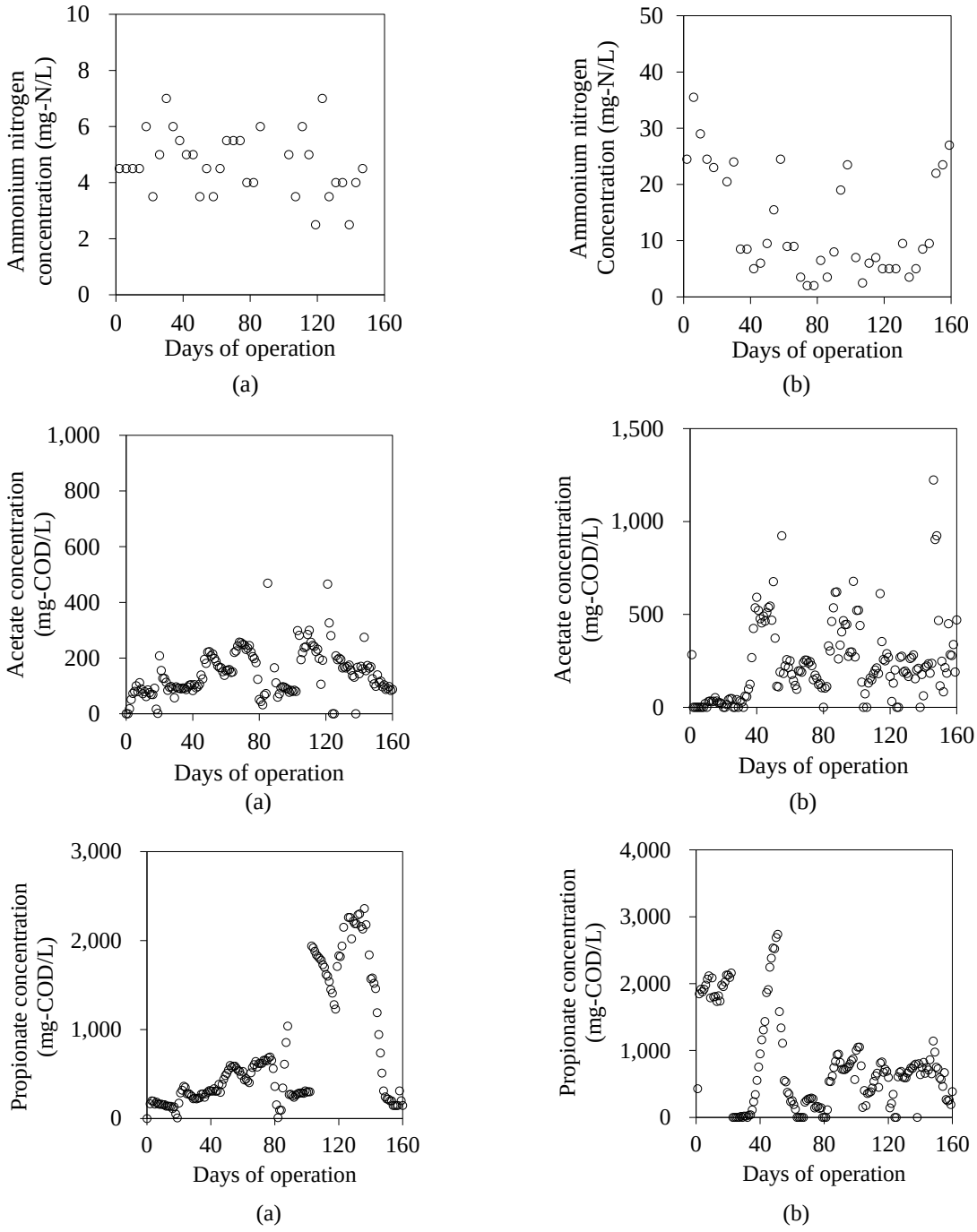

Figure 5. 8. Ammonium nitrogen, acetate and propionate concentration in two reactors ((a): FBR, (b): UASB)

5.3.6 Model calibration

The initial biomass concentrations (Table 5. 2) was used to simulate the performances of fixed-bed reactor (Figure 5. 9). High half-saturation coefficients (K_s) of process rates were used for simulation. Since high K_s was applied the role of biofilm process in fixed-bed reactor was integrated. Nevertheless, the other kinetic parameters for individual organics were almost referred from the results of batch test which conducted in chapter 4 and listed in Table 5. 3. However, the maximum specific uptake rate of propionate (21.5 d^{-1}) and acetate (10 d^{-1}) were remarkably higher than that calibrated from batch test (5 d^{-1} for propionate and 3.8 d^{-1} for acetate). The concentration of the propionate degrader was obtained focusing on the reaction rate of the hydrogenotrophic methanogenic biomass, formate and propionate concentrations in the reactor. To express the hydrogen inhibition for the propionate degrader, a pair of K_I = 0.003 mg-COD/L and m = 0.118 was applied. Moreover, the kinetic of the methanogens on the growth was estimated from the elevation/decrease of MPR.

Table 5. 2. List of initial biomass concentrations

Microorganisms	Concentration (mg-COD/L)
Sugar degrader	400
Amino acid degrader	400
Propionate degrader	300
Acetate utilizer	340
Hydrogen utilizer	300

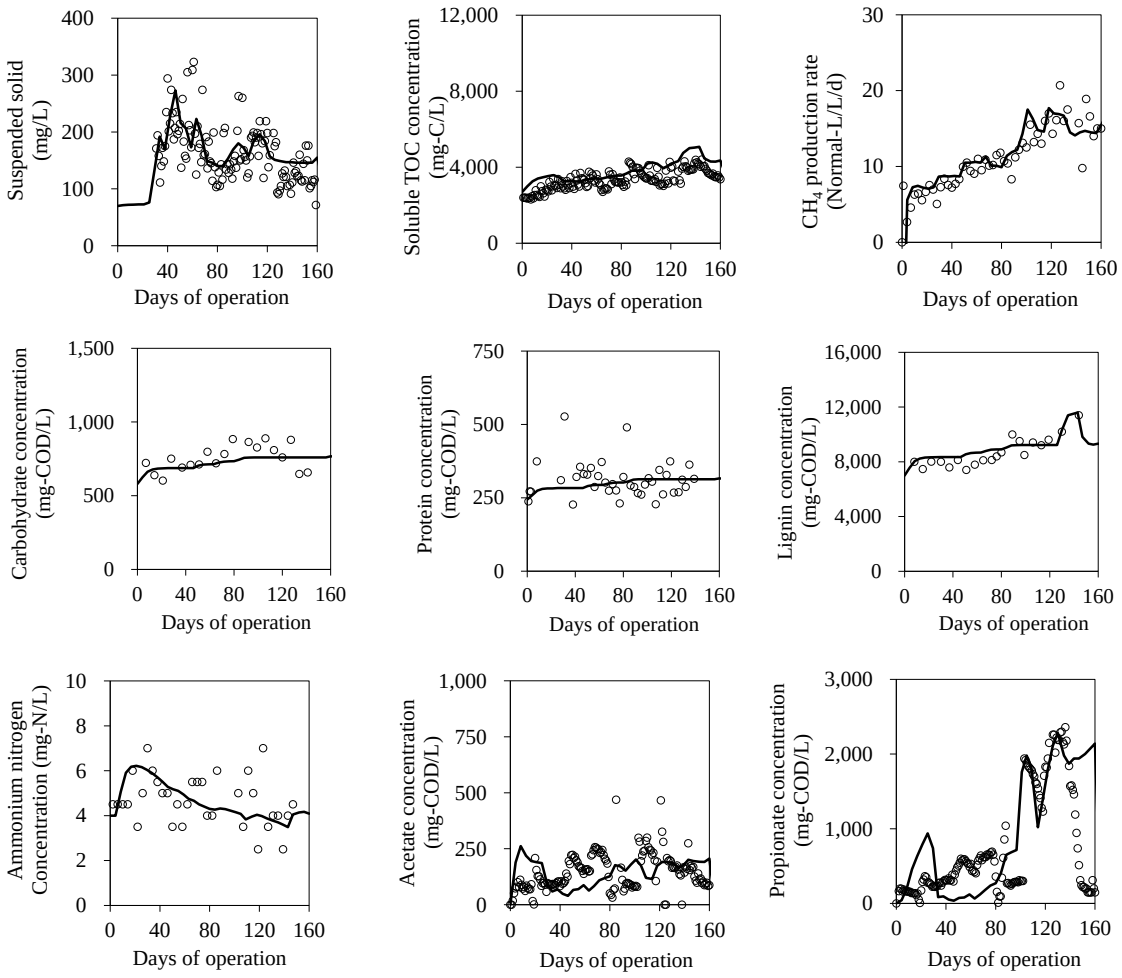

Figure 5. 9. Simulation results for fixed-bed reactor (Unfilled circles: experiment, solid lines: simulation)

Table 5. 3. List of kinetics for anaerobic degradation of steam explosion wastewater

Kinetics	Maximum specific rate (d^{-1})		Half-saturation coefficient (mg-COD/L, -)	
	This study	Batch test	This study	Batch test
Hydrolysis of carbohydrate	10	10	8	8
Hydrolysis of protein	4	4	15	15
Uptake of monosaccharide	3	3	250	10
Uptake of furfural	10	Nil	250	10
Uptake of HMF	10	Nil	250	10
Uptake of lactate	10	Nil	250	10
Uptake of amino acid	2	2	100	10
Uptake of propionate	21.5	5	110 (uptake) 0.003 (inhibition K_I) 0.118 (inhibition m)	10 (uptake) 0.008 (inhibition K_I) 0.05 (inhibition m)
Uptake of acetate	10	3.8	300	5
Uptake of formate	18	Nil	250	5
Uptake of hydrogen	3.4	3	10	10
Decay of sugar degrader	0.01	0.01	Nil	
Decay of amino acid degrader	0.01	0.01	Nil	
Decay of propionate degrader	0.01	0.01	Nil	
Decay of acetate utilizer	0.01	0.01	Nil	
Decay of hydrogen utilizer	0.01	0.01	Nil	

5.3.7 Concentration of microorganisms and sludge withdrawal in the fixed-bed reactor

The dynamic change for acidogens (sugar degrader, amino acid degrader), acetogens (syntrophic propionate degrader) and methanogens (acetate utilizer and hydrogen utilizer) were calculated as shown in Figure 5. 10. Sugar degrader was remained in the reactor at high concentration while amino acid degrader and propionate degrader decreased quickly. The calculated two kinds of active methanogens was kept stable in the reactor.

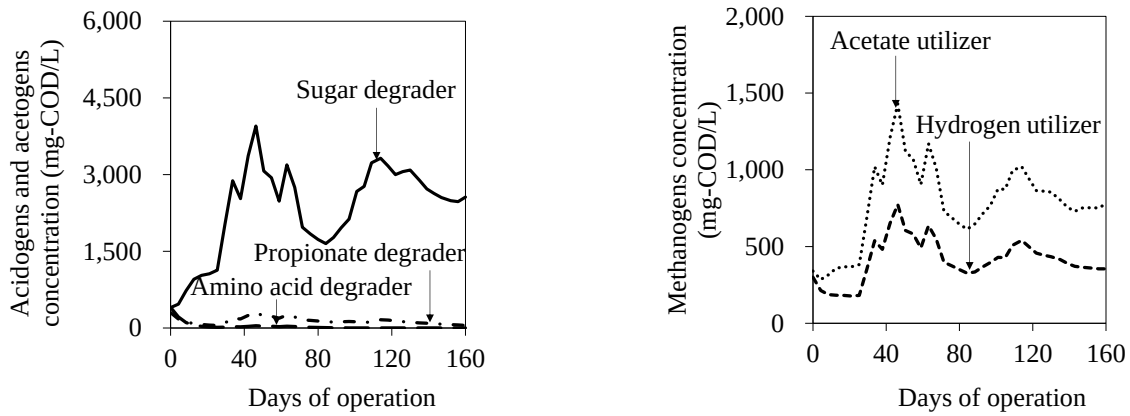

Figure 5. 10. Calculated active biomass concentrations

On the other hand, based on the SS concentration the amount of sludge withdrawal was calculated per day (Figure 5. 11) and from that, cost for disposal of sludge will be estimated. Furthermore, this will be helpful for the design of steam explosion wastewater treatment plant from bioethanol processing.

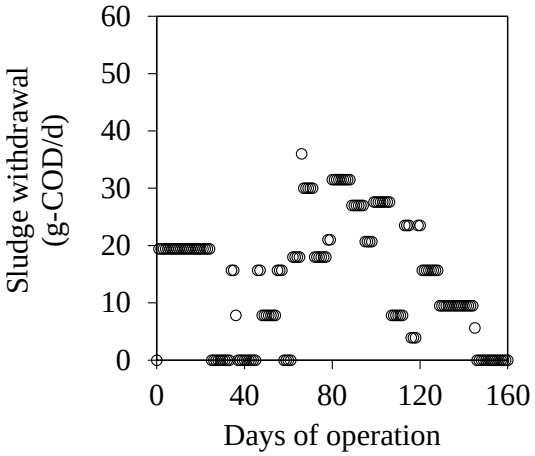

Figure 5. 11. Sludge withdrawal in fixed-bed reactor

5.3.8 Simulation with various VLR at steady state condition

To predict the CH_4 conversion efficiency at different VLR the simulations at steady state condition were conducted. As shown in Table 5. 4 and Figure 5. 12 an insignificant difference of methane conversion efficiency (45-50%) at the VLR from 4.46-9.72 kg-

COD/m^3/d was obtained. Although high organic loading rate (9.72 kg-COD/m^3/d) was applied, 45% of COD was converted to methane with soluble COD and soluble TOC concentrations in the effluent of 11,120 mg-COD/L and 3,604 mg-C/L, respectively.

Table 5. 4. CH_4 conversion efficiency at different VLR in steady state condition

#	VLR (kg-COD/m^3/d)	S-COD_{eff} (mg-COD/L)	CH_4 (kg-COD/m^3/d)	CH_4 conversion efficiency (%)
1	4.46	9,571	2.23	50
2	5.58	10,190	2.75	49
3	7.29	10,350	3.36	46
4	9.72	11,120	4.37	45

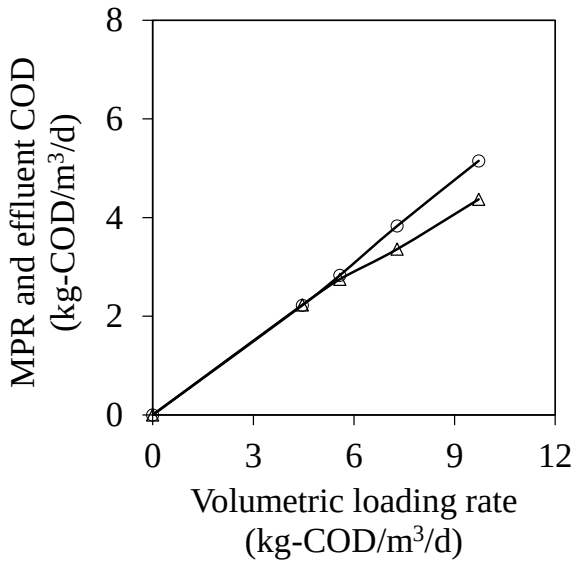

Figure 5. 12. Methane production rate and S-COD concentration at different volumetric loading rates in steady state condition

5.4 Conclusions

The high-rate reactors could be applied to treat steam explosion wastewater from bioethanol processing with volumetric loading rate of 10.94 kg-COD/m^3/d (FBR) and 8.51 kg-COD/m^3/d (UASB).

Most of the organics in the wastewater were supposed to be readily biodegradable except lignin. The average soluble TOC removal efficiencies were 72% (UASB) and 64% (FBR) with a methane conversion efficiency of about 50% for both reactors.

A kinetic model based on a modification of ADM1 and ASMs was used to simulate reasonably the methane production, soluble TOC, suspended solid as well as the soluble effluent constituents in terms of carbohydrate, protein, propionate, acetate, lignin and ammonium nitrogen in FBR. The role of biofilm on digestion efficiency was considered by using high K_s for process rates.

The simulation results at steady state showed that 45% of COD was converted to methane gas with high organic loading rate (9.72 kg-COD/m^3/d).

Chapter 6. Post-treatment of Steam Explosion Wastewater from Bioethanol Processing

6.1 Introduction

Pretreatment of sugar cane bagasse by steam explosion in bioethanol processing generates large volumes of wastewater that is of serious environmental concern. This wastewater is characterized by high organic strength (Steinwinder *et al.* 2011). Anaerobic digestion was suitable process for the wastewater biological treatment (Torry-Smith *et al.* 2003; Uellendahl & Ahring 2010; Choeisai *et al.* 2014; Narra & Balasubramanian 2015). However, the biological processes cannot remove un-biodegradable materials (lignin) as well as color existed in the wastewater. The dark brown color comes from the degradation process of lignocelluloses and is measured indirectly by lignin concentration in the effluent stream (Sari *et al.* 2015). The pollutant can be minimized in available physico-chemical techniques including membrane filtration, adsorption, coagulation/flocculation and advanced oxidation processes (AOPs) (Andersson *et al.* 2011; Shankar *et al.* 2013; Abu Zahrim Yaser 2014).

Oxidation is the most commonly used oxidants (ozone, chlorine, hypochlorite, $OH^{\bullet}$ radical) to breakdown the big molecules to smaller fractions. Coagulation/flocculation method using inorganic coagulants, organic flocculants is one of the best option to treat this wastewater because it is cheaper than other methods (*e.g*. membrane filtration and oxidation process) (Irfan *et al.* 2013; Sari *et al.* 2015). Coagulation is defined as the destabilization of suspension, allowing particle collision and growth of flocs. Flocculation describes the process in which the destabilized particles are agglomerated to form larger aggregates (Bratby 2006; Gregory 2006). On the other hand, adsorption on activated carbon (AC) is widely applied for removal of color and specific organic pollutants due to

its extended surface area, microporus structure and high adsorption capacity (Mane *et al.* 2006; Satyawali & Balakrishnan 2007).

This chapter aimed to determine decolorization and un-degradable removal rate of wastewater by using physico-chemical methods. The efficiency of oxidation and coagulation/flocculation process were evaluated by using different concentrations of sodium hypochlorite (NaClO) and poly aluminum chloride (PAC). In addition, the ability of activated carbon (AC) to decolorize in the wastewater was also studied.

6.2 Material and methods

6.2.1 Experiment for oxidation and coagulation/flocculation

Figure 6. 1 shows experiment process of oxidation and coagulation/flocculation. The effluent from UASB reactor was treated by activated sludge process in 5 days with DO maintained at 1 mg/L to remove some remained biodegradable materials. Next, centrifuging at 8,000 rpm for 5 mins to separate sludge, the supernatant was partial oxidized with sodium hypochlorite (NaClO) (Wako pure chemical industries, Ltd, Japan) in the range of 0.01, 0.1, 0.5, 2, 5, 10, 25, 50, 100 and 200 mg/L and coagulated/flocculated using poly-aluminium chloride (PAC) (contain 30% of Al_2O_3- Osaka chemicals, Japan). The concentration of PAC changed from 50, 100, 150 and 200 mg/L. Then neutralizing pH and waiting for 30 minutes before separating sludge to analyze soluble TOC and color.

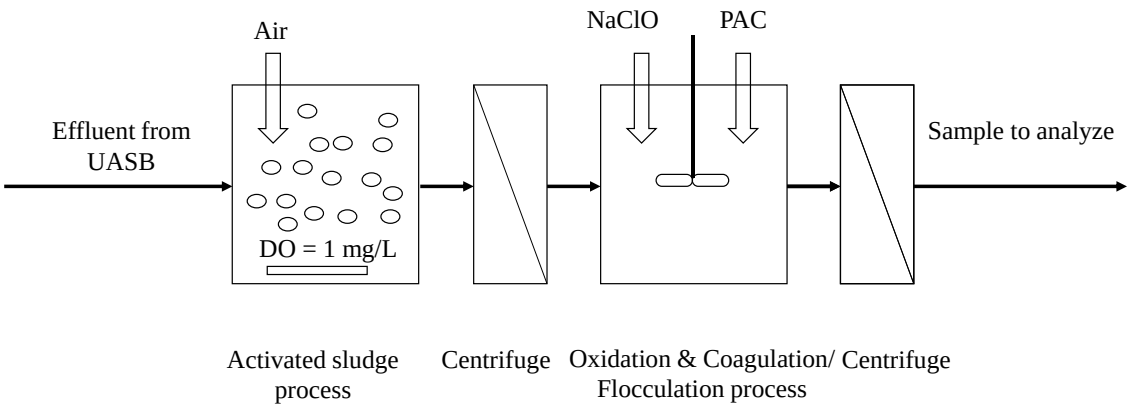

Figure 6. 1. Experiment process of oxidation and coagulation/flocculation

6.2.2 Experiment for adsorption

Figure 6. 2 shows experiment process of adsorption. 50 mL effluent from UASB reactor was added commercial activated charcoal (Wako pure chemical industries, Ltd, Japan) with different dosages (0, 25, 50, 100, 150, 200, 250, 300, 350, 400, 450 and 500 mg). The adsorbent-effluent mixture was kept agitated in 24 hours. The samples were analyzed soluble TOC and color after removal of the suspended activated carbon by centrifugation at 8,000 rpm in 5 mins.

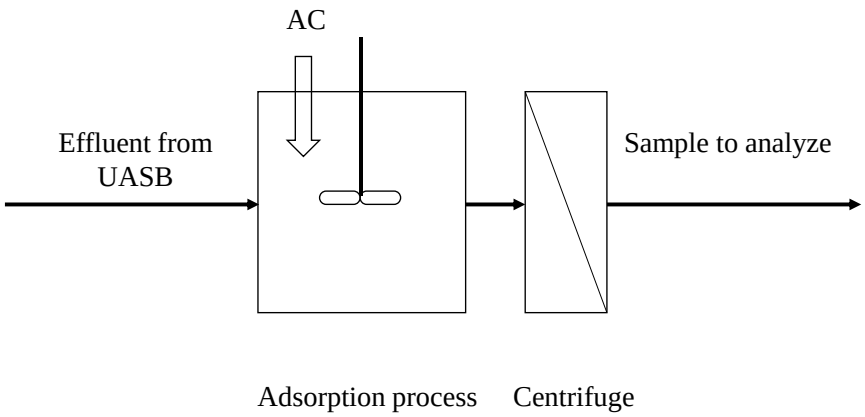

Figure 6. 2. Experiment process of adsorption

6.2.3 Experiment for combining oxidation, coagulation/flocculation and adsorption

Figure 6. 3 shows experiment process of oxidation, coagulation/flocculation and adsorption. Firstly, the effect of oxidation and coagulation/flocculation in different times was studied. Using 50 mg/L NaClO and 100, 300, 500, 750 and 1000 mg/L PAC to oxidize and coagulate/flocculate in 1, 2 and 3 times. After that adding commercial activated charcoal (Wako pure chemical industries, Ltd, Japan) with different dosages (0, 25, 100, 200 and 300 mg) in 25 mL of supernatant. Finally, the wastewater was discharged or recovered for other purposes.

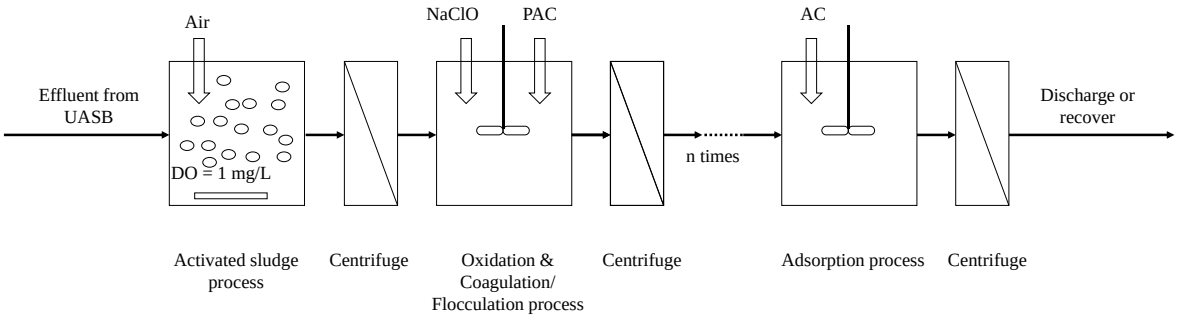

Figure 6. 3. Experiment process of combining oxidation, coagulation/flocculation and adsorption

6.2.4 Analytical procedures

Soluble total organic carbon (S-TOC) and color were measured according to #5310 B and 2120 C in Standard Methods (APHA *et al.* 2012).

6.3 Results and discussions

6.3.1 Removal of un-degradable materials by oxidation process

After aeration in 5 days soluble TOC concentration in the effluent (2,675 mg-C/L) decreased and kept stable at 1,644 mg-C/L while color unit changed from 12,514 to 9,142 ^{0}. Since a great part of the organic matter had already been removed in the anaerobic stage, the remaining biodegradable materials (38.5%) were decomposed in aerobic stage. Next, using NaClO to partly oxidize surface structure of lignin. The oxidation mechanism of lignin is shown in Figure 6. 4.

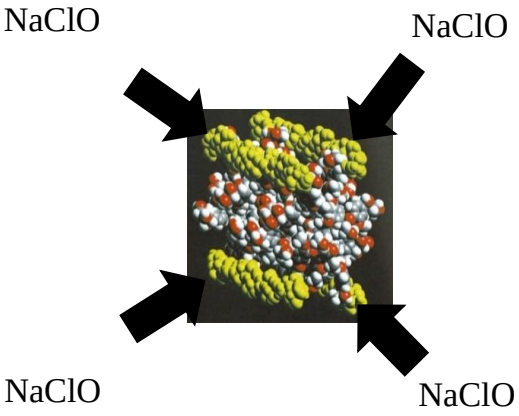

Figure 6. 4. Oxidation mechanism of lignin using NaClO

In addition, the changes of soluble TOC and color in the effluent at different oxidant concentrations are summarized in Figure 6. 5, Figure 6. 6 and Figure 6. 7. As can be seen that the concentration of soluble TOC and color unit seemed to be not change even high concentration of NaClO was used. Therefore, NaClO can only break down surface structure of lignin but cannot degrade lignin.

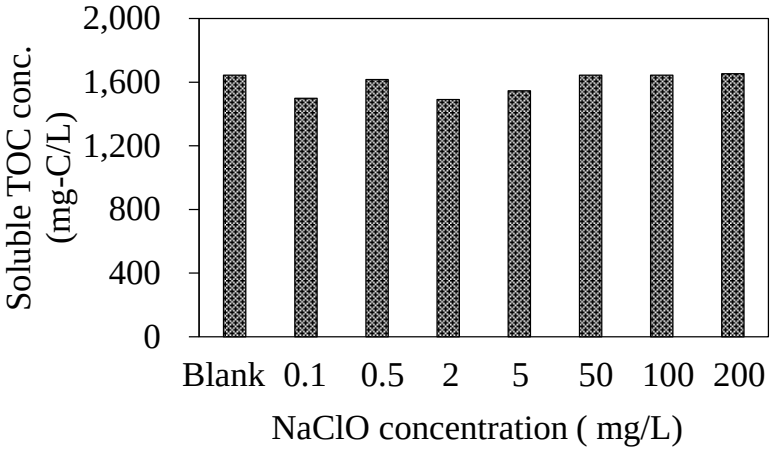

Figure 6. 5. S-TOC concentration at different NaClO concentrations

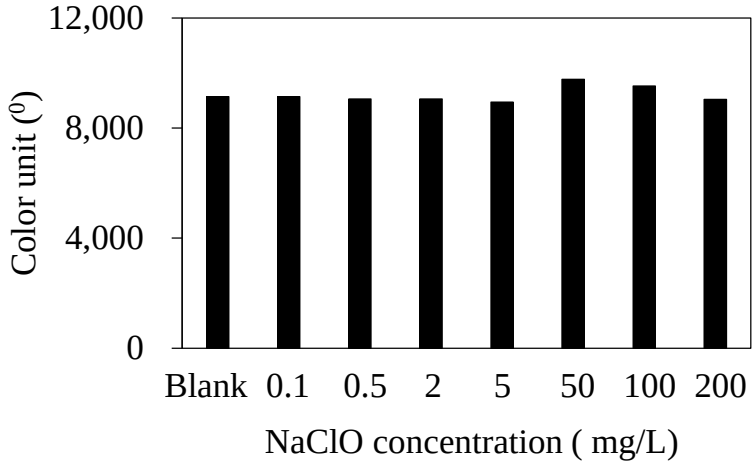

Figure 6. 6. Color unit at different NaClO concentrations

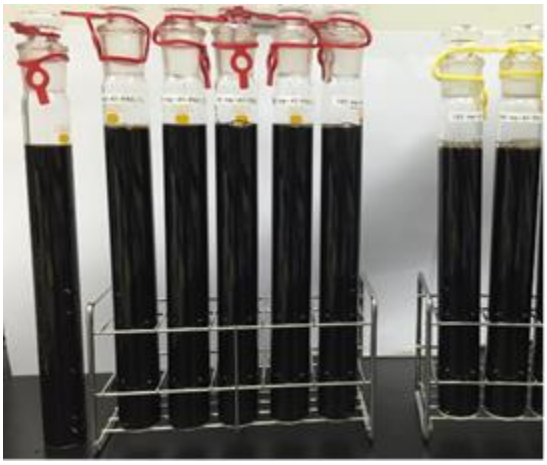

Figure 6. 7. Experimental photo for oxidation process
(from left to right: 0→ 200 mg/L NaClO)

6.3.2 Removal of un-degradable materials by oxidation and coagulation/flocculation process

Due to lignin in wastewater carries negative charge so that after addition of polymeric inorganic coagulant will hydrolyze rapidly to form cationic species, which are adsorbed by negatively charged colloidal particles, resulting in simultaneous surface charge reduction and formation of micro-flocs (Figure 6. 8). The effect of concentrations of PAC and NaClO for soluble TOC removal rate and decolorization are shown in the following figures.

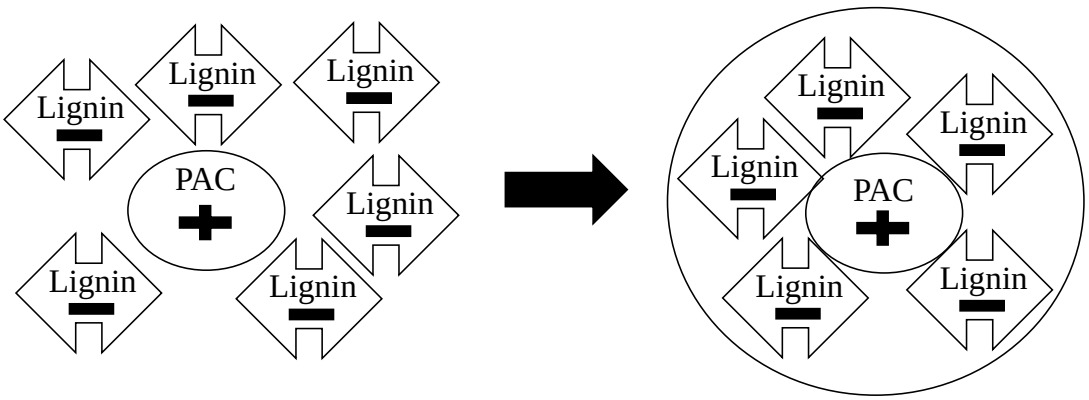

Figure 6. 8. Coagulation/Flocculation mechanism of lignin using PAC

Results from combining 50 mg/L of PAC and 50, 100, 200 mg/L of NaClO after aeration step (1,644 mg-C/L of S-TOC and 9,142 ^{0} of color unit) indicated that concentrations of soluble TOC and color changed insignificantly (Figure 6. 9 and Figure 6. 10).

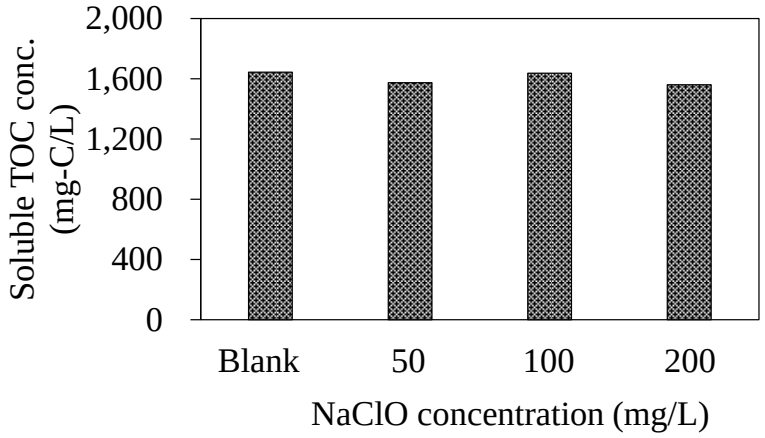

Figure 6. 9. S-TOC concentration at 50 mg/L PAC and different NaClO concentrations

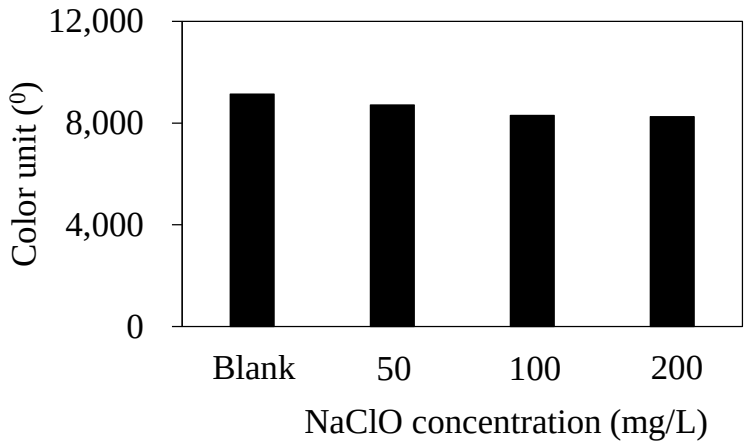

Figure 6. 10. Color unit at 50 mg/L PAC and different NaClO concentrations

As can be seen in Figure 6. 11 and Figure 6. 12 at 100 mg/L of PAC when the concentrations of NaClO were in range of 0.1-50 mg/L, soluble TOC and color removal rate increased from 23-29% and 31-63% while at 100 and 200 mg/L of NaClO the treatment efficiency decreased to 14-16% and 29-37%, respectively.

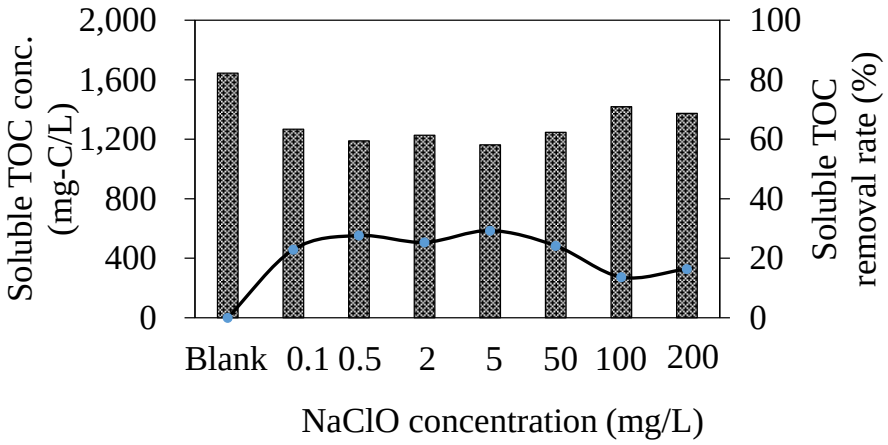

Figure 6. 11. S-TOC concentration and removal rate at 100 mg/L PAC and different NaClO concentrations

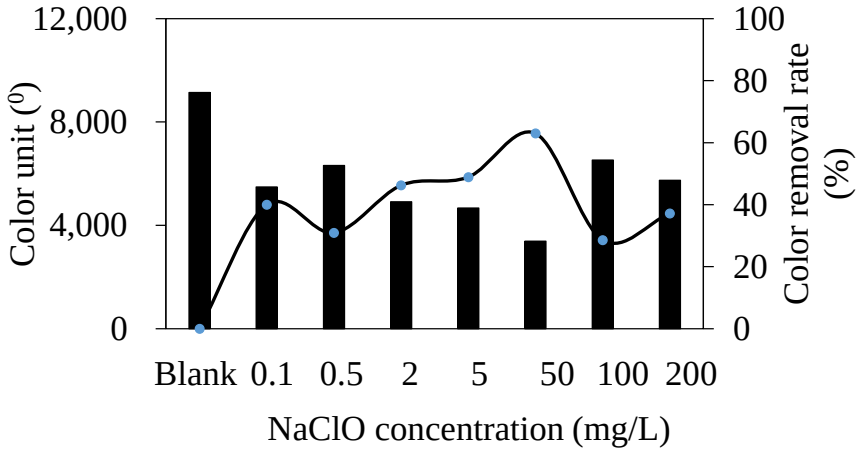

Figure 6. 12. Color unit and removal rate at 100 mg/L PAC and different NaClO concentrations

Figure 6. 13 and Figure 6. 14 shows soluble TOC and color removal rate at 150 mg/L PAC. With 100 mg/L NaClO the treatment efficiencies were highest (42% for S-TOC and 77% for color).

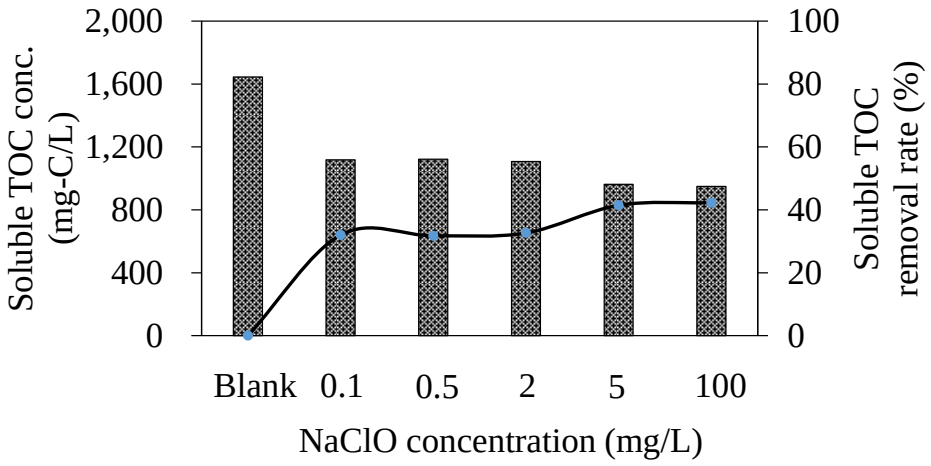

Figure 6. 13. S-TOC concentration and removal rate at 150 mg/L PAC and different NaClO concentrations

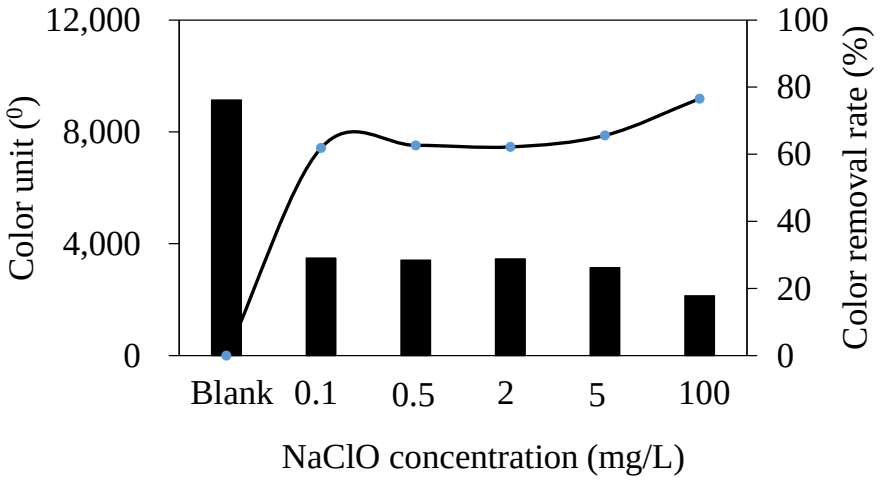

Figure 6. 14. Color unit and removal rate at 150 mg/L PAC and different NaClO concentrations

Although the concentration of PAC increased to 200 mg/L, soluble TOC removal rates only fluctuated in the range of 41-62% with 0.01-200 mg/L of NaClO while color removal rate was rather high (approximately 76%) (Figure 6. 15, Figure 6. 16 and Figure 6. 17).

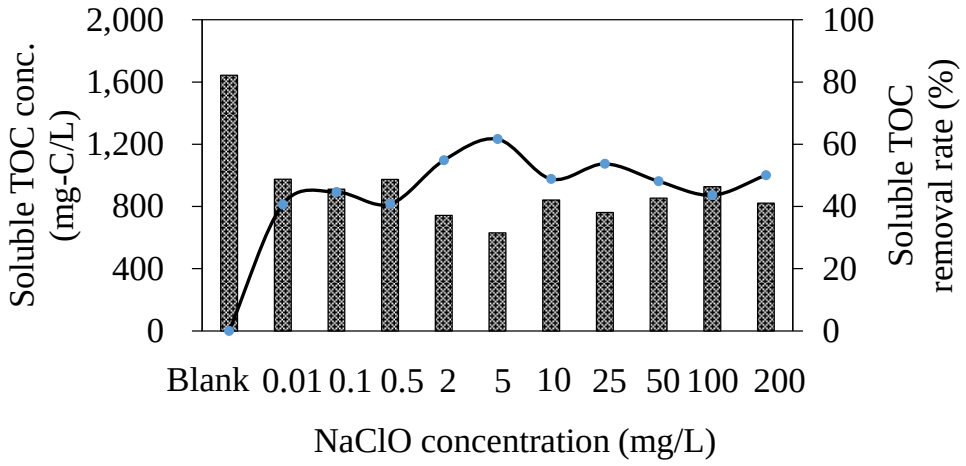

Figure 6. 15. S-TOC concentration and removal rate at 200 mg/L PAC and different NaClO concentrations

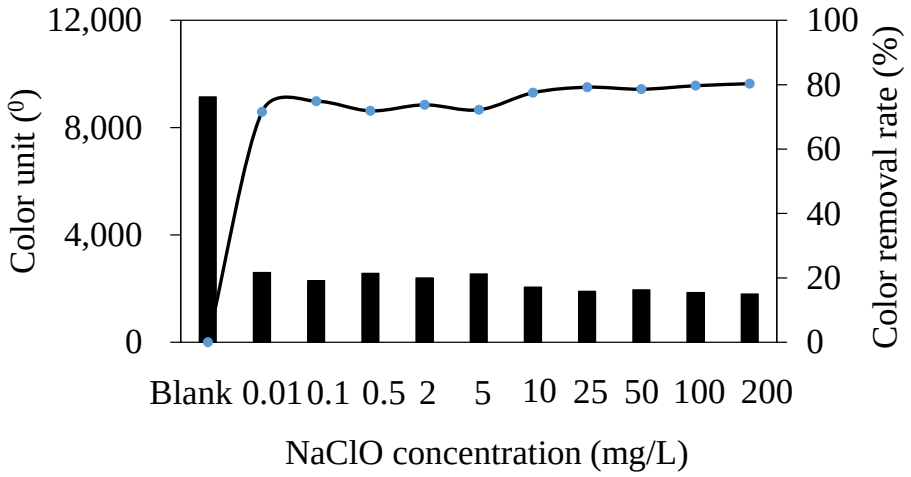

Figure 6. 16. Color unit and removal rate at 200 mg/L PAC and different NaClO concentrations

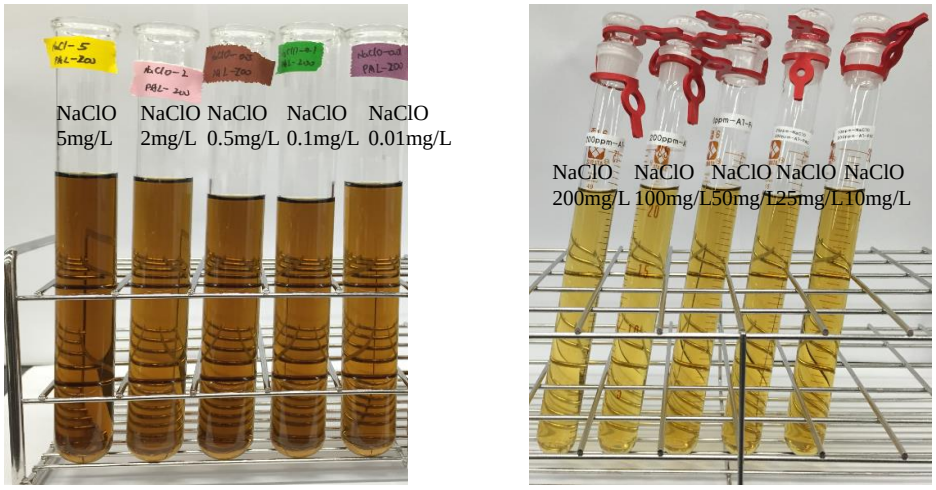

Figure 6. 17. Experimental photo for oxidation and coagulation/flocculation process at 200 mg/L PAC

Based on the above results, it can be concluded that the more PAC was used the lower lignin concentration and color unit were attained. However, the effect of NaClO on lignin and color removal rate was not significant. Possibly, 2 or 5 mg/L NaClO was saturated concentration for partial oxidation process of lignin. Nevertheless, at 200 mg/L PAC and 5 mg/L NaClO soluble TOC and color treatment efficiency achieved the most effective (62% and 72%, respectively).

6.3.3 Removal of un-degradable materials by adsorption process

The effluent from UASB reactor with soluble TOC concentration of 2,687 mg-C/L and color unit of 12,514 ^{0} was directly treated by adsorption process with commercial activated charcoal. The adsorption mechanism of ligin using activated carbon is shown in Figure 6. 18. The adsorbent dose is also an important parameter in adsorption studies because it determines the capacity of adsorbent. Different amounts of adsorbents (0-500 mg in 50 mL) were added. Increase in quantity of activated carbon increased the removal rate of soluble TOC and color from the wastewater. This was due to more surface area availability and more surface functional groups. The maximum treatment efficiencies for soluble TOC (69%) and color (94%) were obtained at dose of 10 g/L (Figure 6. 19, Figure 6. 20 and Figure 6. 21).

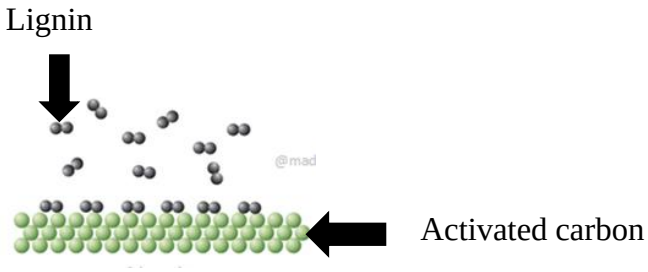

Figure 6. 18. Adsorption mechanism of lignin using activated carbon

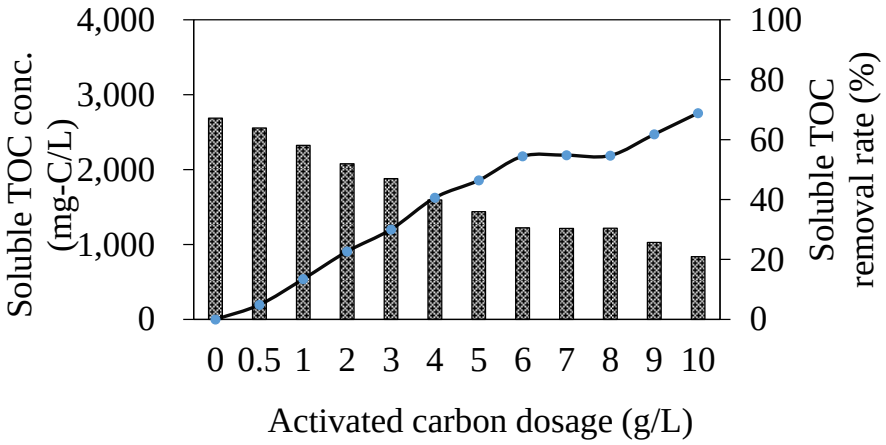

Figure 6. 19. S-TOC concentration and removal rate at different AC dosages

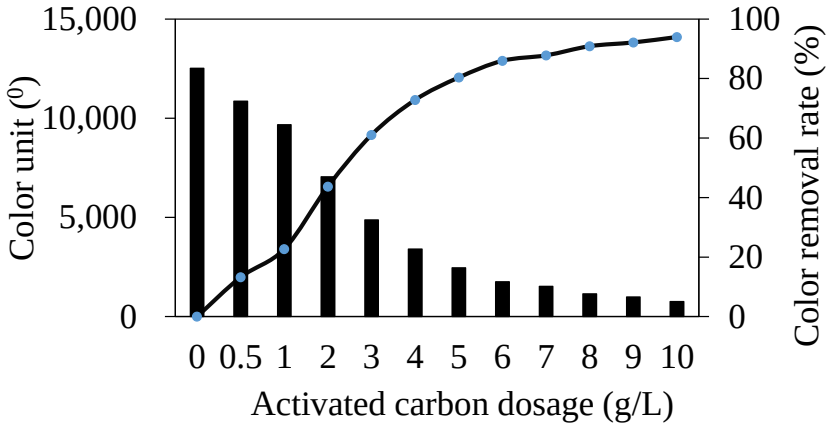

Figure 6. 20. Color unit and removal rate at different AC dosages

Figure 6. 21. Experimental photo for adsorption process
(from left to right: 0→ 10 g/L activated carbon)

Langmuir and Freundlich isotherm

Langmuir isotherm

$$q_e = \frac{q_m b.C_e}{1+b.C_e}$$

The linearized equation of Langmuir expression is as follow

$$\frac{1}{q_e} = \frac{1}{q_m} + \frac{1}{q_m.b} \cdot \frac{1}{C_e}$$

Where, q_e (mg/g) is the equilibrium amount of adsorbed, C_e (mg/L) is the equilibrium concentration of the pollutant and q_m (mg/g) and b (L/mg) are Langmuir constants.

Freundlich isotherm

$$q_e = K_f . C_e^{1/n}$$

The linearized form of the Freundlich expression is as follows

$$\log q_e = \log K_f + 1/n . \log C_e$$

Where, K_f is Freundlich constant and 1/n is the adsorption intensity.

Data for Langmuir and Freundlich isotherm are shown in Table 6. 1 and Figure 6. 22. Results showed that the fit with Langmuir and Freundlich equation were not really good (R^2 = 75% and 73%, respectively).

Table 6. 1. Data for Langmuir and Freundlich isotherm

AC dosage 'M' (g/L)	S-TOC 'C_e' (mg/L)	$X = C_0 - C_e$ (mg/L)	$q_e = X/M$ (mg/g)	$1/C_e$	$1/q_e$	Log C_e	Log q_e
0	2687	0	-	-	-	-	-
0.5	2556	131	262	0.00039	0.0038	3.4075	2.4179
1	2325	362	362	0.00043	0.0028	3.3663	2.5587
2	2077	609	305	0.00048	0.0033	3.3175	2.4838
3	1880	807	269	0.00053	0.0037	3.2741	2.4298
4	1596	1091	273	0.00063	0.0037	3.2029	2.4358
5	1439	1247	249	0.00069	0.0040	3.1581	2.3971
6	1224	1463	244	0.00082	0.0041	3.0877	2.3870
7	1215	1472	210	0.00082	0.0048	3.0844	2.3228
8	1217	1470	184	0.00082	0.0054	3.0852	2.2642
9	1027	1660	184	0.00097	0.0054	3.0114	2.2659
10	836	1850	185	0.00120	0.0054	2.9224	2.2672

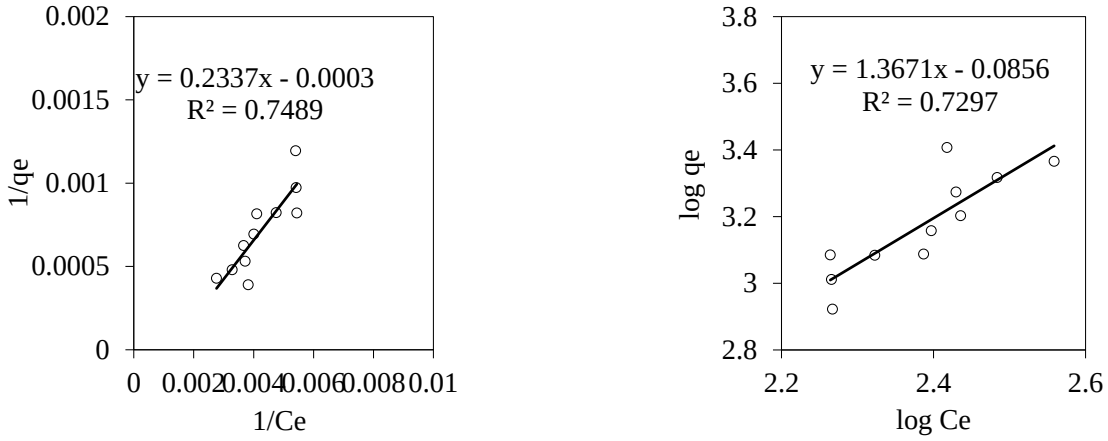

Figure 6. 22. Langmuir and Freundlich isotherm

6.3.4 Removal of un-degradable materials by combining oxidation, coagulation/flocculation and adsorption process

After aeration in 5 days soluble TOC concentration in the effluent (2,058 mg-C/L) decreased and kept stable at 1,375 mg-C/L while color unit changed from 15,357 to 8,571 ^{0}. Next, oxidation and coagulation/flocculation using 50 mg/L NaClO and different concentrations of PAC in 1, 2 and 3 times. The treatment efficiencies for soluble TOC and color are shown in Figure 6. 23 and Figure 6. 24. The greater PAC was used the more S-TOC and color removal rate was obtained. After 3 times coagulation/flocculation the most treatment efficiency was achieved. At 50 mg/L NaClO, 1,000 mg/L PAC and coagulation/flocculation in 3 times, soluble TOC and color removal rate were 49% and 86%, respectively.

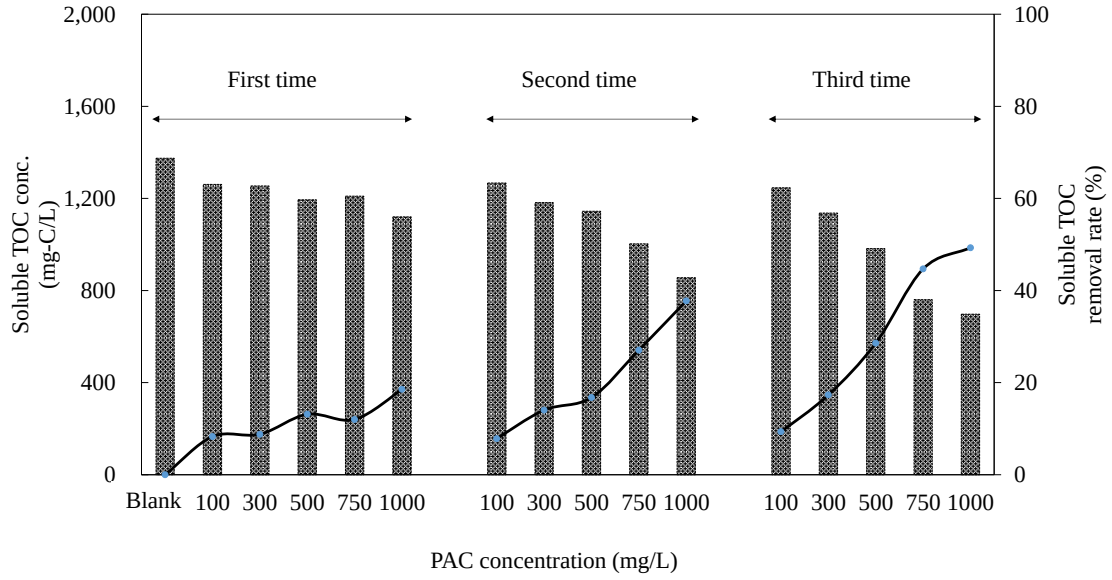

Figure 6. 23. S-TOC concentration and removal rate at different PAC concentrations and addition times

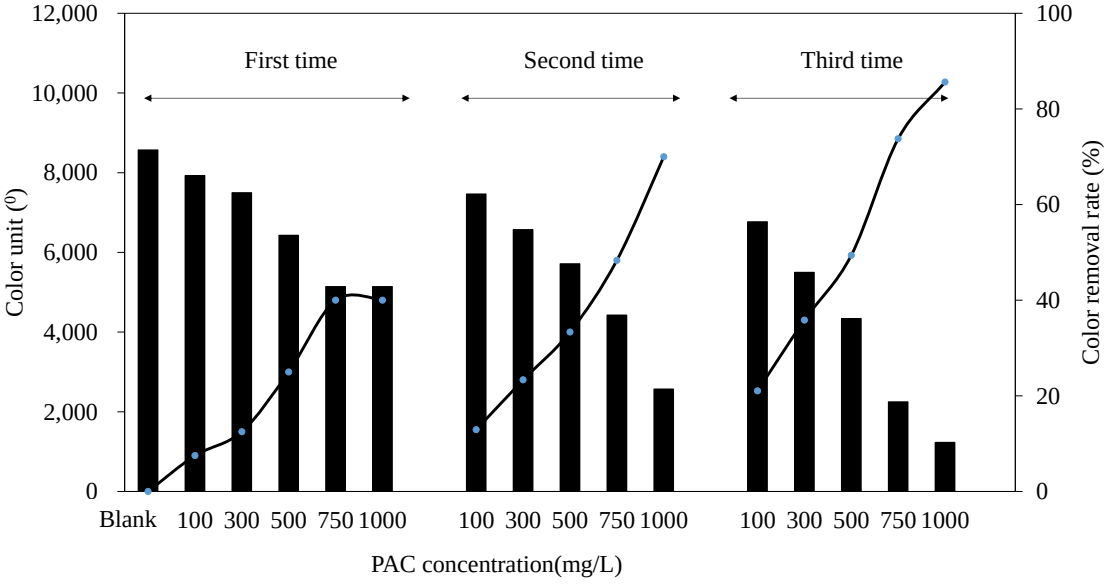

Figure 6. 24. Color unit and removal rate at different PAC concentrations and addition times

After 3 times coagulation/flocculation soluble TOC and color decreased to 697 mg-C/L and 1,232 ^{0}. Using activated carbon (0, 1, 4, 8 and 12 g/L) to treat the remaining un-

degradable materials (Figure 6. 25 and Figure 6. 26). Increasing the adsorbent amount the treatment efficiency was better. At 12 g/L of AC soluble TOC and color removal rate achieved 75% and 95%, correspondingly. Therefore, combining oxidation, coagulation/flocculation and adsorption process could improve the treatment efficiency of S-TOC and color to 87% and 99%, respectively.

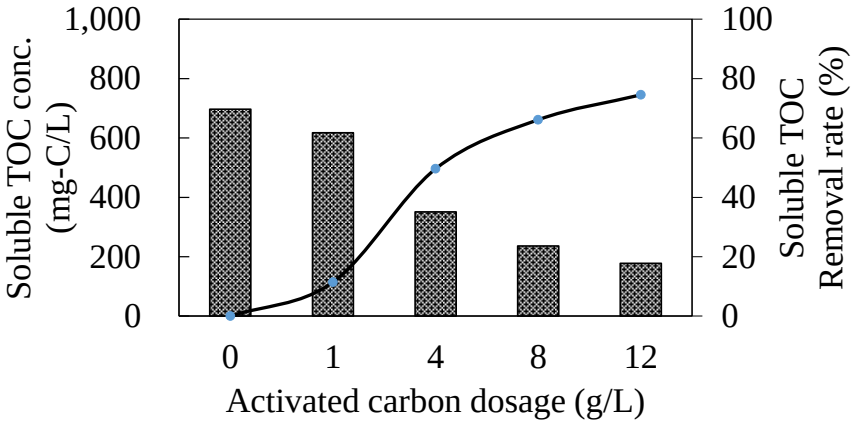

Figure 6. 25. S-TOC concentration and removal rate after 3 times coagulation/flocculation and different activated carbon dosages

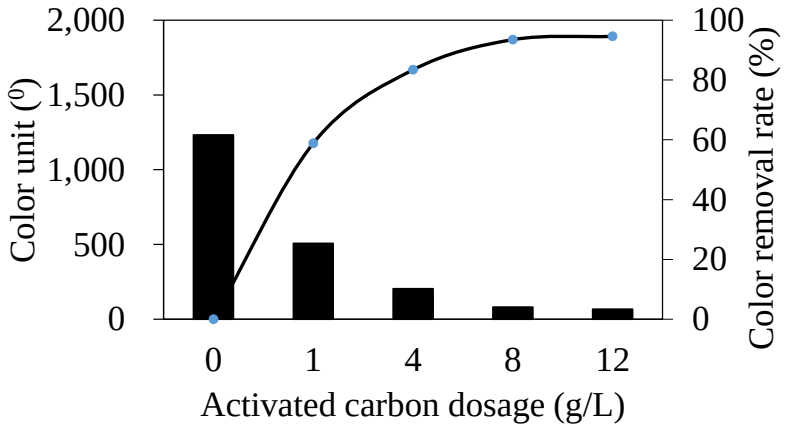

Figure 6. 26. Color and removal rate after 3 times coagulation/flocculation and different activated carbon dosages

Based on the above data set, adsorption isotherm was calculated as shown in Figure 6. 27. From this figure to estimate how much soluble TOC can adsorb in 1 g activated carbon.

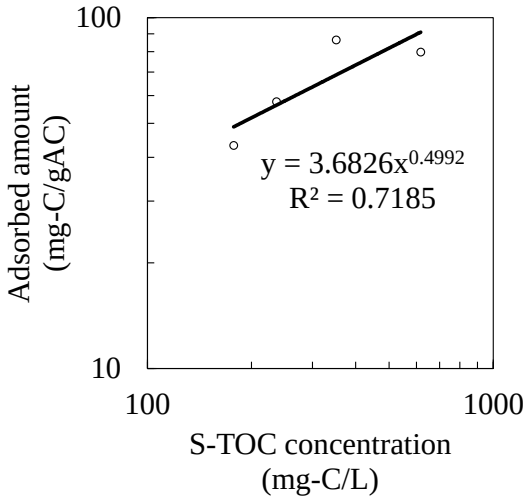

Figure 6. 27. Adsorption isotherm of activated carbon

6.4 Conclusions

Physico-chemical methods were able to apply to remove un-degradable materials (lignin and color) in post-treatment process.

Using 5 mg/L NaClO and 200 mg/L PAC could remove 62% soluble TOC and 72% color while the treatment efficiencies at 10 g/L activated carbon were 69% and 94%, respectively.

Combining oxidation (50 mg/L NaClO), coagulation/flocculation (1,000 mg/L PAC) in 3 times with adsorption (12 g/L AC) the removal rates were increased and achieved 87% for S-TOC and 99% for color.

However, applying these methods required a large amount of chemicals. Therefore, depending on different objectives the appropriate physico-chemical methods for post-treatment should be employed.

Chapter 7. Summary and Further Studies

7.1 Summary

Bioethanol processing factories are being built in many tropical regions where sugar cane is used as raw materials. To maximize the net ethanol production from cellulose in the materials, new technologies using steam explosion pretreatments are being extensively developed to extract more cellulose from lignin-bound sugar cane bagasse. Although, the wastewater from this step with high chemical oxygen demand, high soluble total organic carbon, low pH, strong odor and dark brown color causes serious environmental problems. In this regard, high-rate anaerobic biological treatments are also paid attention as the potential processes. However, the accumulation of VFAs in the high-rate methane fermentation processes often causes an operational failure. Mathematical approach based on the basic models (ASMs and ADM1) provides the understanding deeply about biochemical reactions as well as help predict appropriately this phenomena. But the limitation in many researches is that the inhibition is assumed on the microbial growth stages whilst acceleration of the decay by inhibitory materials is not considered.

This research considered acceleration of the decay by inhibitory materials (VFAs) in the high-rate methane fermentation processes. A lab-scale continuous experiment for the methane fermentation was performed for 110 days by changing the volumetric loading rate from 2.6-9.3 kg-COD/m^3/d. Due to the compositions of the steam explosion wastewater are not high fluctuated, it is difficult to express an acidic failure phenomenon. While organics wastes from food processing factories are typical materials having high fluctuated fraction of readily biodegradable organics, therefore, heterogeneous food wastes were chosen as the alternative influent. In the study, when the VLR was increased from 6 to 8 kg-COD/m^3/d, a sudden decrease of methane production was observed with an accumulation of acetate and propionate in the fermenter. After discontinuation of

feeding for 10 days the digestate in the fermenter was centrifuged and washed with tap water to reduce the VFAs to be acceptable concentration below 1,000 mg-COD/L. Nevertheless no recovery of methane production was observed and VFA concentrations consistently increased. To model the event, a modification of ADM1 was made assuming the methanogens in the fermenter were irreversibly inactivated under very high VFA. Also considering the different nature of the heterogeneous influent materials, decomposition kinetics of individual waste were manipulated. The modified ADM1 with methanogenic activity decay reasonably reproduced the responses for soluble material concentrations and methane gas production rate over the experimental period.

On the other hand, this study applied biological method to treat steam explosion wastewater from bio-ethanol processing. A batch test was conduct to elaborate a reaction map for the anaerobic degradability of organics in steam explosion wastewater from bioethanol processing. Microorganisms were collected from a lab-scale fixed-bed reactor treating the wastewater. The batch test demonstrated that the aldehydes (furfural and hydroxyl-methyl-furfural) were readily degradable and quickly decomposed together with the polysaccharide and lactate while the lignin fraction was found to be biologically inert. The hydrolysis response of soluble protein was comparable to that of polysaccharide. Based on the test a kinetic model for the anaerobic wastewater treatment was developed with a modification of ADM1 and ASMs.

Along with that, the performance of high-rate reactors (fixed-bed reactor and upward anaerobic sludge blanket reactor) for steam explosion wastewater treatment was evaluated. Two lab-scale reactors with each volume of 10.8 L at 35 °C demonstrated acceptable performance for 160 days of the continuous operation under the volumetric loading rates with 8.51 kg-COD/m^3/d (UASB) and 10.9 kg-COD/m^3/d (FBR), respectively. The average soluble TOC removal efficiencies were 72% (UASB) and 64% (FBR) with a methane conversion efficiency of about 50% for both reactors. Comparing two reactors, FBR had more stable operation and applied higher volumetric loading rate than UASB. Therefore, the dynamic simulations were focused on the fixed-bed reactor's responses. A kinetic model based on a modification of ADM1 and ASMs was used to simulate reasonably the methane production, soluble TOC, suspended solid as well as the

soluble effluent constituents in terms of carbohydrate, protein, propionate, acetate, lignin and ammonium nitrogen in FBR.

Although biological treatment resulted in significant soluble TOC removal, the effluent still retained high lignin concentration and the dark brown color. Therefore, post-treatment experiment (oxidation, coagulation/flocculation and adsorption) were conducted to remove un-degradable materials as well as color from the effluent. Firstly, the effluent from UASB reactor (soluble TOC of 2,675 mg-C/L and color of 12,514 unit) was treated by activated sludge process in 5 days with DO maintained at 1 mg/L. Some biodegradable materials continued to remove in this step and soluble TOC decreased to 1,644 mg-C/L and color decreased to 9,142 unit. After centrifuging at 8,000 rpm in 5 mins to separate sludge, the supernatant was partial oxidized with different concentrations of sodium hypochlorite (NaClO) (0.01, 0.1, 0.5, 2, 5, 10, 25, 50 and 100 mg/L) and coagulated/flocculated using 50, 100, 150 and 200 mg/L of poly-aluminium chloride (PAC). Then neutralizing pH and waiting for 30 minutes. As the results, soluble TOC and color removal rate obtained 62% and 72%, respectively with 5 mg/L NaClO and 200 mg/L PAC. On the other hand, applying adsorption process directly after UASB reactor using 0, 0.5, 1, 2, 3, 4, 5, 6, 7, 8, 9 and 10 g/L of commercial activated charcoal (AC) in 24 hours acquired maximum removal rates (69% for S-TOC and 94% for color) at 10g/L AC. Finally, combining oxidation (50 mg/L NaClO) and coagulation/flocculation (100, 300, 500, 750 and 1,000 mg/L PAC) in 1, 2 and 3 times. At 50 mg/L NaClO, 1,000 mg/L PAC and coagulation/flocculation in 3 times, soluble TOC and color removal rate were 49% and 86%, respectively. Using activated carbon (0, 1, 4, 8 and 12 g/L) to treat the remaining un-degradable materials. At 12 g/L of AC soluble TOC and color removal rate achieved 75% and 95%, correspondingly. Therefore, combining oxidation, coagulation/flocculation and adsorption process could improve the treatment efficiency of S-TOC and color to 87% and 99%, correspondingly.

7.2 Further studies

At present, there are many evidences for the reversible inhibitions in the literature, but no study about irreversible inhibition. In future, perhaps both inhibitions should exist in the biological system. Hence proper mapping of the two distinct mechanisms to individual reaction stages in a model will be one of the most important studies to install reliable high-rate methane fermentation processes.

On the other hand, dynamic simulation of UASB reactor need to be conducted to predict and calculate the treatment efficiency for steam explosion wastewater. In addition, the treatment system configuration for SEWW as seen in Figure 7. 1 should be proposed and applied to pilot scale. Firstly, anaerobic treatment (fixed-bed reactor or UASB reactor) is applied to convert the biodegradable materials to methane gas. Then, the effluent is treated by aerobic treatment to remove the remaining biodegradable materials before using physico-chemical methods (oxidation, coagulation/flocculation and adsorption or membrane (reverse osmosis (RO) or nanofiltration (NF) membrane) to remove lignin and color. After centrifuging to separate water and sludge, the effluent can be recovered for other purposes. In addition, for membrane a simple test (lab-scale) using effluent from anaerobic and aerobic treatment should be conducted (Figure 7. 2) before applying this technology to pilot scale. The treatment efficiencies are shown in Table 7. 1 and Figure 7. 3. Using the experimental data to estimate the volume of steam explosion wastewater which would be treated and the amount of sludge that would be generated after biological and physico-chemical methods. From that to design and operate the wastewater treatment plant for bioethanol processing. For example, to treat completely 10 m^3/d of steam explosion wastewater need 50 mg/L NaClO, 1,000 mg/L PAC and 12 g/L activated carbon or apply RO/NF membrane with 2.83 L/m^3.hr (RO) and 8.06 L/m^3.hr (NF). However, the treatment processes would be produce the large amount of sludge (85.5 kg-COD/d), the appropriate sludge disposal solutions should be examined in further studies.

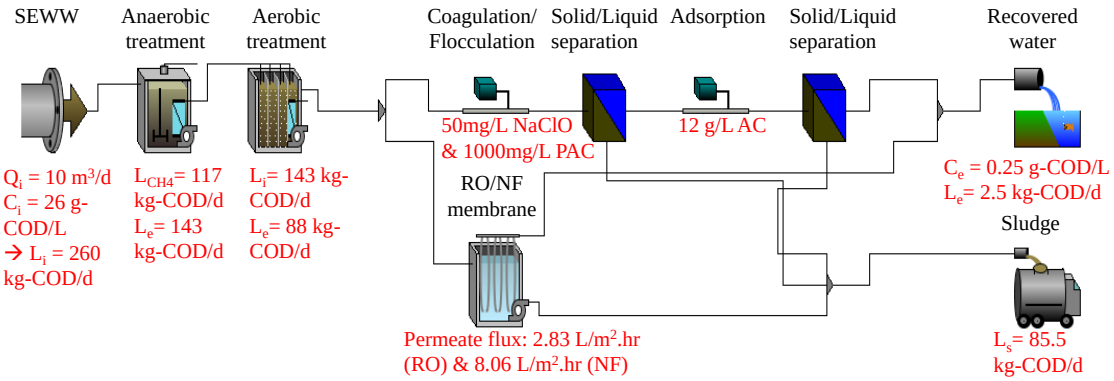

Figure 7. 1. The steam explosion wastewater treatment configuration

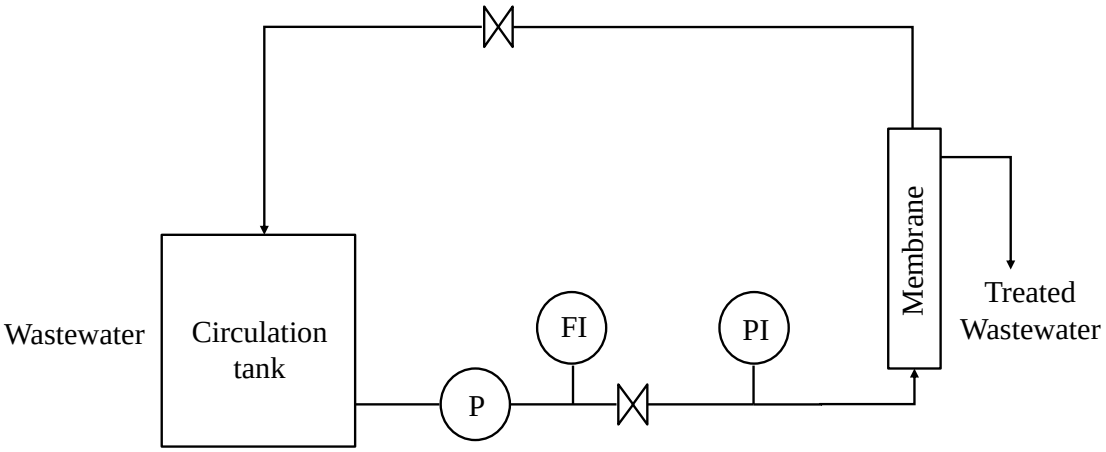

Membrane: low pressure RO (NTR-759HR), NF (NTR-729HF)

Working area: 60 cm2

Operation pressure: 0.5 Mpa

Linear velocity of circulation: 0.15 m/sec

Concentration rate: 1

Figure 7. 2. The membrane system

Table 7. 1. Removal efficiency of un-degradable materials using membrane system

Membrane type	Effluent concentration	Removal rate (%)			Flux ($L/m^2.hr$)
	S-TOC (mg-C/L)	S-TOC	Color (^{o})	Cl^-	
NF	421	87.9	97.0	98.6	8.06
Low pressure RO	72	98.3	99.3	99.9	2.83

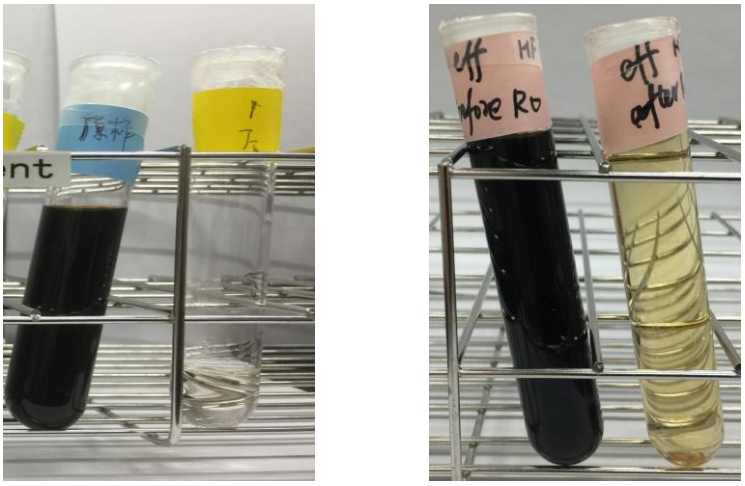

Figure 7. 3. Experimental photo of membrane system (NF (left) and RO (right))

Furthermore, in Vietnam since 2007, several projects with small to medium scales using biomass agricultural residues such as rice husks, sugar cane bagasse have been conducted to produce electricity. Especially in 2010, the government of Vietnam approved the scheme on development of biofuel up to 2015, with a vision to 2025 (Decision No. 177/2007/QD-TTG, 2007), bioethanol production in Vietnam has been sharply increased. However, along with increasing in bioethanol production, wastewater treatment from this process should be consider. Therefore, results obtained from this research can apply in Vietnam to improve the environmental quality.

Reference

A. Mandal K. O., D.N. Ghosh (2003). Removal of color from distillery wastewater by different processes. *Indian Chemical Engineer Section B* **45**(4), 264–7.

A.D. Dhale V. V. M. (2000). Treatment of distillery waste after bio-gas generation: wet oxidation. *Indian Journal of Chemical Technology* **7**, 11–8.

A.G. Vlyssides C. J. I., M. Loizidou, G. Karvouni, V. Mourafeti (1997). Pretreatment of Industrial Wastewaters II. Electrochemical treatment of vinasse from beet molasses. *Water Science and Technology* **36**(2), 271-8.

Abu Zahrim Yaser C. T., Hairul MA and Shazwan AS (2014). Current Review on the Coagulation/Flocculation of Lignin Containing Wastewater. *International Journal of Waste Resources* **4**(2), 1-6.

Akunna J. C. and Clark M. (2000). Performance of a granular-bed anaerobic baffled reactor (GRABBR) treating whisky distillery wastewater. *Bioresour Technol* **74**(3), 257-61.

Alexander J. T., Hai F. I. and Al-aboud T. M. (2012). Chemical coagulation-based processes for trace organic contaminant removal: Current state and future potential. *Journal of Environmental Management* **111**, 195-207.

Alfafara C. G., Migo V. P., Amarante J. A., Dallo R. F. and Matsumura M. (2000). Ozone treatment of distillery slop waste. *Water Science and Technology* **42**(3-4), 193-8.

Ali M. and Sreekrishnan T. R. (2001). Aquatic toxicity from pulp and paper mill effluents: a review. *Advances in Environmental Research* **5**(2), 175-96.

Amani T., Nosrati M., Mousavi S. M. and Kermanshahi R. K. (2011). Study of syntrophic anaerobic digestion of volatile fatty acids using enriched cultures at mesophilic conditions. *International Journal of Environmental Science & Technology* **8**(1), 83-96.

Amarasinghe B. M. W. P. K. and Williams R. A. (2007). Tea waste as a low cost adsorbent for the removal of Cu and Pb from wastewater. *Chemical Engineering Journal* **132**(1–3), 299-309.

Anandkumar J. and Mandal B. (2009). Removal of Cr(VI) from aqueous solution using

Bael fruit (Aegle marmelos correa) shell as an adsorbent. *Journal of Hazardous Materials* **168**(2–3), 633-40.

Andersson K. I., Eriksson M. and Norgren M. (2011). Removal of Lignin from Wastewater Generated by Mechanical Pulping Using Activated Charcoal and Fly Ash: Adsorption Isotherms and Thermodynamics. *Industrial & Engineering Chemistry Research* **50**(13), 7722-32.

Anjaneyulu Y., Sreedhara Chary N. and Samuel Suman Raj D. (2005). Decolourization of Industrial Effluents – Available Methods and Emerging Technologies – A Review. *Reviews in Environmental Science and Bio/Technology* **4**(4), 245-73.

Antonopoulou G., Stamatelatou K., Venetsaneas N., Kornaros M. and Lyberatos G. (2008). Biohydrogen and Methane Production from Cheese Whey in a Two-Stage Anaerobic Process. *Industrial & Engineering Chemistry Research* **47**(15), 5227-33.

APHA, AWWA and WEF (2012). *Standard Methods for the Examination of Water and Wastewater*. American Public Health Association, American Water Works Association, Water Environment Federation, Washington, DC, USA.

Ariffin A., Razali M. A. A. and Ahmad Z. (2012). PolyDADMAC and polyacrylamide as a hybrid flocculation system in the treatment of pulp and paper mills waste water. *Chemical Engineering Journal* **179**, 107-11.

B. Inanc F. C., I. Ozturk (1999). Colour removal from fermentation industry effluents. *Water Science and Technology* **40**(1), 331-8.

B. Wolmarans G. H. d. V. (2002). Start-up of a UASB effluent treatment plant on distillery. *Water SA* **28**(1), 63-8.

Bajaj M., Gallert C. and Winter J. (2008). Biodegradation of high phenol containing synthetic wastewater by an aerobic fixed bed reactor. *Bioresour Technol* **99**(17), 8376-81.

Balat M., Balat H. and Öz C. (2008). Progress in bioethanol processing. *Progress in Energy and Combustion Science* **34**(5), 551-73.

Barrow G. M. (1981). *Appendix I, In: Physical chemistry for the life science 2nd edition*. McGraw-Hillm Inc., USA.

Batstone D. J., Keller J., Angelidaki I., Kalyuzhnyi S. V., Pavlostathis S. G., Rozzi A., Standers W. T. M., Siegrist H. and Vavilin V. A. (2002). *Anaerobic Digestion*

Model No. 1 (ADM1), Report IWA Scientific and Technical report No.13, IWA publishing, UK, IWA publishing U, London, UK.

Bélafi-Bakó E. S. N. N. K. (2010). Anaerobic moving bed biofilm fermenter for biogas production. *Environment Protection Engineering* **36**(4), 117-25.

Bello-Mendoza R. and Castillo-Rivera M. F. (1998). Start-up of an Anaerobic Hybrid (UASB/Filter) Reactor Treating Wastewater from a Coffee Processing Plant. *Anaerobe* **4**(5), 219-25.

Bernardo E. C., Egashira R. and Kawasaki J. (1997). Decolorization of molasses' wastewater using activated carbon prepared from cane bagasse. *Carbon* **35**(9), 1217-21.

Bese F. B. D. a. S. (2001). Treatment of pulping effluents by using alum and clay - Colour removal and sludge characteristics. *Water SA* **27**(3), 361-6.

Bhattacharya A. K., Naiya T. K., Mandal S. N. and Das S. K. (2008). Adsorption, kinetics and equilibrium studies on removal of Cr(VI) from aqueous solutions using different low-cost adsorbents. *Chemical Engineering Journal* **137**(3), 529-41.

Blonskaja V., Menert A. and Vilu R. (2003). Use of two-stage anaerobic treatment for distillery waste. *Advances in Environmental Research* **7**(3), 671-8.

Boeriu C. G., Bravo D., Gosselink R. J. A. and van Dam J. E. G. (2004). Characterisation of structure-dependent functional properties of lignin with infrared spectroscopy. *Industrial Crops and Products* **20**(2), 205-18.

Boubaker F. and Ridha B. C. (2008). Modelling of the mesophilic anaerobic co-digestion of olive mill wastewater with olive mill solid waste using anaerobic digestion model No. 1 (ADM1). *Bioresour Technol* **99**(14), 6565-77.

Bratby J. (2006). *Coagulation and Flocculation in Water and Wastewater Treatment*. IWA Publishing: UK.

Cartier S., Theoleyre M. A. and Decloux M. (1997). Treatment of sugar decolorizing resin regeneration waste using nanofiltration. *Desalination* **113**(1), 7-17.

Chakar F. S. and Ragauskas A. J. (2004). Review of current and future softwood kraft lignin process chemistry. *Industrial Crops and Products* **20**(2), 131-41.

Chandra R. and Pandey P. K. (2000). Decolorization of anaerobically treated distillery effluent by activated charcoal adsorption method. *Indian Journal of Environmental Protection* **21**(2), 134–7.

Chandrasekhar S. and Pramada P. N. (2006). Rice husk ash as an adsorbent for methylene blue—effect of ashing temperature. *Adsorption* **12**(1), 27-43.

Chang I.-S., Choo K.-H., Lee C.-H., Pek U.-H., Koh U.-C., Kim S.-W. and Koh J.-H. (1994). Application of ceramic membrane as a pretreatment in anaerobic digestion of alcohol-distillery wastes. *Journal of Membrane Science* **90**(1), 131-9.

Chaudhari P. K., Mishra I. M. and Chand S. (2007). Decolourization and removal of chemical oxygen demand (COD) with energy recovery: Treatment of biodigester effluent of a molasses-based alcohol distillery using inorganic coagulants *Colloids and Surfaces A: Physicochem. Eng. Aspects* **296**(1), 238-47.

Chiaramonti D., Prussi M., Ferrero S., Oriani L., Ottonello P., Torre P. and Cherchi F. (2012). Review of pretreatment processes for lignocellulosic ethanol production, and development of an innovative method. *Biomass and Bioenergy* **46**, 25-35.

Choeisai P., Jitkam N., Silapanoraset K., Yubolsai C., Yoochatchaval W., Yamaguchi T., Onodera T. and Syutsubo K. (2014). Sugarcane molasses-based bio-ethanol wastewater treatment by two-phase multi-staged up-flow anaerobic sludge blanket (UASB) combination with up-flow UASB and down-flow hanging sponge. *Water Sci Technol* **69**(6), 1174-80.

Chong S., Sen T. K., Kayaalp A. and Ang H. M. (2012). The performance enhancements of upflow anaerobic sludge blanket (UASB) reactors for domestic sludge treatment--a state-of-the-art review. *Water Res* **46**(11), 3434-70.

Correia V. M., Stephenson T. and Judd S. J. (1994). Characterisation of textile wastewaters - a review. *Environmental Technology* **15**(10), 917-29.

Crisafully R., Milhome M. A. L., Cavalcante R. M., Silveira E. R., De Keukeleire D. and Nascimento R. F. (2008). Removal of some polycyclic aromatic hydrocarbons from petrochemical wastewater using low-cost adsorbents of natural origin. *Bioresour Technol* **99**(10), 4515-9.

Da˛ browski A. (2001). Adsorption Theory to practice. *Advances in Colloid and Interface Science* **93**, 135-224.

Davidsson Å. (2013). *Combined biogas and bio-ethanol production for optimal energy utilization*, Lund University.

Del Nery V., Damianovic M. H. and Barros F. G. (2001). The use of upflow anaerobic sludge blanket reactors in the treatment of poultry slaughterhouse wastewater.

Water Sci Technol **44**(4), 83-8.

Demirbaş O., Alkan M. and Doğan M. (2002). The Removal of Victoria Blue from Aqueous Solution by Adsorption on a Low-Cost Material. *Adsorption* **8**(4), 341-9.

Derbal K., Bencheikh-Lehocine M., Cecchi F., Meniai A. H. and Pavan P. (2009). Application of the IWA ADM1 model to simulate anaerobic co-digestion of organic waste with waste activated sludge in mesophilic condition. *Bioresour Technol* **100**(4), 1539-43.

Dias M. O. S., Ensinas A. V., Nebra S. A., Maciel Filho R., Rossell C. E. V. and Maciel M. R. W. (2009). Production of bioethanol and other bio-based materials from sugarcane bagasse: Integration to conventional bioethanol production process. *Chemical Engineering Research and Design* **87**(9), 1206-16.

Dinsdale R. M., Hawkes F. R. and Hawkes D. L. (1997). Comparison of mesophilic and thermophilic upflow anaerobic sludge blanket reactors treating instant coffee production wastewater. *Water Res* **31**(1), 163-9.

Divya Ramchandran V. S., Kishore Rajagopalan, Timothy Strathmann (2013). *Use of Treated Effluent Water in Cellulosic Ethanol Production*, Illinois Sustainable Technology Center, Prairie Research Institute, University of Illinois at Urbana-Champaign, Illinois Sustainable Technology Center.

DuBois M., Gilles K. A., Hamilton J. K., Rebers P. A. and Smith F. (1956). Colorimetric Method for Determination of Sugars and Related Substances. *Analytical Chemistry* **28**(3), 350-6.

Essington M. E. (2003). *Soil and Water Chemistry: An Integrative Approach*. CRC Press, Taylor & Francis Group: Boca Raton, FL.

Farhadian M., Borghei M. and Umrania V. V. (2007). Treatment of beet sugar wastewater by UAFB bioprocess. *Bioresour Technol* **98**(16), 3080-3.

Farhadian M., Duchez D., Vachelard C. and Larroche C. (2008). Monoaromatics removal from polluted water through bioreactors—A review. *Water Res* **42**(6–7), 1325-41.

Fezzani B. and Cheikh R. B. (2008). Implementation of IWA anaerobic digestion model No. 1 (ADM1) for simulating the thermophilic anaerobic co-digestion of olive mill wastewater with olive mill solid waste in a semi-continuous tubular digester. *Chemical Engineering Journal* **141**(1–3), 75-88.

Fukuzaki S., Nishio N., Shobayashi M. and Nagai S. (1990). Inhibition of the Fermentation of Propionate to Methane by Hydrogen, Acetate, and Propionate. *Appl Environ Microbiol* **56**(3), 719-23.

Gaikwad R. W. and Naik a. P. K. (2000). Technology for the removal of sulfate from distillery wastewater. *Indian Journal of Environmental Protection* **20**(2), 106–8.

Gali A., Benabdallah T., Astals S. and Mata-Alvarez J. (2009). Modified version of ADM1 model for agro-waste application. *Bioresour Technol* **100**(11), 2783-90.

Ganesh R., Rajinikanth R., Thanikal J. V., Ramanujam R. A. and Torrijos M. (2010). Anaerobic treatment of winery wastewater in fixed bed reactors. *Bioprocess and Biosystems Engineering* **33**(5), 619-28.

Garcia-Calderon D., Buffiere P., Moletta R. and Elmaleh S. (1998). Anaerobic digestion of wine distillery wastewater in down-flow fluidized bed. *Water Res* **32**(12), 3593-600.

Garcia H., Rico C., Garcia P. A. and Rico J. L. (2008). Flocculants effect in biomass retention in a UASB reactor treating dairy manure. *Bioresour Technol* **99**(14), 6028-36.

Garrote G., Domínguez H. and Parajó C. J. (1999). Hydrothermal processing of lignocellulosic materials. *Holz als Roh- und Werkstoff* **57**(3), 191-202.

Goodwin J. A. S. and Stuart J. B. (1994). Anaerobic digestion of malt whisky distillery pot ale using upflow anaerobic sludge blanket reactors. *Bioresour Technol* **49**(1), 75-81.

Goyal S. K., Seth R. and Handa B. K. (1996). Diphasic fixed-film biomethanation of distillery spentwash. *Bioresour Technol* **56**(2), 239-44.

Gregory J. (2006). *Particles in Water: Properties and Processes*. CRC Press, Taylor & Francis Group: Boca Raton, FL.

Grover R., Marwaha S. S. and Kennedy J. F. (1999). Studies on the use of an anaerobic baffled reactor for the continuous anaerobic digestion of pulp and paper mill black liquors. *Process Biochemistry* **34**(6–7), 653-7.

Hamelinck C. N., Hooijdonk G. v. and Faaij A. P. C. (2003). Prospects for ethanol from lignocellulosic biomass: techno-economic performance as development progresses Scientific report- NWS-E-2003-55. In, Copernicus Institute, Department of Science, Technology and Society, Utrecht University, Utrecht, The

Netherlands p. 35.

Hamelinck C. N., Hooijdonk G. v. and Faaij A. P. C. (2005). Ethanol from lignocellulosic biomass: techno-economic performance in short-, middle- and long-term. *Biomass and Bioenergy* **28**(4), 384-410.

Hampannavar U. S., Shivayogimath, C.B (2010). Anaerobic treatment of sugar industry wastewater by Upflow anaerobic sludge blanket reactor at ambient temperature. *International Journal of Environmental Sciences* **1**(4), 631-9.

Harada H., Uemura S., Chen A.-C. and Jayadevan J. (1996). Anaerobic treatment of a recalcitrant distillery wastewater by a thermophilic UASB reactor. *Bioresour Technol* **55**(3), 215-21.

Henze M., Gujer W., Mino T. and van Loosdrecht M. C. M. (2000). *Activated Sludge Models ASM1, ASM2, ASM2D, ASM3*, Report IWA Scientific and Technical report No.9, IWA publishing, UK, IWA publising U, UK.

Hill A. V. (1910). The possible effects of the aggregation of the molecules of haemoglobin on its dissociation curves. *Journal of Physiology* **40**, iv-vii.

IEA (2011). *Technology Roadmap. Biofuels for Transport*, IEA, Paris.

Irfan M., Butt T., Imtiaz N., Abbas N., Khan R. A. and Shafique A. (2013). The removal of COD, TSS and colour of black liquor by coagulation–flocculation process at optimized pH, settling and dosing rate. *Arabian Journal of Chemistry*.

Itzhaki R. F. and Gill D. M. (1964). A micro-biuret method for estimating proteins. *Anal Biochem* **9**, 401-10.

Jain A. K., Gupta V. K., Bhatnagar A. and Suhas (2003). Utilization of industrial waste products as adsorbents for the removal of dyes. *Journal of Hazardous Materials* **101**(1), 31-42.

Johns M. R. (1995). Developments in wastewater treatment in the meat processing industry: A review. *Bioresour Technol* **54**(3), 203-16.

Kaar W. E., Gutierrez C. V. and Kinoshita C. M. (1998). Steam explosion of sugarcane bagasse as a pretreatment for conversion to ethanol. *Biomass and Bioenergy* **14**(3), 277-87.

Kalfas H., Skiadas I. V., Gavala H. N., Stamatelatou K. and Lyberatos G. (2006). Application of ADM1 for the simulation of anaerobic digestion of olive pulp under mesophilic and thermophilic conditions. *Water Science & Technology* **54**(4),

149.

Kallas M. K. a. J. (2006). Degradation of lignins by wet oxidation: model water solutions In: *The Estonian Academy of Sciences. Chemistry*, pp. 132–44.

Khattri S. D. and Singh M. K. (2009). Removal of malachite green from dye wastewater using neem sawdust by adsorption. *Journal of Hazardous Materials* **167**(1–3), 1089-94.

King H. H., Avni E., Coughlin R. W. and Solomon P. R. (1983). *Modeling tar composition in lignin pyrolysis*.

Kleerebezem R. and van Loosdrecht M. C. M. (2006). Critical analysis of some concepts proposed in ADM1. *Water Science & Technology* **54**(4), 51.

Klinke H. B., Thomsen A. B. and Ahring B. K. (2004). Inhibition of ethanol-producing yeast and bacteria by degradation products produced during pre-treatment of biomass. *Appl Microbiol Biotechnol* **66**(1), 10-26.

Koehler A. G. a. T. (2000). *Oregon cellulose-ethanol study: an evaluation of the potential for ethanol production in Oregon using cellulose-based feedstocks*, Salem, Oregon, USA.

Kumar U. and Bandyopadhyay M. (2006). Sorption of cadmium from aqueous solution using pretreated rice husk. *Bioresour Technol* **97**(1), 104-9.

Kumaresan T., Meera Sheriffa Begum K. M., Sivashanmugam P., Anantharaman N. and Sundaram S. (2003). Experimental studies on treatment of distillery effluent by liquid membrane extraction. *Chemical Engineering Journal* **95**(1–3), 199-204.

Kuo C. H. and Lee C. K. (2009). Enhanced enzymatic hydrolysis of sugarcane bagasse by N-methylmorpholine-N-oxide pretreatment. *Bioresour Technol* **100**(2), 866-71.

Lalov I. G., Guerginov I. I., Krysteva M. A. and Fartsov K. (2000). Treatment of waste water from distilleries with chitosan. *Water Res* **34**(5), 1503-6.

Leal K., Chacin E., Behling E., Gutierez E., Fernandez N. and Forster C. F. (1998). A mesophilic digestion of brewery wastewater in an unheated anaerobic filter. *Bioresour Technol* **65**(1), 51-5.

Lew B., Lustig I., Beliavski M., Tarre S. and Green M. (2011). An integrated UASB-sludge digester system for raw domestic wastewater treatment in temperate climates. *Bioresour Technol* **102**(7), 4921-4.

Li Y., Zhang F. S. and Xiu F. R. (2009). Arsenic (V) removal from aqueous system using

adsorbent developed from a high iron-containing fly ash. *Sci Total Environ* **407**(21), 5780-6.

Lier J. B. v., Mahmoud N. and Zeeman a. G. (2008). Anaerobic Wastewater Treatment. In: *Biological Wastewater Treatment: Principles, Modelling and Design* Henze M, Loosdrecht MCMv, Ekama GA and Brdjanovic aD (eds), IWA Publishing, London, UK.

Lowry O. H., Rosebrough N. J., Farr A. L. and Randall R. J. (1951). Protein measurement with the Folin phenol reagent. *J Biol Chem* **193**(1), 265-75.

Mahmoud N. (2008). High strength sewage treatment in a UASB reactor and an integrated UASB-digester system. *Bioresour Technol* **99**(16), 7531-8.

Mairet F., Bernard O., Ras M., Lardon L. and Steyer J. P. (2011). Modeling anaerobic digestion of microalgae using ADM1. *Bioresour Technol* **102**(13), 6823-9.

Mall I. D. and Kumar V. (1997). Removal of organic matter from distillery effluent using low cost adsorbent. *Chemical Engineering World* **XXXII**(7), 89-96.

Mane J. D., Modi S., Nagawade S., Phadnis S. P. and Bhandari V. M. (2006). Treatment of spentwash using chemically modified bagasse and colour removal studies. *Bioresour Technol* **97**(14), 1752-5.

Mannina G. and Viviani G. (2009). Hybrid moving bed biofilm reactors: an effective solution for upgrading a large wastewater treatment plant. *Water Sci Technol* **60**(5), 1103-16.

Martin M., Svensson N., Fonseca J. and Eklund M. (2014). Quantifying the environmental performance of integrated bioethanol and biogas production. *Renewable Energy* **61**, 109-16.

Mata-Alvarez J. (2005). Biomethanization of the Organic Fraction of Municipal Solid Wastes. *Water Intelligence Online* **4**.

Mechichi T. and Sayadi S. (2005). Evaluating process imbalance of anaerobic digestion of olive mill wastewaters. *Process Biochemistry* **40**(1), 139-45.

Migo V. P., Matsumura M., Del Rosario E. J. and Kataoka H. (1993). Decolorization of molasses wastewater using an inorganic flocculant. *Journal of Fermentation and Bioengineering* **75**(6), 438-42.

Mosier N., Wyman C., Dale B., Elander R., Lee Y. Y., Holtzapple M. and Ladisch M. (2005). Features of promising technologies for pretreatment of lignocellulosic

biomass. *Bioresour Technol* **96**(6), 673-86.

Nacheva P. M., Chavez G. M., Chacon J. M. and Chuil A. C. (2009). Treatment of cane sugar mill wastewater in an upflow anaerobic sludge bed reactor. *Water Sci Technol* **60**(5), 1347-52.

Narra M. and Balasubramanian V. (2015). Utilization of solid and liquid waste generated during ethanol fermentation process for production of gaseous fuel through anaerobic digestion--a zero waste approach. *Bioresour Technol* **180**, 376-80.

Nataraj S. K., Hosamani K. M. and Aminabhavi T. M. (2006). Distillery wastewater treatment by the membrane-based nanofiltration and reverse osmosis processes. *Water Res* **40**(12), 2349-56.

Nikolaeva S., Sanchez E., Borja R., Raposo F., Colmenarejo M. F., Montalvo S. and Jimenez-Rodriguez A. M. (2009). Kinetics of anaerobic degradation of screened dairy manure by upflow fixed bed digesters: effect of natural zeolite addition. *J Environ Sci Health A Tox Hazard Subst Environ Eng* **44**(2), 146-54.

OECD/IEA (2014). *Medium Term Renewable Energy Market Report 2014. Executive Summary*, IEA, Paris.

Orhon D., Di Pinto A. C., Tilche A., Tasli R., Yilmazer G. and Yenigün O. (1999). Waste Management Problems in Agro-Industires 1998Two-phase anaerobic treatment of cheese whey. *Water Science and Technology* **40**(1), 289-95.

Pandey R. A., Malhotra S., Tankhiwale A., Pande S., Pathe P. P. and Kaul S. N. (2003). Treatment Of Biologically Treated Distillery Effluent - A Case Study. *International Journal of Environmental Studies* **60**(3), 263-75.

Parajuli R., Dalgaard T., Jørgensen U., Adamsen A. P. S., Knudsen M. T., Birkved M., Gylling M. and Schjørring J. K. (2015). Biorefining in the prevailing energy and materials crisis: a review of sustainable pathways for biorefinery value chains and sustainability assessment methodologies. *Renewable and Sustainable Energy Reviews* **43**, 244-63.

Pedro Silva J., Sousa S., Rodrigues J., Antunes H., Porter J. J., Gonçalves I. and Ferreira-Dias S. (2004). Adsorption of acid orange 7 dye in aqueous solutions by spent brewery grains. *Separation and Purification Technology* **40**(3), 309-15.

Peña M., Coca M., González G., Rioja R. and García M. T. (2003). Chemical oxidation of wastewater from molasses fermentation with ozone. *Chemosphere* **51**(9), 893-

900.

Pikaev A. K., Ponomarev A. V., Bludenko A. V., Minin V. N. and Elizar'eva L. M. (2001). Combined electron-beam and coagulation purification of molasses distillery slops. Features of the method, technical and economic evaluation of large-scale facility. *Radiation Physics and Chemistry* **61**(1), 81-7.

R. Chandra H. S. (1999). Chemical decolorization of anaerobically treated distillery effluent. *Indian Journal of Environmental Protection* **19**(11), 833–7.

R. Seth S. K. G., B.K. Handa (1995). Fixed film biomethanation of distillery spentwash using low cost porous media. *Resources, Conservation and Recycling* **14**(2), 79-89.

Rabelo S. C., Carrere H., Maciel Filho R. and Costa A. C. (2011). Production of bioethanol, methane and heat from sugarcane bagasse in a biorefinery concept. *Bioresour Technol* **102**(17), 7887-95.

Rajagopal R., Mehrotra I., Kumar P. and Torrijos M. (2010). Evaluation of a hybrid upflow anaerobic sludge-filter bed reactor: effect of the proportion of packing medium on performance. *Water Sci Technol* **61**(6), 1441-50.

Rajesh Banu J., Kaliappan S. and Beck D. (2006). High rate anaerobic treatment of Sago wastewater using HUASB with PUF as carrier. *International Journal of Environmental Science & Technology* **3**(1), 69-77.

Rajeshwari K. V., Balakrishnan M., Kansal A., Lata K. and Kishore V. V. N. (2000). State-of-the-art of anaerobic digestion technology for industrial wastewater treatment. *Renewable and Sustainable Energy Reviews* **4**(2), 135-56.

Rajinikanth R., Ganesh R., Escudie R., Mehrotra I., Kumar P., Thanikal J. V. and Torrijos M. (2009). High rate anaerobic filter with floating supports for the treatment of effluents from small-scale agro-food industries. *Desalination and Water Treatment* **4**(1-3), 183-90.

Sangave P. C. and Pandit A. B. (2004). Ultrasound pre-treatment for enhanced biodegradability of the distillery wastewater. *Ultrasonics Sonochemistry* **11**(3–4), 197-203.

Sari A. A., Kurniawan H. H., Nurdin M. and Abimanyu H. (2015). Decolorization of Black Liquor Wastewater Generated from Bioethanol Process by Using Oil Palm Empty Fruit Bunches. *Energy Procedia* **68**, 254-62.

Satyawali Y. and Balakrishnan M. (2007). Removal of color from biomethanated distillery spentwash by treatment with activated carbons. *Bioresour Technol* **98**(14), 2629-35.

Saxena R. C., Adhikari D. K. and Goyal H. B. (2009). Biomass-based energy fuel through biochemical routes: A review. *Renewable and Sustainable Energy Reviews* **13**(1), 167-78.

Sekar D. and Murthy D. V. S. (1998). Color removal of distillery spentwash by adsorption technique. *Indian Chemical Engineer, Section A* **40**(4), 176–81.

Şen S. and Demirer G. N. (2003). Anaerobic treatment of real textile wastewater with a fluidized bed reactor. *Water Res* **37**(8), 1868-78.

Shankar R., Singh L., Mondal P. and Chand S. (2013). Removal of Lignin from Wastewater through Electro-Coagulation. *World Journal of Environmental Engineering* **1**(2), 16-20.

Shao X., Peng D., Teng Z. and Ju X. (2008). Treatment of brewery wastewater using anaerobic sequencing batch reactor (ASBR). *Bioresour Technol* **99**(8), 3182-6.

Show K.-Y. and Tay J.-H. (1999). Influence of support media on biomass growth and retention in anaerobic filters. *Water Res* **33**(6), 1471-81.

Siegrist H., Vogt D., Garcia-Heras J. L. and Gujer W. (2002). Mathematical model for meso- and thermophilic anaerobic sewage sludge digestion. *Environ Sci Technol* **36**(5), 1113-23.

Somasiri W., Li X.-F., Ruan W.-Q. and Jian C. (2008). Evaluation of the efficacy of upflow anaerobic sludge blanket reactor in removal of colour and reduction of COD in real textile wastewater. *Bioresour Technol* **99**(9), 3692-9.

Srivastava V. C., Mall I. D. and Mishra I. M. (2005). Treatment of pulp and paper mill wastewaters with poly aluminium chloride and bagasse fly ash. *Colloids and Surfaces A: Physicochemical and Engineering Aspects* **260**(1–3), 17-28.

Steinwinder T., Gill E. and Gerhardt M. (2011). Process design of wastewater treatment for the NREL cellulosic ethanol model. In: Gill E and Gerhardt M (eds). [Revision]. edn, National Renewable Energy Laboratory, Golden, CO :.

Suhas, Carrott P. J. M. and Ribeiro Carrott M. M. L. (2007). Lignin – from natural adsorbent to activated carbon: A review. *Bioresour Technol* **98**(12), 2301-12.

Sundin J. and massateknik T. h. i. S. I. f. p.-o. (2000). *Precipitation of Kraft Lignin Under*

Alkaline Conditions.

Syutsubo K., Harada H., Ohashi A. and Suzuki H. (1997). Anaerobic Digestion VIII. An effective start-up of thermophilic UASB reactor by seeding mesophilically-grown granular sludge. *Water Science and Technology* **36**(6-7), 391-8.

Tchobanoglous G., Burton F. L., Stensel H. D., Metcalf and Eddy I. (2003). *Wastewater Engineering: Treatment and Reuse*. McGraw-Hill Education.

Teh C. Y., Budiman P. M., Shak K. P. Y. and Wu T. Y. (2016). Recent Advancement of Coagulation–Flocculation and Its Application in Wastewater Treatment. *Industrial & Engineering Chemistry Research* **55**(16), 4363-89.

Tokuda M., Fujiwara Y. and Kida K. (1999). Pilot plant test for removal of organic matter, N and P from whisky pot ale. *Process Biochemistry* **35**(3–4), 267-75.

Torry-Smith M., Sommer P. and Ahring B. K. (2003). Purification of bioethanol effluent in an UASB reactor system with simultaneous biogas formation. *Biotechnol Bioeng* **84**(1), 7-12.

U.Satyanarayana and U.Chakrapani (2006). *Biochemistry 3rd edition*. Books and Applied (P) Ltd.

Uellendahl H. and Ahring B. K. (2010). Anaerobic digestion as final step of a cellulosic ethanol biorefinery: Biogas production from fermentation effluent in a UASB reactor-pilot-scale results. *Biotechnol Bioeng* **107**(1), 59-64.

Vavilin V. A., Fernandez B., Palatsi J. and Flotats X. (2008). Hydrolysis kinetics in anaerobic degradation of particulate organic material: an overview. *Waste Manag* **28**(6), 939-51.

Vavilin V. A., Rytov S. V. and Lokshina a. L. Y. (1996). A description of hydrolysis kinetics in anaerobic degradation of particulate organic matter. *Bioresour Technol* **56**(2-3), 229-37.

Vijayaraghavan K. and Ramanujam K. T. (2000). Performance of anaerobic contact filter in series for treating distillery spentwash. *Bioprocess Engineering* **22**(2), 109-14.

Wang J.-P., Chen Y.-Z., Yuan S.-J., Sheng G.-P. and Yu H.-Q. (2009a). Synthesis and characterization of a novel cationic chitosan-based flocculant with a high water-solubility for pulp mill wastewater treatment. *Water Res* **43**(20), 5267-75.

Wang S., Boyjoo Y. and Choueib A. (2005). A comparative study of dye removal using fly ash treated by different methods. *Chemosphere* **60**(10), 1401-7.

Wang Y., Zhang Y., Wang J. and Meng L. (2009b). Effects of volatile fatty acid concentrations on methane yield and methanogenic bacteria. *Biomass and Bioenergy* **33**(5), 848-53.

Wichern M., Gehring T., Fischer K., Andrade D., Lubken M., Koch K., Gronauer A. and Horn H. (2009). Monofermentation of grass silage under mesophilic conditions: measurements and mathematical modeling with ADM 1. *Bioresour Technol* **100**(4), 1675-81.

Wiegant W. M., Claassen J. A. and Lettinga G. (1985). Thermophilic anaerobic digestion of high strength wastewaters. *Biotechnol Bioeng* **27**(9), 1374-81.

Wyman C. E., Dale B. E., Elander R. T., Holtzapple M., Ladisch M. R. and Lee Y. Y. (2005). Coordinated development of leading biomass pretreatment technologies. *Bioresour Technol* **96**(18), 1959-66.

Y. Zahrim A. and Rajin M. (2014). Diluted Biologically Digested Palm Oil Mill Effluent as a Nutrient Source for Eichornia crassipes. *Current Environmental Engineering* **1**(1), 45-50.

Yeoh B. G. (1997). Anaerobic Digestion VIII.Two-phase anaerobic treatment of cane-molasses alcohol stillage. *Water Science and Technology* **36**(6), 441-8.

Yi Zheng Z. P., Ruihong Zhang (2009). Overview of biomass pretreatment for cellulosic ethanol production. *Int J Agric & Biol Eng* **2**(3), 51-68.

Zaldivar J., Martinez A. and Ingram L. O. (1999). Effect of selected aldehydes on the growth and fermentation of ethanologenic Escherichia coli. *Biotechnol Bioeng* **65**(1), 24-33.

Zaldivar J., Martinez A. and Ingram L. O. (2000). Effect of alcohol compounds found in hemicellulose hydrolysate on the growth and fermentation of ethanologenic Escherichia coli. *Biotechnol Bioeng* **68**(5), 524-30.

Zanin G. M., Santana C. C., Bon E. P., Giordano R. C., de Moraes F. F., Andrietta S. R., de Carvalho Neto C. C., Macedo I. C., Fo D. L., Ramos L. P. and Fontana J. D. (2000). Brazilian bioethanol program. *Appl Biochem Biotechnol* **84-86**, 1147-61.

Zeng Y. and Park J. (2009). Characterization and coagulation performance of a novel inorganic polymer coagulant—Poly-zinc-silicate-sulfate. *Colloids and Surfaces A: Physicochemical and Engineering Aspects* **334**(1–3), 147-54.

Zheng Y., Zhao J., Xu F. and Li Y. (2014). Pretreatment of lignocellulosic biomass for

enhanced biogas production. *Progress in Energy and Combustion Science* **42**(0), 35-53.

Publication list

Journal paper

1. **Ngo Van Anh**, Vuong Thi Huyen, Le Van Chieu, Nguyen Thi Ha, Mitsuharu Terashima, Hidenari Yasui (2014). High-rate Moving-bed Biofilm Anaerobic Digestion for Waste Activated Sludge Treatment. **Journal of Water and Environmental Technology**, Vol.12, No.6, 501-509.
2. **Anh Van Ngo**, Ha Thi Nguyen, Chieu Van Le, Rajeev Goel, Mitsuharu Terashima, Hidenari Yasui (2015). A Dynamic Simulation of Methane Fermentation Process Receiving Heterogeneous Food Wastes and Modelling Acidic Failure. **Journal of Material Cycles and Waste Management,** Vol.18, No.12, 239-247.
3. **Anh Van Ngo**, Bing Liu, Mitsuharu Terashima, Hidenari Yasui. High-rate Anaerobic Treatment of the Steam Explosion Wastewater from Bioethanol Processing using Sugar Cane Bagasse. (Under review, **Journal of Water and Environmental Technology).**
4. **Ngo Van Anh**, Bing Liu, Mitsuharu Terashima, Hidenari Yasui. Anaerobic Degradation of the Organics in Steam Explosion Wastewater from Bioethanol Processing. (In progress).

International conference paper

1. **Ngo Van Anh**, Vuong Thi Huyen, Le Van Chieu, Nguyen Thi Ha, Mitsuharu Terashima, Hidenari Yasui (2014). High-rate Moving-bed Biofilm Anaerobic Digestion for Waste Activated Sludge Treatment. **Proceeding of Water and Environment Technology conference 2014**, Tokyo, Japan, P.25.
2. **Ngo Van Anh,** Nguyen Thi Ha, Le Van Chieu, Rajeev Goel, Mitsuharu Terashima, Hidenari Yasui (2014). Expression of Acidic Failure for the Methane Fermentation in Food Waste Digestion. **Proceeding of 9th IWA International Symposium on Waste Management Problems in Agro-Industries**, Kochi, Japan, PP.443-450.
3. **Ngo Van Anh**, Bing Liu, Mitsuharu Terashima, Hidenari Yasui (2015). Anaerobic Biodegradation of the Steam Explosion Wastewater from Sugar Cane Bagasse for Bioethanol Processing. **Proceeding of the 6th IWA-ASPIRE Conference and**

Exhibition, Beijing, China, P.64.

4. **Ngo Van Anh**, Bing Liu, Mitsuharu Terashima, Hidenari Yasui (2016). Anaerobic Treatment of the Steam Explosion Wastewater from Bioethanol Processing using Sugar Cane Bagasse. **Proceeding of Water and Environment Technology conference 2016**, Tokyo, Japan, P. 30.